UNIVERSITY OF MINNESOTA

This is to certify that I have examined this bound copy of a Doctoral thesis by

Nikhil Chandra Admal

and have found that it is complete and satisfactory in all respects,
and that any and all revisions required by the final
examining committee have been made.

Ellad B. Tadmor

Name of Faculty Adviser

Signature of Faculty Adviser

Date

GRADUATE SCHOOL

Results on the interaction between atomistic and continuum models

A THESIS
SUBMITTED TO THE FACULTY OF THE GRADUATE SCHOOL
OF THE UNIVERSITY OF MINNESOTA
BY

Nikhil Chandra Admal

IN PARTIAL FULFILLMENT OF THE REQUIREMENTS
FOR THE DEGREE OF
Doctor of Philosophy

Ellad B. Tadmor, Adviser

August 2014

Abstract

In this thesis, we develop continuum notions for atomistic systems which play an important role in developing accurate constitutive relations for continuum models, and robust multiscale methods for studying systems with multiple length and time scales. We use a unified framework to study the Irving–Kirkwood and Murdoch–Hardy procedures used to obtain definitions for continuum fields in atomistic systems. We identify and investigate the following three problems.

1. Continuum fields derived for atomistic systems using the Irving–Kirkwood or the Murdoch–Hardy procedures correspond to a spatial description. Due to the absence of a deformation mapping field in atomistic simulations, it is uncommon to define atomistic fields in the reference configuration. We show that the Murdoch–Hardy procedure can be modified to obtain pointwise continuum fields in the reference configuration using the motion of particles as a surrogate for the deformation mapping. In particular, we obtain definitions for the first and second atomistic Piola–Kirchhoff stress tensors. An interesting feature of the atomistic first Piola–Kirchhoff stress tensor is the absence of a kinetic contribution, which in the atomistic Cauchy stress tensor accounts for thermal fluctuations. We show that this effect is also included in the atomistic first Piola–Kirchhoff stress tensor through the motion of the particles.

2. We investigate the non-uniqueness of the atomistic stress tensor stemming from the non-uniqueness of the potential energy representation. In particular, we show using rigidity theory that the distribution associated with the potential part of the atomistic stress tensor can be decomposed into an irrotational part that is independent of the potential energy representation, and a traction-free solenoidal part. Therefore, we have identified for the atomistic stress tensor a discrete analog of the continuum generalized Beltrami representation (a version of the vector Helmholtz decomposition for symmetric tensors).

3. We show that an ambiguity in the original Irving–Kirkwood procedure resulting due to the non-uniqueness of the energy decomposition between particles can be completely avoided through an alternate derivation for the energy balance. It is found that the expressions for the specific internal energy and the heat flux obtained through the alternate derivation are quite different from the original Irving–Kirkwood procedure and appear to be more physically reasonable. Next, we apply spatial averaging to the pointwise field to obtain the corresponding macroscopic quantities. These lead to expressions suitable for computation in molecular dynamics simulations.

Contents

List of Figures

Chapter 1

Thesis introduction

Continuum mechanics provides an efficient theoretical framework for modeling materials science phenomena.[1] To characterize the behavior of materials, *constitutive relations* serve as an input to the continuum theory. These constitutive models have functional forms which must be consistent with material frame-indifference and the laws of thermodynamics and include parameters that are fitted to reproduce experimental observations. With the advent of modern computing power, atomistic simulations through "numerical experiments" offer the potential for studying different materials and arriving at their constitutive laws from first principles. This could make it possible to design new materials and to improve the properties of existing materials in a systematic fashion. To use the data obtained from an atomistic simulation to build a constitutive law that is framed in the language of continuum mechanics, it is necessary to understand the connection between continuum fields and the underlying microscopic dynamics.

Another arena where the connection between continuum and atomistic concepts is important is the field of *multiscale modeling of materials*. This discipline involves the development of computational tools for studying problems where two or more length and/or time scales play a major role in determining macroscopic behavior. A prototypical example is fracture mechanics where the behavior of a crack is controlled by atomic-scale phenomena at the crack-tip, while at the same time long-range elastic stress fields are set up in the body. Many advances have been made in the area of multiscale modeling in recent years. Some common atomistic/continuum coupling methods are quasicontinuum [TOP96, SMT$^+$99], coupling of length scales [RB00], cluster quasicontinuum [KO01],

[1] Some portions of this introductory chapter are adopted either in essence or verbatim from our earlier publication [AT10].

bridging domain [XB04], coupled atomistics and discrete dislocations [SMC04], and heterogeneous multiscale methods [EEL+07], to name just a few. Refer to [TM09] for a comparison of some prominent atomistic/continuum coupling multiscale methods. In a multiscale method, a key issue involves the transfer of information between the discrete model and the continuum model. It is therefore of practical interest to understand how to construct definitions of continuum fields for an atomistic system, to ensure a smooth transfer of information between the discrete and continuum domains.

The main theme of this work is to develop continuum notions for atomistic systems within a unified framework. The idea of defining continuum fields from particle mechanics (for the special case of pair potential interactions) was pioneered in the landmark paper of Irving and Kirkwood [IK50]. Irving and Kirkwood derived the equations of hydrodynamics from the principles of non-equilibrium classical statistical mechanics and in the process established pointwise definitions for various continuum fields. Under this procedure, basic continuum fields including the mass density, momentum density, and the specific internal energy are defined *a priori* using a probability density function. Using these definitions, expressions for the stress tensor and the heat flux vector fields are obtained that identically satisfy the balance laws of continuum mechanics. The continuum fields obtained in Irving and Kirkwood's original paper [IK50] involved a series expansion of the Dirac delta distribution, which is not mathematically rigorous.[2] In a follow-up study, Noll [Nol55, LVLT10] proved two lemmas, which allowed him to avoid the use of the delta distribution and to obtain closed-form analytical expressions for the continuum fields.

Since the Irving–Kirkwood procedure is stochastic in nature, many problems arise when one tries to use the resulting expressions for a practical calculation — a key one being our lack of knowledge of the probability density function. To avoid these difficulties, Hardy [Har82, HRS02] and independently Murdoch [Mur82, MB93, MB94, Mur03, Mur07] developed a simpler spatial averaging procedure that avoids the mathematical complexity of the Irving–Kirkwood procedure. In this procedure, continuum fields are defined as direct spatial averages of the discrete equations of motion using a normalized weighting function. This approach also leads to a set of definitions that identically satisfy the balance equations. The continuum fields developed by Hardy and Murdoch are extensively used in numerical simulations due to their deterministic nature and simplicity. The Irving–Kirkwood and Murdoch–Hardy procedures were originally developed only for the special case of pair po-

[2]The derivation is non-rigorous in the sense that expressing the stress tensor as a series expansion is only possible when the probability density function, which is used in the derivation, is an analytic function of the spatial variables (see [Nol55]).

tential interactions. Although there have been a number of attempts to generalize these approaches to multi-body potentials (see [ZWS08, Che06, ZT04, HPB05]), these attempts are restricted to specific potentials (see [Che06, ZT04]). This limitation was addressed by Admal and Tadmor in [Adm10, AT10] where a unified framework that applies to *arbitrary* multi-body potentials was developed. We use this unified framework throughout this work.

Although the fields obtained in the Murdoch–Hardy and Irving–Kirkwood procedures identically satisfy the continuum balance laws (mass, momentum and energy), they do not have dual material and spatial descriptions as seen in continuum mechanics. In continuum mechanics, a reference configuration is chosen to represent a convenient fixed state of the body to which the deformed configuration is compared. Once the reference configuration is chosen, constitutive relations are described using the gradient (or higher-order gradients) of a deformation which tracks the motion of material points from the reference to the deformed configuration. Therefore, the reference configuration plays an important role in defining constitutive relations in continuum mechanics. Moreover, continuum fields can be expressed *materially* on the reference configuration, or *spatially* on the deformed configuration. A material field can be obtained as a "pull-back" of the corresponding spatial field with respect to the deformation map.

In contrast to the continuum definitions, since the potential energy of an atomistic body is defined in terms of the current positions of particles, a reference configuration of particles is not needed to describe the physical properties of the system. As a result, the fields obtained in the Murdoch–Hardy and Irving–Kirkwood procedures correspond to a spatial description. In the absence of a deformation map, atomistic fields cannot be readily pulled-back to a reference configuration, which hampers the definition of constitutive relations. This issue is addressed in Chapter 2 in which we obtain material (or referential) descriptions for atomistic fields and study their relation to the spatial fields obtained in the original Murdoch–Hardy procedure.

Next we turn to the specific case of the stress tensor field, which of all the continuum fields, has been studied most extensively due to its importance. In addition to the definitions for the stress tensor obtained from the Murdoch–Hardy and Irving–Kirkwood procedures, several other definitions have been proposed over the years dating back to the 1800s in the work of Cauchy [Cau28a, Cau28b] on the stress vector, and Clausius [Cla70] on the virial stress.[3] Efforts at obtaining microscopic definitions for the stress tensor (as well as other continuum variables) are ongoing; see for example [Tsa79, WAD95, CRD01, ZIH+04, HPB05, Del05,

[3] See [AT10] for a more detailed historical review.

MRT06, Che06, MJP09b, MJP09a, TPM09, RT10] for some important contributions. Admal and Tadmor [AT10] have extensively studied the definition for the stress tensor within a unified framework based on a generalization of the Irving–Kirkwood procedure to arbitrary multi-body potentials followed by a process of spatial averaging. In that work it was shown that all existing definitions, including the virial stress tensor [Cla70], Hardy stress tensor [Har82], and Cauchy/Tsai stress tensor [Cau28a, Cau28b, Tsa79], which all seem to be derived from disparate approaches, follow as special cases from a single stress expression. Moreover, various sources of non-uniqueness of the stress tensor in the Murdoch–Hardy and Irving–Kirkwood procedures are identified.

One source of non-uniqueness in the Murdoch–Hardy procedure is associated with the choice of weighting function used for spatial averaging. An optimal weighting function minimizes the noise resulting from the discrete nature of an atomistic model, while at the same time preserving the macroscopic profile of the continuum field. A recent article by Ulz et al. [UMP13] proposes an optimal weighting function based on the correlation length of the potential energy function. A second source of non-uniqueness is a consequence of the non-uniqueness of the force decomposition used in the stress derivation as first pointed out in [AT10]. A recent work by Arroyo et al. [VTSA14] discusses the significance of the force decomposition on the atomistic stress in lipid bilayers used to evaluate the material constants of a bilayer membrane.

Although significant, the non-uniqueness of the atomistic stress due to the force decomposition has not been as extensively studied as that resulting due to the weighting function. The rigorous analysis in [AT10] shows that the non-uniqueness of the force decomposition is directly related to the non-uniqueness of potential energy representation. We explore this issue in more depth in Chapter 3, where we apply rigidity theory to obtain a Helmholtz-like decomposition of the atomistic stress tensor into an *irrotational* part that is independent of the potential energy representation, and a *traction-free solenoidal* part. We show that a similar decomposition of the Cauchy stress tensor can be constructed in continuum mechanics using the generalized Beltrami representation. We identify analogies between the two decompositions, and in the process obtain a strain tensor equivalent in atomistics. The Helmholtz decomposition of the atomistic stress tensor has the potential to systematically reduce the noise associated with atomistic fields, which was originally addressed using the weighting function alone.

In Chapter 4, we use the unified framework developed in [AT10] to study the energy balance equation of continuum mechanics in the context of multi-body potentials. (This work

has been published in [AT11].) In the original Irving–Kirkwood procedure, the definition for the potential part of the specific internal energy (for the special case of pair potentials in a mono-atomic system) is assumed *a priori* and the expression for the heat flux vector is then derived to ensure that the energy balance equation is identically satisfied. Unfortunately, this approach does not generalize to arbitrary multi-body potentials (or even pair potentials with multiple species types) since it involves an ambiguous definition for the "energy of an atom". To the best of the our knowledge, all the existing works (see [ZWS08, Che06, ZT04, MR83, TNO08]) which attempt to derive a microscopic definition for the heat flux in the case of multi-body potentials by generalizing the Irving–Kirkwood procedure suffer from this ambiguity. Furthermore, even for the case of pair potential interactions, the original Irving–Kirkwood approach leads to an expression for the heat flux vector which is not invariant with respect to the addition of a constant to the potential energy of the system — a result which is clearly not physically reasonable. In contrast, in the spatial averaging procedure proposed by Murdoch [MB94], the specific internal energy and heat flux vector are obtained together as part of the derivation and the resulting expressions are consistent with physical expectations. Motivated by this, in Chapter 4, we reformulate the Irving–Kirkwood procedure using Murdoch's approach [MB94]. This method leads to physically-acceptable expressions for the internal energy density and heat flux vector which are grounded in rigorous statistical mechanics principles and which do not require an arbitrary energy decomposition between the particles.

The following notation is used in this thesis. Vectors are denoted by lower case letters in bold font, while tensors of higher order are denoted by capital letters in bold font. The inner product of two vectors is given by a dot "$\cdot$", and their tensor product is given by the symbol "$\otimes$". The inner product of two second-order tensors is denoted by ":". The gradient of a vector field, $\boldsymbol{v}(\boldsymbol{x})$, is denoted by $\nabla_{\boldsymbol{x}}\boldsymbol{v}(\boldsymbol{x})$. A second-order tensor, $\boldsymbol{T}$, operating on a vector, $\boldsymbol{v}$, is denoted by $\boldsymbol{T}\boldsymbol{v}$. The divergence of a tensor field, $\boldsymbol{T}(\boldsymbol{x})$, is denoted by $\mathrm{div}_{\boldsymbol{x}}\,\boldsymbol{T}(\boldsymbol{x})$, which corresponds to $\partial \boldsymbol{T}_{ij}/\partial \boldsymbol{x}_j$ in indicial notation (with Einstein's summation convention).

The main results of this thesis are presented in Chapter 2, Chapter 3 and Chapter 4 which are written as three separate papers. (The papers in Chapters 2 and 3 are to be submitted for publication in peer-reviewed journals. The paper in Chapter 4 has already been published in the *Journal of Chemical Physics* [AT11].) We summarize our results in Chapter 5.

Chapter 2

Referential continuum fields in atomistics

2.1 Introduction

Atomistic and continuum models have been extensively used to study material behavior. Atomistic simulations can be used to construct accurate constitutive relations for continuum models, and atomistic and continuum descriptions coexist in multiscale methods that study systems with two or more length/time scales [TM11]. Both cases require an exchange of information between the atomistic and continuum models, which requires an understanding of the relationship between them.

Data in an atomistic model exists in the form of positions and velocities of particles, which has to be reinterpreted in the language of continuum mechanics. This is done by developing continuum notions for atomistic systems. Work on this dates back at least to Cauchy in the 1820s with his aim to define stress in crystalline solids. Later, Irving and Kirkwood [IK50] derived continuum fields for an atomistic system that is probabilistic in nature using principles of non-equilibrium classical statistical mechanics. More recently, Hardy [Har82, HRS02] and Murdoch [Mur82] defined continuum fields for an atomistic model using spatial averaging. From a practical viewpoint, the spatial averaging procedure of Murdoch and Hardy has been very successful, and has been extensively used in computer simulations. Although continuum fields obtained in the Murdoch–Hardy procedure or the Irving–Kirkwood procedure satisfy all the balance laws (mass, momentum and energy), they do not have the dual material and spatial description as seen in continuum mechanics.

In continuum mechanics, a reference configuration is chosen to represent a convenient fixed state of the body to which the deformed configuration is compared. Once the reference configuration is chosen, constitutive relations are described using the gradient (or higher-order gradients) of a deformation which tracks the motion of material points from the reference configuration to the deformed configuration. Therefore, the reference configuration plays an important role in defining constitutive relations in continuum mechanics. Moreover, continuum fields can be expressed *materially* on the reference configuration, or *spatially* on the deformed configuration. A material field can be obtained as a "pull-back" of the corresponding spatial field with respect to the deformation map. (See Tadmor et al. [TME12] for a discussion of material and spatial descriptions in continuum mechanics and the definitions of the terms used in this paper.)

In contrast to the continuum definitions, since the potential energy of an atomistic body is usually defined using current positions of particles, a reference configuration of particles is not needed to describe the physical properties of the system. Since the fields obtained in the Murdoch–Hardy or the Irving–Kirkwood procedures depend on the current configuration of the atomistic body, they correspond to a spatial description. In the absence of a deformation map, atomistic fields cannot be readily pulled-back to a reference configuration, which hampers the definition of constitutive relations.

The main focus of this paper is to obtain material (or referential) descriptions for atomistic fields and study their relation to the spatial fields obtained in the original Murdoch–Hardy procedure. We begin by fixing a reference configuration of particles, and show that the Murdoch–Hardy procedure can be modified to obtain pointwise continuum fields in the reference configuration using the motion of particles as a surrogate for the deformation map. Through this procedure, we obtain definitions for certain material fields such as reference density, reference momentum density, reference body field and the first Piola–Kirchhoff stress, which identically satisfy the material form of the balance laws. One of the key feature of this procedure is that these material fields are obtained without defining a deformation map.

The procedure described above does *not* yield definitions for the material descriptions of the spatial mass density and the Cauchy stress. Material fields for these quantities are obtained using a pull-back of the distributions associated with the atomistic Cauchy stress and the density fields obtained in the original Murdoch–Hardy procedure with respect to an arbitrary deformation map that tracks the particles. This results in material fields for the atomistic Cauchy stress and the mass density, that depend on the choice of the deformation

map. With these definitions, we show that the relationship between the spatial and material atomistic fields are identically satisfied in a distributional sense.

Finally, we observe the interesting fact that atomistic first Piola–Kirchhoff stress tensor does not have a kinetic contribution, which in the atomistic Cauchy stress tensor accounts for thermal fluctuations. We show that this effect is also included in the atomistic first Piola–Kirchhoff stress tensor through the motion of the particles.

The paper is organized as follows. In Section 2.2, we review the material and spatial description of fields in continuum mechanics. In Section 2.3, we obtain definitions of material and spatial fields for an atomistic system, study the relationship between them, and compare it to the relationship seen in continuum mechanics. In Section 2.4, we demonstrate the validity of the definition for the first Piola–Kirchhoff stress through a numerical example involving finite deformation of a slab containing a notch under tension. We conclude with a summary in Section 2.5.

2.2 Material and spatial description of fields in continuum mechanics

A shape or configuration of a body is represented as an open subset of $\mathbb{E}^3$, which denotes the three-dimensional Euclidean space. A reference configuration, denoted by an open set $\mathcal{B}_{\mathrm{c}}^0 \subset \mathbb{E}^3$, is chosen to represent a convenient fixed state of the body to which other configurations are compared. The subscript c in $\mathcal{B}_{\mathrm{c}}^0$ and in other variables defined for the continuum model is used to differentiate them from their analogs defined for an atomistic model in later sections. The position of an arbitrary continuum particle in the reference configuration is denoted by $\boldsymbol{X}$. A time-dependent deformation of the body is described by a C^1 continuous deformation mapping $\varphi_{\mathrm{c}} : \mathcal{B}_{\mathrm{c}}^0 \times \mathbb{R}^+ \to \mathcal{B}_{\mathrm{c}}^t$ which maps the reference configuration $\mathcal{B}_{\mathrm{c}}^0$ to a deformed configuration $\mathcal{B}_{\mathrm{c}}^t$ at time t. Thus $\boldsymbol{x}(t) = \varphi_{\mathrm{c}}(\boldsymbol{X}, t)$, where $\boldsymbol{x}(t)$ is the position at time t of the continuum particle located at $\boldsymbol{X}$ in the reference configuration.

Continuum fields defined in the reference and the deformed configuration are commonly referred to as the *material* and *spatial* fields, respectively (see for example Tadmor et al. [TME12]). The two descriptions are related to each other through the deformation mapping: $\breve{\boldsymbol{g}}_{\mathrm{c}}(\boldsymbol{X}, t) = \boldsymbol{g}_{\mathrm{c}}(\boldsymbol{\varphi}_{\mathrm{c}}(\boldsymbol{X}, t), t)$, where $\breve{\boldsymbol{g}}_{\mathrm{c}}$ denotes the material description of an arbitrary continuum field whose spatial description is denoted by $\boldsymbol{g}_{\mathrm{c}}$.[1] In addition to fields, the balance laws of continuum mechanics can also be described in the reference or the deformed

[1] In mathematics, $\breve{\boldsymbol{g}}_{\mathrm{c}}$ is referred to as the *pull-back* of $\boldsymbol{g}_{\mathrm{c}}$ with respect to the deformation map $\boldsymbol{\varphi}_{\mathrm{c}}$.

configurations. For example, the continuity equation (conservation of mass) in the deformed configuration is given by

$$\frac{\partial \rho_{\mathrm{c}}}{\partial t} + \operatorname{div}_{\boldsymbol{x}}(\rho_{\mathrm{c}} \boldsymbol{v}_{\mathrm{c}}) = 0, \tag{2.2.1}$$

where ρ_{c} and $\boldsymbol{v}_{\mathrm{c}}$ denote the spatial mass density and the velocity fields, respectively. The velocity field $\boldsymbol{v}_{\mathrm{c}}$ is related to the deformation mapping $\breve{\boldsymbol{v}}_{\mathrm{c}} = \dot{\boldsymbol{\varphi}}_{\mathrm{c}}(\boldsymbol{X}, t)$. The continuity equation in the reference configuration is given by

$$\mathring{\rho}_{\mathrm{c}} = J_{\mathrm{c}} \breve{\rho}_{\mathrm{c}}, \tag{2.2.2}$$

where $\mathring{\rho}_{\mathrm{c}}$ is the *reference mass density* which is independent of time, $J_{\mathrm{c}} = \det \boldsymbol{F}_{\mathrm{c}}$, and $\boldsymbol{F}_{\mathrm{c}} = \nabla_{\boldsymbol{X}} \boldsymbol{\varphi}_{\mathrm{c}}$ is the deformation gradient.

The equations of motion in the deformed configuration are given by

$$\operatorname{div}_{\boldsymbol{x}} \boldsymbol{\sigma}_{\mathrm{c}} + \rho_{\mathrm{c}} \boldsymbol{b}_{\mathrm{c}} = \frac{\partial (\rho_{\mathrm{c}} \boldsymbol{v}_{\mathrm{c}})}{\partial t} + \operatorname{div}_{\boldsymbol{x}}(\rho_{\mathrm{c}} \boldsymbol{v}_{\mathrm{c}} \otimes \boldsymbol{v}_{\mathrm{c}}), \tag{2.2.3}$$

where $\boldsymbol{\sigma}_{\mathrm{c}}$ denotes the Cauchy stress and $\boldsymbol{b}_{\mathrm{c}}$ denotes the body force field. In the reference configuration the equations of motion are

$$\operatorname{div}_{\boldsymbol{X}} \boldsymbol{P}_{\mathrm{c}} + \mathring{\rho}_{\mathrm{c}} \breve{\boldsymbol{b}}_{\mathrm{c}} = \mathring{\rho}_{\mathrm{c}} \breve{\boldsymbol{a}}_{\mathrm{c}}, \tag{2.2.4}$$

where $\boldsymbol{P}_{\mathrm{c}}$ denotes the first Piola–Kirchhoff stress tensor, and $\breve{\boldsymbol{a}}_{\mathrm{c}} = \ddot{\boldsymbol{\varphi}}_{\mathrm{c}}(\boldsymbol{X}, t)$ denotes the material acceleration field. The relationship between the first Piola–Kirchhoff stress tensor and the Cauchy stress tensor is given by

$$\boldsymbol{P}_{\mathrm{c}}(\boldsymbol{X}, t) = J_{\mathrm{c}} \breve{\boldsymbol{\sigma}}_{\mathrm{c}} \boldsymbol{F}_{\mathrm{c}}^{-\mathrm{T}}. \tag{2.2.5}$$

In the next section, we discuss the material and spatial descriptions of continuum fields for atomistic systems.

2.3 Material and spatial descriptions of continuum fields in atomistics

Continuum fields for atomistic systems can be obtained using the Irving–Kirkwood [IK50] or Murdoch–Hardy [Har82, HRS02, MB93] procedures. The former is used for a probabilistic system, while the latter is used for a deterministic system. The Murdoch–Hardy procedure is often used in practice because most numerical experiments, carried out in the

form of molecular statistics or molecular dynamics, are deterministic in nature. For the purpose of this paper, we use the Murdoch–Hardy framework, although a similar procedure can be carried out for the Irving–Kirkwood framework.

An atomistic body is modeled as a collection of N classical interacting point particles. We use the notation m_α, $\boldsymbol{x}_\alpha$ and $\boldsymbol{v}_\alpha$ to denote the mass, position and velocity of particle α, respectively. A configuration of the atomistic body is given by the positions of particles in $\mathbb{E}^3$. A reference configuration is chosen to represent a fixed state of the atomistic body to which other configurations can be compared. The position of an arbitrary particle α in the reference configuration is denoted by $\boldsymbol{X}_\alpha$. A time-dependent deformation of the atomistic body is described by a C^1 continuous deformation mapping $\boldsymbol{\varphi}(\cdot, t)$, which maps the position $\boldsymbol{X}_\alpha$ of an arbitrary particle in the reference configuration to a position $\boldsymbol{x}_\alpha$ in the deformed configuration at time t. (The nature of this mapping is the subject of discussion below.) The velocity of a particle α at time t is then given by

$$\boldsymbol{v}_\alpha(t) = \dot{\boldsymbol{\varphi}}(\boldsymbol{X}_\alpha, t). \tag{2.3.1}$$

We assume that the particles interact through a potential energy function

$$\mathcal{V} = \mathcal{V}(\boldsymbol{x}_1, \ldots, \boldsymbol{x}_N), \tag{2.3.2}$$

which is divided into two parts, an *internal* part $\mathcal{V}_{\text{int}}$ associated with short-range particle interactions, and an *external* part $\mathcal{V}_{\text{ext}}$ associated with long-range interactions. For the remainder of this paper, we assume $\mathcal{V}_{\text{ext}} = 0$. The force on particle α is given by

$$\boldsymbol{f}_\alpha = -\nabla_{\boldsymbol{x}_\alpha} \mathcal{V}. \tag{2.3.3}$$

Continuum fields can now be obtained using the Murdoch–Hardy procedure.

2.3.1 A brief description of the Murdoch–Hardy procedure

In the Murdoch–Hardy procedure, continuum fields are defined as direct spatial averages of microscopic variables. The spatial averaging is performed with respect to a weighting function $w : \mathbb{R}^3 \to \mathbb{R}^+$ that has a compact support and satisfies the normalization condition, $\int_{\mathbb{R}^3} w = 1$. For example, the density, momentum density, and the body force fields are

defined as

$$\rho_w(\boldsymbol{x},t) := \sum_\alpha m_\alpha w(\boldsymbol{x}-\boldsymbol{x}_\alpha), \tag{2.3.4}$$

$$\boldsymbol{p}_w(\boldsymbol{x},t) := \sum_\alpha m_\alpha \boldsymbol{v}_\alpha w(\boldsymbol{x}-\boldsymbol{x}_\alpha), \tag{2.3.5}$$

$$\boldsymbol{b}_w(\boldsymbol{x},t) := \sum_\alpha \boldsymbol{b}_\alpha w(\boldsymbol{x}-\boldsymbol{x}_\alpha), \tag{2.3.6}$$

where α ranges from 1 to N, and the subscript w on the left indicates the role of the weighting function. The body force $\boldsymbol{b}_\alpha$ in (2.3.6) is defined as $\boldsymbol{b}_\alpha := -\nabla_{\boldsymbol{x}_\alpha}\mathcal{V}_{\text{ext}}$. Since we have assumed $\mathcal{V}_{\text{ext}} = 0$ for the purpose of this presentation, it follows that $\boldsymbol{b}_w = \boldsymbol{0}$. The velocity field $\boldsymbol{v}_w$ is defined as

$$\boldsymbol{v}_w(\boldsymbol{x},t) := \begin{cases} \dfrac{\boldsymbol{p}_w}{\rho_w}(\boldsymbol{x},t), & \text{if } \rho_w(\boldsymbol{x},t) \neq 0, \\ \boldsymbol{0} & \text{otherwise.} \end{cases} \tag{2.3.7}$$

In order to obtain a definition for the atomistic Cauchy stress tensor, the definitions given in (2.3.4) and (2.3.7) are substituted into the equations of motion (see (2.2.3)) to obtain an expression in divergence form, given by

$$\operatorname{div}_{\boldsymbol{x}} \boldsymbol{\sigma}_w(\boldsymbol{x},t) = \sum_\alpha \boldsymbol{f}_\alpha w(\boldsymbol{x}_\alpha - \boldsymbol{x}) - \operatorname{div}_{\boldsymbol{x}} \sum_\alpha m_\alpha (\boldsymbol{v}_\alpha^{\text{rel}} \otimes \boldsymbol{v}_\alpha^{\text{rel}}) w(\boldsymbol{x}-\boldsymbol{x}_\alpha), \tag{2.3.8}$$

where $\boldsymbol{f}_\alpha$ is defined in (2.3.3), and $\boldsymbol{v}_\alpha^{\text{rel}}(\boldsymbol{x},t) := \boldsymbol{v}_\alpha(t) - \boldsymbol{v}_w(\boldsymbol{x},t)$. From (2.3.8), it is clear that the atomistic Cauchy stress tensor has two contributions:

$$\boldsymbol{\sigma}_w = \boldsymbol{\sigma}_{w,v} + \boldsymbol{\sigma}_{w,\text{k}}, \tag{2.3.9}$$

where $\boldsymbol{\sigma}_{w,v}$ and $\boldsymbol{\sigma}_{w,\text{k}}$ are commonly referred to as the *potential* and *kinetic* parts of the stress tensor, respectively. The kinetic part, is given by

$$\boldsymbol{\sigma}_{w,\text{k}}(\boldsymbol{x},t) = -\sum_\alpha m_\alpha (\boldsymbol{v}_\alpha^{\text{rel}} \otimes \boldsymbol{v}_\alpha^{\text{rel}}) w(\boldsymbol{x}_\alpha - \boldsymbol{x}), \tag{2.3.10}$$

and the potential part of the stress tensor satisfies the equation

$$\operatorname{div}_{\boldsymbol{x}} \boldsymbol{\sigma}_{w,v}(\boldsymbol{x},t) = \sum_\alpha \boldsymbol{f}_\alpha w(\boldsymbol{x}-\boldsymbol{x}_\alpha). \tag{2.3.11}$$

Clearly, there are many candidates for $\boldsymbol{\sigma}_{w,v}$ that satisfy (2.3.11). The most commonly used definition for $\boldsymbol{\sigma}_{w,v}$ that satisfies (2.3.11) is given by[2]

$$\boldsymbol{\sigma}_{w,v}(\boldsymbol{x},t) = \sum_{\substack{\alpha,\beta \\ \alpha<\beta}} -\boldsymbol{f}_{\alpha\beta} \otimes (\boldsymbol{x}_\alpha - \boldsymbol{x}_\beta) b(\boldsymbol{x}, \boldsymbol{x}_\alpha, \boldsymbol{x}_\beta), \tag{2.3.12}$$

where $\sum_{\substack{\alpha,\beta \\ \alpha<\beta}} \equiv \sum_{\alpha=1}^{N-1} \sum_{\beta=\alpha+1}^{N}$, b is the bond function defined by

$$b(\boldsymbol{x}, \boldsymbol{x}_\alpha, \boldsymbol{x}_\beta) := \int_{s=0}^{1} w((1-s)\boldsymbol{x}_\alpha + s\boldsymbol{x}_\beta - \boldsymbol{x})\, ds, \tag{2.3.13}$$

and the forces $\boldsymbol{f}_{\alpha\beta}$ satisfy the conditions

$$\sum_{\beta} \boldsymbol{f}_{\alpha\beta} = \boldsymbol{f}_\alpha, \tag{2.3.14a}$$

$$\boldsymbol{f}_{\alpha\beta} = -\boldsymbol{f}_{\beta\alpha}. \tag{2.3.14b}$$

If in addition, the forces $\boldsymbol{f}_{\alpha\beta}$ are assumed to be central (i.e. $f_{\alpha\beta} \parallel \boldsymbol{x}_\beta - \boldsymbol{x}_\alpha$), then the resulting stress tensor is always symmetric. Although $\boldsymbol{\sigma}_{w,v}$ is commonly referred to as the Hardy stress tensor, we refer to it as the Cauchy–Hardy stress tensor to differentiate it from the referential stress tensors defined later. We also note that the fields ρ_w, $\boldsymbol{p}_w$, and $\boldsymbol{\sigma}_{w,v}$ obtained in the Murdoch–Hardy procedure can be written as a convolution[3] of the

[2]The expression for $\boldsymbol{\sigma}_{w,v}$ given in (2.3.12) is obtained from (2.3.11) in two steps. In the first step, each force $\boldsymbol{f}_\alpha$ is decomposed into forces $\boldsymbol{f}_{\alpha\beta}$ such that (2.3.14) is satisfied, to obtain

$$\operatorname{div}_{\boldsymbol{x}} \boldsymbol{\sigma}_{w,v} = \sum_{\substack{\alpha,\beta \\ \alpha<\beta}} \boldsymbol{f}_{\alpha\beta} w(\boldsymbol{x} - \boldsymbol{x}_\alpha).$$

In the second step, the right-hand-side of the above equation is recast as an integral of an anti-symmetric function, from which (2.3.12) is obtained followed by an application of Nolls lemma [Nol55]. See [AT10] for a derivation of various other definitions of $\boldsymbol{\sigma}_{w,v}$ such as the virial, Tsai or the doubly-averaged stress tensor, and [AT14] for a discussion on the non-uniqueness of the atomistic Cauchy stress tensor, and its interpretation from a continuum mechanics viewpoint.

[3]See [Hör90] for the formal definition of a convolution of a function with a distribution. Here, we do not require such a general definition since algebra on a Dirac-delta distribution can be carried out as if it were a function. Therefore we use the following definition for the convolution of two smooth functions u and v that have a compact support in $\mathbb{R}^3$,

$$u \star v(\boldsymbol{x}) := \int_{\mathbb{R}^3} u(\boldsymbol{x} - \boldsymbol{y}) v(\boldsymbol{y})\, d\boldsymbol{y},$$

where v is replaced by the Dirac-delta distribution.

weighting function w with a corresponding distribution[4]. In other words,

$$\rho_w(\boldsymbol{x},t) = w \star \rho, \quad \boldsymbol{p}_w(\boldsymbol{x},t) = w \star \boldsymbol{p}, \quad \boldsymbol{\sigma}_{w,v}(\boldsymbol{x},t) = w \star \boldsymbol{\sigma}_{\mathrm{v}}, \tag{2.3.15}$$

where $\star$ denotes the convolution operator, and the distributions ρ and $\boldsymbol{p}$ are given by

$$\rho(\boldsymbol{x},t) = \sum_{\alpha} m_\alpha \delta(\boldsymbol{x} - \boldsymbol{x}_\alpha), \tag{2.3.16}$$

$$\boldsymbol{p}(\boldsymbol{x},t) = \sum_{\alpha} m_\alpha \boldsymbol{v}_\alpha \delta(\boldsymbol{x} - \boldsymbol{x}_\alpha) \tag{2.3.17}$$

respectively,with support[5] on the current configuration of the particles $\{\boldsymbol{x}_\alpha : \alpha = 1, \dots, N\}$. Further, $\boldsymbol{\sigma}_v$ in (2.3.15) is a distribution given by

$$\boldsymbol{\sigma}_v(\boldsymbol{x},t) = \sum_{\substack{\alpha,\beta \\ \alpha<\beta}} -\boldsymbol{f}_{\alpha\beta} \otimes (\boldsymbol{x}_\alpha - \boldsymbol{x}_\beta) \int_{s=0}^{1} \delta((1-s)\boldsymbol{x}_\alpha + s\boldsymbol{x}_\beta - \boldsymbol{x})\, ds, \tag{2.3.18}$$

with support on the *current bonds* of the system, where a current bond refers to a line joining any pair of particles α and β in the deformed configuration, such that $\boldsymbol{f}_{\alpha\beta} \neq \boldsymbol{0}$. Therefore, the support of $\boldsymbol{\sigma}_v$ is given by

$$\bigcup_{\substack{\alpha,\beta: \\ \boldsymbol{f}_{\alpha\beta}\neq\boldsymbol{0}}} \{s\boldsymbol{x}_\alpha + (1-s)\boldsymbol{x}_\beta : s \in [0,1]\}. \tag{2.3.19}$$

By writing the spatially-averaged fields ρ_w, $\boldsymbol{p}_w$ and $\boldsymbol{\sigma}_{w,v}$ in convolution form, we are able to separate out the role of the weighting function, and thereby arrive at distributions ρ, $\boldsymbol{p}$ and $\boldsymbol{\sigma}$, which by definition exist without reference to a weighting function. It is important to note that the fields $\boldsymbol{v}_w$ and $\boldsymbol{\sigma}_{w,\mathrm{k}}$ cannot be written in a convolution form, or in other words, their corresponding distributions do not exist. Since the continuum fields obtained in the Murdoch–Hardy procedure depend on the positions and velocities of particles in the deformed configuration of the atomistic body, they correspond to a spatial description. One of our goals in this paper is to obtain a material description of continuum fields that appear in the equations of motion expressed in the reference configuration (see (2.2.4)). This includes the reference density $\mathring{\rho}$, and the first Piola–Kirchhoff stress tensor $\boldsymbol{P}$. The distributions defined in (2.3.15) will play an important role in obtaining the material definitions

[4] A distribution is a linear map from the space of smooth functions with compact support to the real line $\mathbb{R}$.

[5] Intuitively, the support of a distribution is the closed set on which the distribution is "concentrated". See [Hör90] for a rigorous definition.

of continuum fields for atomistics. Recall from Section 2.2, a material field in continuum mechanics is obtained as a pull-back of the spatial field with respect to the deformation map. In the next section, we discuss the idea of pulling-back the spatial fields obtained in Murdoch–Hardy procedure in order to arrive at definitions for $\mathring{\rho}$ and $\boldsymbol{P}$.

2.3.2 A notion of a material point in atomistics

In continuum mechanics, material fields are obtained as a pull-back of the spatial fields with respect to the deformation mapping. In order to pull-back the spatial fields obtained in Section 2.3.1, we need a continuum deformation mapping that maps an open subset, representing the reference configuration of the atomistic body, to an open subset representing the deformed configuration. In other words, we need a definition for the shape of the atomistic body. [Mur06] proposed a definition for the shape of the body at time t, given by

$$\mathcal{B}_w^t := \{\boldsymbol{x} \in \mathbb{R}^3 : \rho_w(\boldsymbol{x}, t) \neq 0\}. \tag{2.3.20}$$

Clearly, the set given in (2.3.20) is an open set that includes the positions of all the particles of the system. In addition, Murdoch proposed a deformation mapping based on his interpretation of a material point for atomistic systems. (We describe this approach here, but adopt a different line of reasoning in our own work as explained below.) According to Murdoch, an arbitrary point $\boldsymbol{X} \in \mathcal{B}_w^0$ defines the position of a material point in the continuum associated with the reference configuration of the atomistic body. As the atomistic body evolves from its reference configuration, the corresponding continuum body $\mathcal{B}_w^0$ evolves to $\mathcal{B}_w^t$ at time t. An evolution for a material point $\boldsymbol{X} \in \mathcal{B}_w^0$ is given by a mapping $\hat{\boldsymbol{\varphi}}_w(\cdot, t) : \mathcal{B}_w^0 \to \mathbb{R}^3$ that satisfies the ordinary differential equation

$$\dot{\hat{\boldsymbol{\varphi}}}_w(\boldsymbol{X}, t) = \boldsymbol{v}_w(\hat{\boldsymbol{\varphi}}_w(\boldsymbol{X}, t), t), \tag{2.3.21a}$$

$$\hat{\boldsymbol{\varphi}}_w(\boldsymbol{X}, 0) = \boldsymbol{X}, \tag{2.3.21b}$$

where $\boldsymbol{v}_w$ defined in (2.3.7), depends on the evolution of the atomistic body. A solution to the evolution equation given in (2.3.21) has the following interpretation: $\hat{\boldsymbol{\varphi}}_w(\boldsymbol{X}, t)$ gives the position of a material point that started at $\boldsymbol{X}$ at time $t = 0$. The velocity of a material point, positioned at $\hat{\boldsymbol{\varphi}}_w(\boldsymbol{X}, t)$ at time time t is equal to a local spatial average of velocities of the particles in the neighborhood of $\hat{\boldsymbol{\varphi}}_w(\boldsymbol{X}, t)$, given by $\boldsymbol{v}_w(\hat{\boldsymbol{\varphi}}_w(\boldsymbol{X}, t), t)$. It is important to note that $\hat{\boldsymbol{\varphi}}_w$ does not track the motion of particles, i.e. we do not necessarily have the

equality $\hat{\boldsymbol{\varphi}}_w(\boldsymbol{X}_\alpha, t) = \boldsymbol{x}_\alpha$.

If the above differential equation has a solution, then we can obtain a material description for the continuum fields defined in Section 2.2, by pulling-back the spatial fields obtained in Section 2.3.1 with respect to the deformation mapping $\hat{\boldsymbol{\varphi}}_w$. We *do not* follow this approach for the following reasons. First, it is not a priori clear under what conditions the solution $\hat{\boldsymbol{\varphi}}_w$ maps the set $\mathcal{B}_w^0$ to $\mathcal{B}_w^t$. Second, the solution to (2.3.21) not only depends on the initial and final configuration of the atomistic body, but also depends on the path traversed by the atomistic body. For example, consider a non-trivial deformation of the atomistic body indexed by time $t \in [0, 1]$, such that the $\boldsymbol{x}_\alpha(1) = \boldsymbol{x}_\alpha(0) = \boldsymbol{X}_\alpha$. In other words, the system is deformed and brought back to its original configuration. Using the field $\boldsymbol{v}_w$ generated by this deformation in solving (2.3.21), results in a deformation $\hat{\boldsymbol{\varphi}}_w$ that does not necessarily satisfy the condition $\hat{\boldsymbol{\varphi}}_w(\boldsymbol{X}, 0) = \hat{\boldsymbol{\varphi}}_w(\boldsymbol{X}, 1)$ because $\hat{\boldsymbol{\varphi}}$ does not track the motion of particles. Finally, from a practical point of view, solving (2.3.21) can be computationally expensive. In the next section, we show that definitions for certain material fields ($\mathring{\rho}$, $\breve{\boldsymbol{v}}$ and $\boldsymbol{P}$) can be obtained without defining a deformation mapping for the continuum associated with the atomistic body. These definitions satisfy the equations of motion given in (2.2.4).

2.3.3 Murdoch–Hardy procedure in the reference configuration

In analogy to Section 2.3.1, we define the reference density field $\mathring{\rho}_w$, momentum density field[6] $\mathring{\rho}_w \breve{\boldsymbol{v}}_w$, and the body force field $\breve{\boldsymbol{b}}_w$ as

$$\mathring{\rho}_w(\boldsymbol{X}, t) := \sum_\alpha m_\alpha w(\boldsymbol{X} - \boldsymbol{X}_\alpha), \tag{2.3.22}$$

$$\mathring{\rho}_w \breve{\boldsymbol{v}}_w(\boldsymbol{X}, t) := \sum_\alpha m_\alpha \boldsymbol{v}_\alpha w(\boldsymbol{X} - \boldsymbol{X}_\alpha), \tag{2.3.23}$$

$$\breve{\boldsymbol{b}}_w(\boldsymbol{X}, t) := \sum_\alpha \boldsymbol{b}_\alpha w(\boldsymbol{X} - \boldsymbol{X}_\alpha). \tag{2.3.24}$$

We note the following: (1) since $\boldsymbol{X}_\alpha$ is independent of time, so is $\mathring{\rho}$; (2) Although $\breve{\boldsymbol{v}}_w$ defined in (2.3.23) is not strictly a pull-back of $\boldsymbol{v}_w$, we use the notation of a pull-back for a reason that will be motivated in the next section.

Substituting the definitions given in (2.3.22) and (2.3.23) into the material description of the equations of motion (cf. (2.2.4)),

$$\operatorname{div}_{\boldsymbol{x}} \boldsymbol{P}_w + \mathring{\rho}_w \breve{\boldsymbol{b}}_w = \mathring{\rho}_w \breve{\boldsymbol{a}}_w, \tag{2.3.25}$$

[6]Similar to the definition of $\boldsymbol{v}_w$ in (2.3.7), $\breve{\boldsymbol{v}}_w$ given in (2.3.23), is defined to be zero whenever $\mathring{\rho} = 0$.

and invoking our assumption $\boldsymbol{b}_\alpha = \mathbf{0}$, we obtain an expression for the divergence of the spatially-averaged first Piola–Kirchhoff stress tensor:

$$\operatorname{div}_{\boldsymbol{X}} \boldsymbol{P}_w = \sum_\alpha \boldsymbol{f}_\alpha w(\boldsymbol{X} - \boldsymbol{X}_\alpha). \tag{2.3.26}$$

Since the right-hand side of (2.3.26) and (2.3.11) are of the same form, we arrive at the following definition for the atomistic first Piola–Kirchhoff stress:

$$\boldsymbol{P}_w(\boldsymbol{X}, t) = \sum_{\substack{\alpha,\beta \\ \alpha<\beta}} -\boldsymbol{f}_{\alpha\beta} \otimes (\boldsymbol{X}_\alpha - \boldsymbol{X}_\beta) b(\boldsymbol{X}, \boldsymbol{X}_\alpha, \boldsymbol{X}_\beta), \tag{2.3.27}$$

where the scalar bonding function b is defined in (2.3.13). We note some interesting features of the definition given in (2.3.27):

1. Since $\boldsymbol{f}_{\alpha\beta} \nparallel (\boldsymbol{X}_\alpha - \boldsymbol{X}_\beta)$, $\boldsymbol{P}_w$ is non-symmetric.
2. Unlike the atomistic Cauchy stress, which has an additive decomposition into potential and kinetic parts, the atomistic first Piola–Kirchhoff stress only has a potential part. The dependence of $\boldsymbol{P}_w$ on thermal vibrations enters through the term $\boldsymbol{f}_{\alpha\beta}$, since $\boldsymbol{X}_\alpha$ in (2.3.27) is independent of time.

The spatially-averaged quantities in (2.3.22), (2.3.23) and (2.3.27) can be written in convolution form as

$$\mathring{\rho}_w(\boldsymbol{X}) = w \star \mathring{\rho}, \quad \mathring{\rho}_w \breve{\boldsymbol{v}}_w(\boldsymbol{X}, t) = w \star \mathring{\boldsymbol{p}}, \quad \boldsymbol{P}_w(\boldsymbol{X}, t) = w \star \boldsymbol{P}, \tag{2.3.28}$$

where $\mathring{\rho}$ and $\mathring{\boldsymbol{p}}$ are distributions given by

$$\mathring{\rho}(\boldsymbol{X}) = \sum_\alpha m_\alpha \delta(\boldsymbol{X} - \boldsymbol{X}_\alpha), \tag{2.3.29}$$

$$\mathring{\boldsymbol{p}}(\boldsymbol{X}, t) = \sum_\alpha m_\alpha \boldsymbol{v}_\alpha \delta(\boldsymbol{X} - \boldsymbol{X}_\alpha), \tag{2.3.30}$$

with support on the reference configuration of the particles $\{\boldsymbol{X}_\alpha : \alpha = 1, \dots, N\}$, and $\boldsymbol{P}$ is a distribution given by

$$\boldsymbol{P}(\boldsymbol{X}, t) = \sum_{\substack{\alpha,\beta \\ \alpha<\beta}} -\boldsymbol{f}_{\alpha\beta} \otimes (\boldsymbol{X}_\alpha - \boldsymbol{X}_\beta) \int_{s=0}^{1} \delta((1-s)\boldsymbol{X}_\alpha + s\boldsymbol{X}_\beta - \boldsymbol{X})\, ds, \tag{2.3.31}$$

with support on the *reference bonds* of the system. We define a "reference bond" as a line joining any pair of particles α and β in the reference configuration, such that $\boldsymbol{f}_{\alpha\beta} \neq \boldsymbol{0}$. Since $\boldsymbol{f}_{\alpha\beta}$ is calculated using the current configuration of particles, the reference bonds change with time. Therefore, the support of $\boldsymbol{P}$ is given by

$$\bigcup_{\substack{\alpha,\beta:\\ \boldsymbol{f}_{\alpha\beta}\neq\boldsymbol{0}}} \{s\boldsymbol{X}_\alpha + (1-s)\boldsymbol{X}_\beta : s \in [0,1]\}. \tag{2.3.32}$$

From the above derivation, we see that the material fields $\mathring{\rho}_w$, $\breve{\boldsymbol{v}}_w$ and $\boldsymbol{P}_w$ can be obtained using the Murdoch–Hardy procedure without explicitly defining a deformation mapping for the continuum $\mathcal{B}_w^0$. In the next section, we explore the relations between these referential measures and the spatial measures obtained in Section 2.3.1. This will lead to definitions for the pull-back fields $\breve{\rho}_w$ and $\breve{\boldsymbol{\sigma}}_w$.

2.3.4 Relationship between material and spatial fields in atomistics

Our objective in this section is to show that the continuum relations between $\breve{\rho}_{\mathrm{c}}$ and $\mathring{\rho}_{\mathrm{c}}$ defined in (2.2.2), and $\breve{\boldsymbol{\sigma}}_{\mathrm{c}}$ and $\boldsymbol{P}_{\mathrm{c}}$ defined in (2.2.5), also hold in atomistics in the sense of distributions. In order to arrive at these relations, we intend to pull-back the distributions ρ and $\boldsymbol{\sigma}$, defined in (2.3.16) and (2.3.18), with respect to a C^1 deformation mapping $\boldsymbol{\varphi}(\cdot,t) : \mathcal{B}_w^0 \to \mathbb{R}^3$, that tracks the motion of the particles, such that[7]

$$\boldsymbol{\varphi}(\boldsymbol{X}_\alpha, t) = \boldsymbol{x}_\alpha. \tag{2.3.33}$$

The mapping $\boldsymbol{\varphi}$ need not be continuous in time. We note that one such mapping always exists. This can be obtained by using a Delaunay triangulation on the reference configuration and fitting a C^1 function on the resulting mesh to the data $\boldsymbol{\varphi}(\boldsymbol{X}_\alpha, t)$. Although the condition given in (2.3.33) does not result in a unique $\boldsymbol{\varphi}$, we show below that certain distributions, such as ρ and $\boldsymbol{P}$, are independent of the choice of $\boldsymbol{\varphi}$.

2.3.4.1 Relationship between ρ and $\mathring{\rho}$

In this section, we study the relationship between the distributions ρ and $\mathring{\rho}$ defined in (2.3.16) and (2.3.29). From continuum mechanics, we know that $\mathring{\rho}_{\mathrm{c}}$ is related to the pull-back of ρ_{c} through (2.2.2). We will now show that a similar relationship holds for the distributions $\mathring{\rho}$ and $\breve{\rho}$, where $\breve{\rho}$ is defined as the pull-back of the distribution ρ with respect

[7] Recall that (2.3.33) is not satisfied by the deformation mapping $\hat{\boldsymbol{\varphi}}_w$ defined in Section 2.3.2.

to the map $\boldsymbol{\varphi}$:

$$\breve{\rho}(\boldsymbol{X},t) := \sum_{\alpha} m_\alpha \delta(\boldsymbol{\varphi}(\boldsymbol{X},t) - \boldsymbol{x}_\alpha). \tag{2.3.34}$$

Similarly, we define the pull-back of the momentum density distribution $\boldsymbol{p}$ as

$$\breve{\boldsymbol{p}}(\boldsymbol{X},t) := \sum_{\alpha} m_\alpha \boldsymbol{v}_\alpha \delta(\boldsymbol{\varphi}(\boldsymbol{X},t) - \boldsymbol{x}_\alpha). \tag{2.3.35}$$

Theorem 1. *For a mapping $\boldsymbol{\varphi} : \mathcal{B}_w^0 \to \mathcal{B}_w^t \times \mathbb{R}^+$ that satisfies (2.3.33), we have*

$$J\breve{\rho}(\boldsymbol{X},t) = \mathring{\rho}, \tag{2.3.36}$$

$$J\breve{\boldsymbol{p}}(\boldsymbol{X},t) = \mathring{\boldsymbol{p}}, \tag{2.3.37}$$

where $J(\boldsymbol{X},t) := \det \nabla_{\boldsymbol{X}} \boldsymbol{\varphi}(\boldsymbol{X},t)$.

Proof. Equation (2.3.36) is satisfied if and only if

$$w \star (J\breve{\rho}) = w \star \mathring{\rho}, \tag{2.3.38}$$

for all smooth functions w with a compact support. This can be shown as follows:

$$\begin{aligned} w \star (J\breve{\rho})(\boldsymbol{X},t) &= \sum_{\alpha} \int_{\mathbb{R}^3} m_\alpha w(\boldsymbol{X}-\boldsymbol{Y}) \delta(\boldsymbol{\varphi}(\boldsymbol{Y},t) - \boldsymbol{x}_\alpha) J(\boldsymbol{Y})\, d\boldsymbol{Y} \\ &= \sum_{\alpha} \int_{\mathbb{R}^3} m_\alpha w(\boldsymbol{X} - \boldsymbol{\varphi}^{-1}(\boldsymbol{y},t)) \delta(\boldsymbol{y} - \boldsymbol{x}_\alpha)\, d\boldsymbol{y} \\ &= \sum_{\alpha} m_\alpha w(\boldsymbol{X} - \boldsymbol{X}_\alpha) \\ &= w \star \mathring{\rho}(\boldsymbol{X}), \end{aligned}$$

where we have performed a change of variable from $\boldsymbol{Y}$ to $\boldsymbol{y}$ $(= \boldsymbol{\varphi}(\boldsymbol{Y},t))$ in the second equality, followed by the substitution $\boldsymbol{\varphi}^{-1}(\boldsymbol{x}_\alpha,t) = \boldsymbol{X}_\alpha$ in the third equality. Equation (2.3.37) follows from a similar argument. □

From (3.39) and (3.40), we note that although the distributions $\breve{\rho}$ and $\breve{\boldsymbol{p}}$ depend on the choice of $\boldsymbol{\varphi}$, the distributions $J\breve{\rho}$ and $J\breve{\boldsymbol{p}}$ are independent of it. We also make the following observations regarding the relationship between the spatial and material fields defined in this section by comparing them to their analogs in continuum mechanics.

1. Although $\breve{\rho}_w$ and $\breve{\boldsymbol{p}}_w$ are obtained by convolving w with the pull-back of distributions ρ and $\boldsymbol{p}$ respectively, Theorem 1 *does not* imply $\breve{\rho}_w = \rho_w(\boldsymbol{\varphi}(\boldsymbol{X}))$, or $\breve{\boldsymbol{p}}_w = \boldsymbol{p}_w(\boldsymbol{\varphi}(\boldsymbol{X}))$.

2. The relation given in Theorem 1 *does not* generally imply that $J\breve{\rho}_w = \mathring{\rho}_w$. This relation only holds if $\boldsymbol{\varphi}$ is a uniform deformation mapping. This follows from (2.3.38), and the equality $w\star(J\breve{\rho}) = J(w\star\breve{\rho})$, where J is now a constant. Similarly, $J\breve{\boldsymbol{p}}_w = \mathring{\boldsymbol{p}}_w$ for a uniform deformation mapping $\boldsymbol{\varphi}$.

3. The nearest equivalent of (3.40) in continuum mechanics is given by

$$\mathring{\rho}_{\mathrm{c}}\breve{\boldsymbol{v}}_{\mathrm{c}} = J_{\mathrm{c}}\breve{\rho}_{\mathrm{c}}\breve{\boldsymbol{v}}_{\mathrm{c}}. \tag{2.3.39}$$

   Compared with the analogy between (2.2.2) and (2.3.36), the analogy between (2.3.39) and (2.3.37) is not perfect since we do not have a distributional definition for $\breve{\boldsymbol{v}}$.

2.3.4.2 Relationship between the atomistic Piola–Kirchhoff and Cauchy stresses

In this section, we study the relationship between the distributions $\boldsymbol{P}$ and $\boldsymbol{\sigma}$ defined in (2.3.31) and (2.3.18), respectively. From continuum mechanics, we know that $\boldsymbol{P}$ is related to the pull-back of $\boldsymbol{\sigma}$ through (2.2.5). We now show that a similar relationship holds between the distributions $\boldsymbol{P}$ and $\breve{\boldsymbol{\sigma}}_v$, where $\breve{\boldsymbol{\sigma}}_v$ is defined as the pull-back of the distribution $\boldsymbol{\sigma}_v$ with respect to the mapping $\boldsymbol{\varphi}$:

$$\breve{\boldsymbol{\sigma}}_v(\boldsymbol{X}, t) = \boldsymbol{\sigma}_v(\boldsymbol{\varphi}(\boldsymbol{X}, t), t). \tag{2.3.40}$$

Theorem 2. *For a mapping $\boldsymbol{\varphi} : \mathcal{B}_w^0 \to \mathcal{B}_w^t \times \mathbb{R}^+$ that satisfies (2.3.33), we have*

$$\boldsymbol{P}^{\mathrm{G}}(\boldsymbol{X}, t) = J\breve{\boldsymbol{\sigma}}_v\boldsymbol{F}^{-\mathrm{T}}, \tag{2.3.41}$$

where $J(\boldsymbol{X}, t) := \det \boldsymbol{F}$, $\boldsymbol{F}(\boldsymbol{X}, t) = \nabla_{\boldsymbol{X}}\boldsymbol{\varphi}$, and

$$\boldsymbol{P}^{\mathrm{G}}(\boldsymbol{X}, t) := \sum_{\substack{\alpha,\beta \\ \alpha<\beta}} \boldsymbol{f}_{\alpha\beta} \otimes \int_{s=0}^{1} \delta((\boldsymbol{\varphi}^{-1} \circ \boldsymbol{\Upsilon}_{\alpha\beta})(s, t) - \boldsymbol{X})(\boldsymbol{\varphi}^{-1} \circ \boldsymbol{\Upsilon}_{\alpha\beta})'(s, t)\, ds, \tag{2.3.42}$$

where $\boldsymbol{\Upsilon}_{\alpha\beta}(s, t) = (1 - s)\boldsymbol{x}_\alpha + s\boldsymbol{x}_\beta$, represents a point indexed by s on the line joining particles α and β at time t, $(\boldsymbol{\varphi}^{-1}\circ\boldsymbol{\Upsilon}_{\alpha\beta})(s, t) = \boldsymbol{\varphi}^{-1}(\Upsilon_{\alpha\beta}(s, t), t)$ is a function composition, and the prime denotes differentiation with respect to s.

We refer to $\boldsymbol{P}^{\mathrm{G}}$ as the *Generalized first Piola–Kirchhoff stress tensor*. Before we discuss the proof of Theorem 2, we list a few properties of the definition given in (2.3.42). For the purpose of this discussion, let us assume that the set of reference bonds given by (2.3.32) are contained in the set $\mathcal{B}_w^0$.

1. The support of the distribution $\boldsymbol{P}^{\mathrm{G}}$ is the inverse image of the set of reference bonds under the mapping $\boldsymbol{\varphi}$. For non-uniform deformation mappings, this support differs from the set of current bonds given by (2.3.19).

2. The spatially averaged field $\boldsymbol{P}_w^{\mathrm{G}} = w \star \boldsymbol{P}^{\mathrm{G}}$ is given by

$$\boldsymbol{P}_w^{\mathrm{G}}(\boldsymbol{X}, t) = \sum_{\substack{\alpha,\beta \\ \alpha<\beta}} -\boldsymbol{f}_{\alpha\beta} \otimes \mathfrak{b}(\boldsymbol{X}, \boldsymbol{X}_\alpha, \boldsymbol{X}_\beta), \tag{2.3.43}$$

   where

$$\mathfrak{b}(\boldsymbol{X}, \boldsymbol{X}_\alpha, \boldsymbol{X}_\beta) := \int_{s=0}^{1} w(\boldsymbol{X} - \boldsymbol{\varphi}^{-1} \circ \boldsymbol{\Upsilon}_{\alpha\beta})(\boldsymbol{\varphi}^{-1} \circ \boldsymbol{\Upsilon}_{\alpha\beta})' \, ds. \tag{2.3.44}$$

   Note that $\boldsymbol{P}_w^{\mathrm{G}}$ also satisfies the equations of motion given in (2.3.25). This can be easily shown using our earlier results (see [AT10]) on the atomistic stress tensor obtained for *curved paths of interaction*).

3. Comparing equations (2.2.5) and (2.3.41) we note that the right-hand side of (2.3.41) includes only the potential part of the atomistic Cauchy stress, whereas the right-hand side of (2.2.5) includes the entire continuum Cauchy stress. This discrepancy can be addressed by noting that in continuum mechanics, for a body in equilibrium, the deformation gradient $\boldsymbol{F}_{\mathrm{c}}$ is independent of time. In contrast, $\boldsymbol{F}$ in (2.3.41), oscillates about a mean value due to thermal vibrations of the particles. It is precisely these oscillations that lead to a thermal contribution to $\boldsymbol{P}^{\mathrm{G}}$. In Appendix A, we study this contribution through an example of an ideal gas enclosed in a container. In particular, we show that $\boldsymbol{P}_w$ and $\boldsymbol{\sigma}_w$ exactly agree in a Tsai calculation.[8]

We now turn to the proof of Theorem 2.

[8] Recall that the Tsai stress tensor at a point is obtained from the Cauchy–Hardy stress tensor in the limit as the support of the weighting function collapses to a plane [AT10].

Proof. From the definition of $\breve{\boldsymbol{\sigma}}_v$ in (2.3.40), we have

$$\begin{aligned}\breve{\boldsymbol{\sigma}}_v(\boldsymbol{X},t) &= \sum_{\substack{\alpha,\beta\\ \alpha<\beta}} -\boldsymbol{f}_{\alpha\beta}\otimes(\boldsymbol{x}_\alpha-\boldsymbol{x}_\beta)\int_{s=0}^{1}\delta((1-s)\boldsymbol{x}_\alpha+s\boldsymbol{x}_\beta-\boldsymbol{\varphi}(\boldsymbol{X},t))\,ds\\ &= \sum_{\substack{\alpha,\beta\\ \alpha<\beta}} \boldsymbol{f}_{\alpha\beta}\otimes\int_{s=0}^{1}\delta(\boldsymbol{\Upsilon}_{\alpha\beta}(s,t)-\boldsymbol{\varphi}(\boldsymbol{X},t))\boldsymbol{\Upsilon}'_{\alpha\beta}(s,t)\,ds, \end{aligned}\tag{2.3.45}$$

where we have used $\boldsymbol{\Upsilon}'_{\alpha\beta}(s,t)=\boldsymbol{x}_\beta-\boldsymbol{x}_\alpha$. It can be easily shown that the Dirac-delta distribution in the integrand of (2.3.45) satisfies the relation

$$J\delta(\boldsymbol{\Upsilon}_{\alpha\beta}(s,t)-\boldsymbol{\varphi}(\boldsymbol{X},t))=\delta(\boldsymbol{\varphi}^{-1}\circ\boldsymbol{\Upsilon}_{\alpha\beta}(s,t)-\boldsymbol{X}).\tag{2.3.46}$$

From (2.3.45), and using (2.3.46), we obtain

$$J\breve{\boldsymbol{\sigma}}_v(\boldsymbol{X},t)=\sum_{\substack{\alpha,\beta\\ \alpha<\beta}} \boldsymbol{f}_{\alpha\beta}\otimes\int_{s=0}^{1}\delta(\boldsymbol{\varphi}^{-1}\circ\boldsymbol{\Upsilon}_{\alpha\beta}(s,t)-\boldsymbol{X})\boldsymbol{\Upsilon}'_{\alpha\beta}(s,t)\,ds.\tag{2.3.47}$$

Post-multiplying both sides of (2.3.47) with $\boldsymbol{F}^{-\mathrm{T}}$, and using $\boldsymbol{F}^{-1}\boldsymbol{\Upsilon}'_{\alpha\beta}(s,t)=(\boldsymbol{\varphi}^{-1}\circ\boldsymbol{\Upsilon}_{\alpha\beta})'(s,t)$, we obtain the desired result:

$$\begin{aligned}J\breve{\boldsymbol{\sigma}}_v(\boldsymbol{X},t)\boldsymbol{F}^{-\mathrm{T}} &= \sum_{\substack{\alpha,\beta\\ \alpha<\beta}} \boldsymbol{f}_{\alpha\beta}\otimes\int_{s=0}^{1}\delta(\boldsymbol{\varphi}^{-1}\circ\boldsymbol{\Upsilon}_{\alpha\beta}(s,t)-\boldsymbol{X})(\boldsymbol{\varphi}^{-1}\circ\boldsymbol{\Upsilon}_{\alpha\beta})'(s,t)\,ds\\ &= \boldsymbol{P}^{G}(\boldsymbol{X},t). \end{aligned}\tag{2.3.48}$$

□

Corollary 1. *For a uniform deformation mapping $\boldsymbol{\varphi}$, we have*

$$\boldsymbol{P}=\boldsymbol{P}^{\mathrm{G}}.\tag{2.3.49}$$

Proof. Under uniform deformation, we observe that $\boldsymbol{\varphi}^{-1}\circ\Upsilon_{\alpha\beta}=(1-s)\boldsymbol{X}_\alpha+s\boldsymbol{X}_\beta$, i.e. the inverse image of the line joining $\boldsymbol{x}_\alpha$ and $\boldsymbol{x}_\beta$ is equal to the line joining $\boldsymbol{X}_\alpha$ and $\boldsymbol{X}_\beta$. Therefore, (2.3.42) simplifies to (2.3.31). □

Note that both $\boldsymbol{P}_w=w\star\boldsymbol{P}$ and $\boldsymbol{P}^{\mathrm{G}}_w=w\star\boldsymbol{P}^{\mathrm{G}}$ qualify to be definitions for the atomistic first Piola–Kirchhoff stress because they satisfy the equations of motion given in (2.3.25). We prefer the definition $\boldsymbol{P}$ to $\boldsymbol{P}^{\mathrm{G}}$ because $\boldsymbol{P}^{\mathrm{G}}$ depends on the choice of $\boldsymbol{\varphi}$, whereas $\boldsymbol{P}$

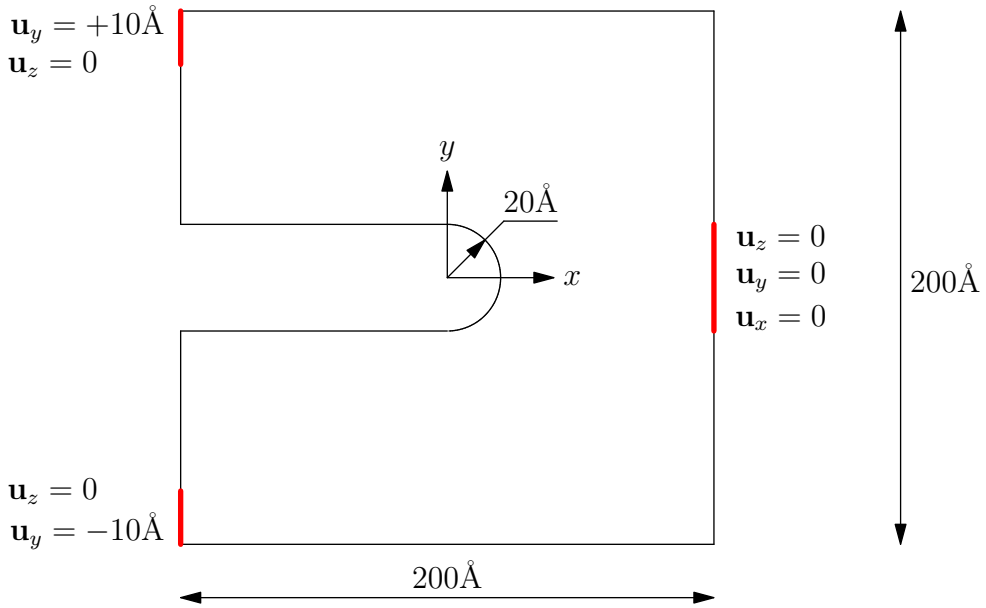

Figure 2.1: A schematic of the geometry of the studied boundary-value problem, with displacement boundary conditions enforced on a part of the boundary shown in red.

is independent of it and only depends on the reference and the deformed configuration of particles.

It is easy to see that the definition of the first Piola–Kirchhoff stress tensor also results in the following definition for the second Piola–Kirchhoff stress tensor $\boldsymbol{S}$,

$$\boldsymbol{S}(\boldsymbol{X},t) = \sum_{\substack{\alpha,\beta \\ \alpha<\beta}} -\boldsymbol{f}^{\leftarrow}_{\alpha\beta} \otimes (\boldsymbol{X}_\alpha - \boldsymbol{X}_\beta) \int_{s=0}^{1} \delta((1-s)\boldsymbol{X}_\alpha + s\boldsymbol{X}_\beta - \boldsymbol{X})\, ds, \qquad (2.3.50)$$

where $\boldsymbol{f}^{\leftarrow}_{\alpha\beta}(\boldsymbol{X},t) := \boldsymbol{F}^{-1}\boldsymbol{f}_{\alpha\beta}$ is the pull-back of the force $\boldsymbol{f}_{\alpha\beta}$ under the mapping $\boldsymbol{\varphi}$. The definition given in (2.3.50) satisfies the condition $\boldsymbol{F}\boldsymbol{S} = \boldsymbol{P}$. Since $\boldsymbol{f}^{\leftarrow}_{\alpha\beta}$ depends on the mapping $\boldsymbol{\varphi}$, so does $\boldsymbol{S}$.

2.4 Numerical example

In this section, we compare the atomistic first Piola–Kirchhoff stress tensor $\boldsymbol{P}_w$ given in (2.3.27), to the continuum first Piola–Kirchhoff stress $\boldsymbol{P}_{\mathrm{c}}$ using a numerical example. In order to capture the asymmetry of the first Piola–Kirchhoff stress we choose an example with large geometric nonlinearity. We study a system that exhibits this property — a two-dimensional plane strain slab containing a rounded notch under tension. The slab is a

200 Å $\times$ 200 Å square with a notch of size 40 Å as illustrated in Fig. 2.1. It consists of single crystal Al in the face-centered cubic (fcc) structure with the x, y, z axes (see Fig. 2.1) oriented along the $[111]$, $[\bar{1}10]$, $[\bar{1}\bar{1}2]$ crystallographic directions. The notch is stretched in tension by displacement boundary conditions applied at the top and bottom left corners of the model as shown in red in Fig. 2.1. Rigid-body motion is prevented by constraining a portion of the right edge of the slab. Periodic boundary conditions are applied in the out-of-plane (z) direction. The system is studied at zero temperature, $T = 0$ K.

The above problem is simulated in two different ways: (1) an atomistic molecular statics simulation is performed from which $\boldsymbol{P}_w$ is computed; (2) a continuum finite element simulation using a constitutive relation consistent with the atomistic model in (1) is performed from which $\boldsymbol{P}_{\text{c}}$ is computed.

2.4.1 Atomistic simulation of a notched slab

In the atomistic simulation, the notched slab system is modeled using a collection of Al atoms.[9] An embedded-atom method (EAM) interatomic potential due to [EA94] archived in OpenKIM [Ella, Ellb, TES$^+$11] is used to model the interaction between the Al atoms. The equilibrium fcc lattice parameter at 0 K calculated for this potential is $a_0 = 4.03208$Å. The reference (unloaded) configuration of the notched slab (shown in Fig. 2.1 is obtained by cutting out a 200 Å $\times$ 200 Å square from a perfect fcc single crystal with the orientation described above and removing all atoms that fall inside the notch. The thickness in the z direction is taken equal to the minimum crystallographic repeat distance in that direction which is $a_0\sqrt{3/2} = 4.93827$ Å. The resulting system consists of 10,560 atoms. The boundary conditions shown in Fig. 2.1 are applied by identifying the atoms lying on the part of the boundary on which the displacements are applied. The maximum magnitude of the displacements (10 Å) on the upper-left and the lower-left corners of the system is reached in 50 steps of 0.2 Å each. At each time step, the displacement boundary conditions are updated, and the system is evolved by minimizing its potential energy with respect to the positions of the atoms using a conjugate gradient algorithm (see for example [TM11]). This corresponds to a molecular statics simulation.

The atomistic first Piola–Kirchhoff stress field is obtained using the expression given in

[9] Given the physical nature of the system, we switch from the more generic term "particles" used so far to "atoms."

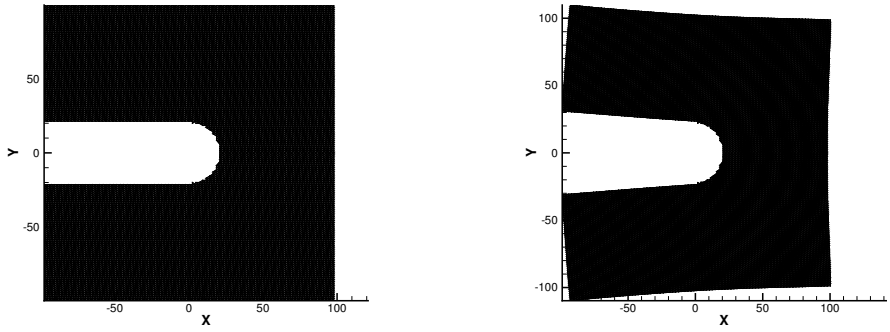

(a) (b)

Figure 2.2: A plot of the mesh used to discretize the domain in (a) the reference configuration, and (b) the deformed configuration.

(2.3.27). The forces $\boldsymbol{f}_{\alpha\beta}$ in (2.3.27) are given by

$$\boldsymbol{f}_{\alpha\beta} = -\frac{\partial \mathcal{V}_{\mathrm{EAM}}}{\partial r_{\alpha\beta}} \frac{\boldsymbol{x}_\alpha - \boldsymbol{x}_\beta}{r_{\alpha\beta}}, \tag{2.4.1}$$

where $\mathcal{V}_{\mathrm{EAM}}$ denotes the EAM potential energy which is a function of the distances between atoms $r_{\alpha\beta} = \|\boldsymbol{x}_\beta - \boldsymbol{x}_\alpha\|$, and $\boldsymbol{x}_\alpha$ and $\boldsymbol{x}_\beta$ are the positions of atoms α and β in the deformed configuration obtained at the end of the atomistic simulation. We compute two stress fields, $\boldsymbol{P}_w$ and $\boldsymbol{P}_{\tilde{w}}$, corresponding to two different uniform weighting functions, $w(\boldsymbol{X}) = \hat{w}(\boldsymbol{X}, 2.5\ \text{Å})$ and $\tilde{w}(\boldsymbol{X}) = \hat{w}(\boldsymbol{X}, 5\ \text{Å})$, where

$$\hat{w}(\boldsymbol{X}, R) = \begin{cases} c_R & \text{if } \|\boldsymbol{X}\| < R - \epsilon, \\ \frac{1}{2} c_R \left[1 - \cos\left(\frac{R - \|X\|}{\epsilon}\pi\right)\right] & \text{if } R - \epsilon < \|\boldsymbol{X}\| < R, \\ 0 & \text{otherwise.} \end{cases} \tag{2.4.2}$$

The support of the weighting function is a sphere of radius R, and c_R in (2.4.2) is chosen such that $\hat{w}$ is a normalized function. We use two weighting functions with different supports ($R = 2.5$ Å and $R = 5$ Å, with $\epsilon = 0.12R$) to explore the effect of weighting function on the atomistic stress at the surfaces.

2.4.2 Continuum simulation of a notched slab

In order to obtain the continuum first Piola–Kirchhoff field $\boldsymbol{P}_{\mathrm{c}}$, a continuum simulation must be performed. The comparison to the atomistic results is only meaningful if the

continuum constitutive relation is consistent with the atomistic simulation. To this end, we apply the local Quasicontinuum (QC) method of [TOP96]. Local QC corresponds to a finite deformation (nonlinear) finite element simulation in which the constitutive relation is obtained from an atomistic model using the Cauchy–Born rule (see for example Tadmor and Miller [TM11]). Briefly, the constitutive response at an integration point is obtained by applying the deformation gradient at that point to a periodic unit cell of the underlying crystal structure and computing the energy from the resulting deformed configuration of atoms using an interatomic potential energy function. The strain energy density follows as

$$W_{\mathrm{c}}(\boldsymbol{F}_{\mathrm{c}}) = \frac{1}{\Omega_0} E_{\mathrm{unit}}(\boldsymbol{F}_{\mathrm{c}}), \tag{2.4.3}$$

where Ω_0 is the unit cell volume in the reference configuration, and E_{unit} is the energy per unit cell subjected to a uniform (affine) deformation $\boldsymbol{F}_{\mathrm{c}}$. In our case, E_{unit} is computed using the same EAM potential used in the atomistic simulation. The first Piola–Kirchhoff at the integration point is obtained by differentiation,

$$\boldsymbol{P}_{\mathrm{c}} = \frac{\partial W_{\mathrm{c}}}{\partial \boldsymbol{F}_{\mathrm{c}}}. \tag{2.4.4}$$

See Tadmor et al. [TOP96] or Tadmor and Miller [TM11] for more details and specific local QC expressions for W_{c} and $\boldsymbol{P}_{\mathrm{c}}$.

For the notched slab boundary-value problem, a two-dimensional local QC simulation is performed. As in the atomistic simulation, periodic boundary conditions are applied in the out-of-plane direction. The finite element mesh consists of linear triangular elements. The mesh in the reference configuration is uniform and symmetric about the $y = 0$ plane. The nodes of the mesh coincide with the positions of the atoms. In QC terminology this is referred to as a "fully-refined" mesh. The QC mesh in the reference and deformed configurations is shown in Fig. 2.2. The local QC simulation is performed in a similar manner to the atomistic molecular statics simulation. The boundary conditions are incremented in steps of 0.2 Å and the potential energy of the system is minimized using the previously converged result as an initial guess. At the end of the simulation, the first Piola–Kirchhoff field is computed at the integration points (element centroids) using (2.4.4).

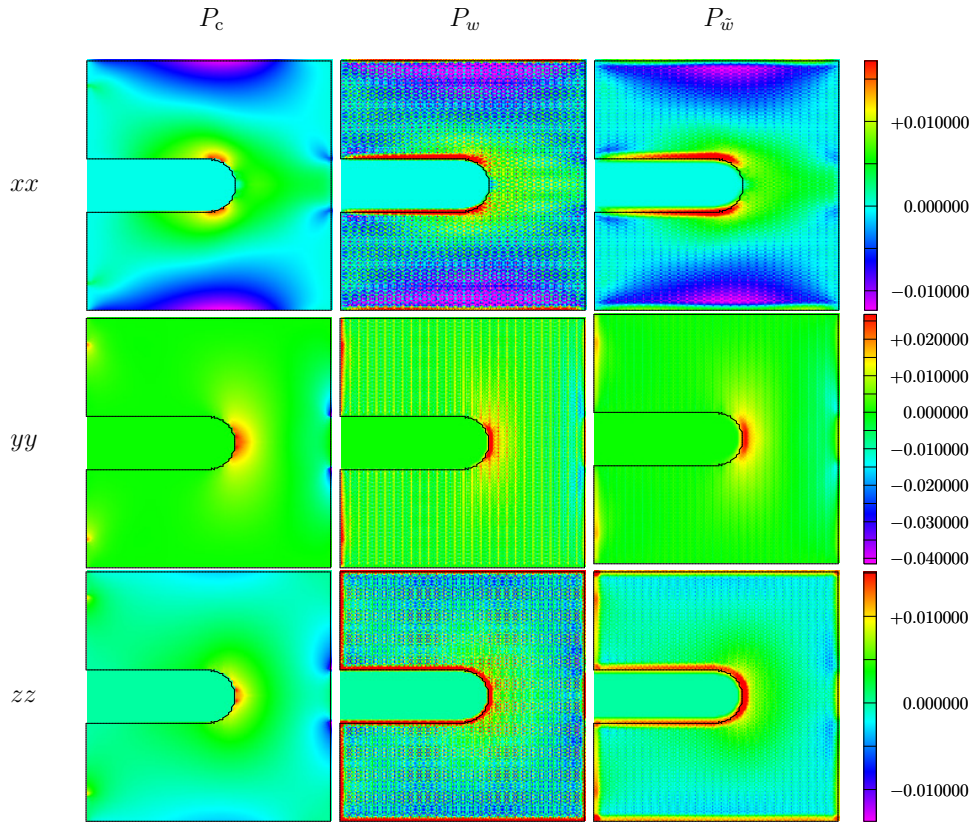

Figure 2.3: A plot of the xx, yy and zz components of the continuum and atomistic first Piola–Kirchhoff stress tensor fields in units of eV/Å^3. The atomistic stress is given for two weighting functions, w and $\tilde{w}$.

2.4.3 Comparison of the continuum and atomistic first Piola–Kirchhoff stress

The stress profiles obtained from the continuum solution are compared to those obtained from the atomistic solution in Figs. 2.3–2.5. Based on these results we make the following observations.

1. From Figs. 2.3–2.5 we see that the atomistic first Piola–Kirchhoff stress tensors corresponding to the weighting functions w and $\tilde{w}$ are in good agreement with the continuum first Piola–Kirchhoff stress in bulk regions of the system (i.e. away from surfaces).

2. The effect of surfaces on the atomistic first Piola–Kirchhoff stress are clear in the xx, yy and zz plots shown in Fig. 2.3. In particular, we see that the presence of surfaces results in a localized surface stress with a magnitude that is comparable to the bulk stress. We also see from Figs. 2.3–2.5 that the localization decreases as the support of the weighting function increases.

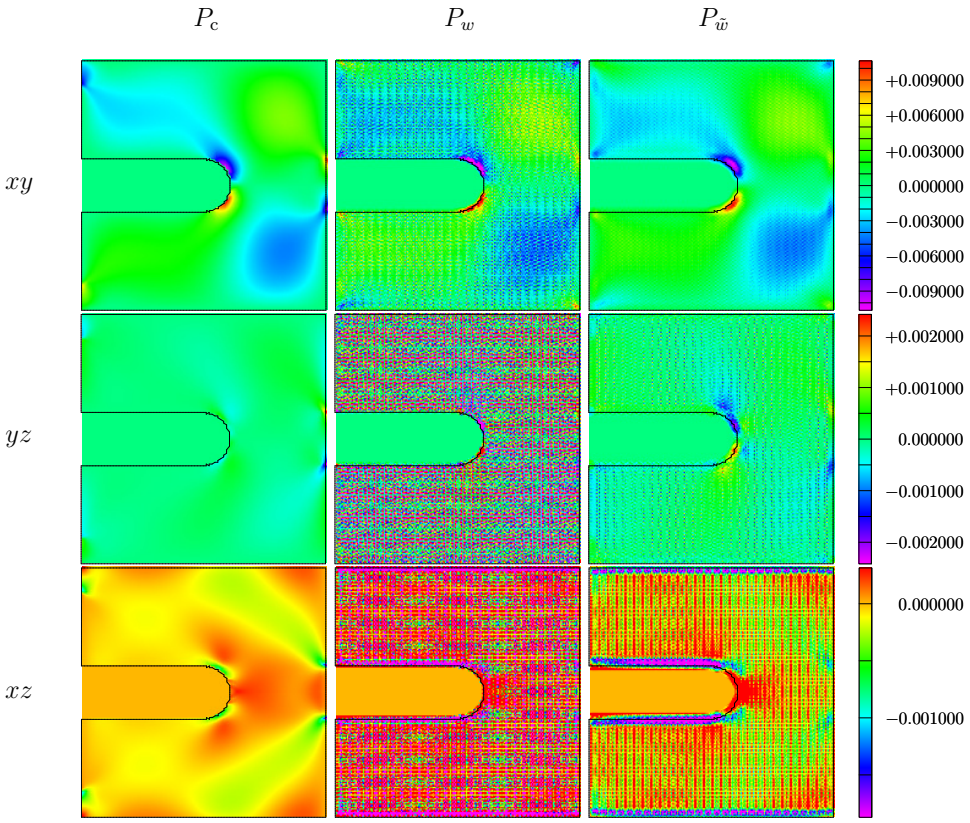

Figure 2.4: A plot of the xy, yz and xz components of the continuum and atomistic first Piola–Kirchhoff stress tensor fields in units of eV/Å^3. The atomistic stress is given for two weighting functions, w and $\tilde{w}$.

3. The surface effect on the xx component is negligible on planes perpendicular to the x-axis, such as the region at the rounded surface of the notch and the outer boundary surfaces at $x = \pm 100$ Å. Similarly, the effect of surfaces on the yy component is negligible on the $y = \pm 20$Å surfaces of the notch.

From the above observations, we conclude that the definition of the atomistic first Piola–Kirchhoff stress given in (2.3.27) is in good agreement with continuum first Piola–Kirchhoff stress.

2.5 Conclusion

In this paper, we obtained material fields for atomistic systems by carrying out the Murdoch–Hardy procedure on a reference configuration of discrete particles. The fields resulting from this procedure are the reference mass density, reference momentum density, reference body field, and first Piola–Kirchhoff stress. These fields identically satisfy the material form of

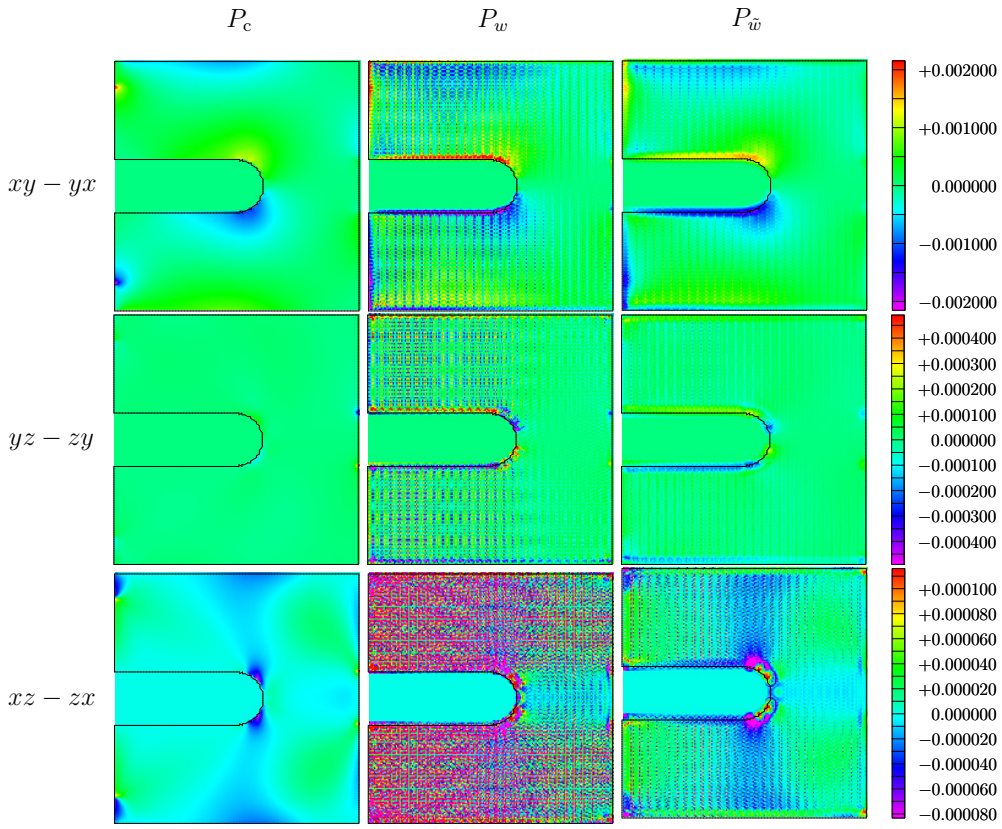

Figure 2.5: A plot showing the asymmetry of the continuum and atomistic first Piola–Kirchhoff stress tensor fields in units of eV/Å^3. The atomistic stress is given for two weighting functions, w and $\tilde{w}$.

the balance laws. One of the key feature of this procedure is that these fields are obtained without defining a deformation map. In addition, a pull-back procedure is defined in terms of an arbitrary deformation map that tracks the particles, which provides definitions for the material description of the spatial mass density and Cauchy stress. Although the resulting distributions obtained through the pull-back depend on the choice of the deformation map, the relationship between the spatial and material fields are identically satisfied in a distributional sense.

An interesting observation from our derivation is that the atomistic first Piola–Kirchhoff stress tensor does not have a kinetic contribution, which in the atomistic Cauchy stress tensor accounts for thermal fluctuations. We show that this effect is also included in the atomistic first Piola–Kirchhoff stress tensor through the motion of particles with the example of an ideal gas.

Finally, we demonstrate the validity of our definition for the first Piola–Kirchhoff stress through a numerical example involving finite deformation of a slab containing a notch

under tension.

Chapter 3

The non-uniqueness of the atomistic stress tensor and its relationship to the generalized Beltrami representation

3.1 Introduction

Atomistic simulations are extensively used as a tool to obtain accurate constitutive relations for continuum models. In order to do so, the data generated in an atomistic simulation, which is in the form of positions and velocities of particles, has to be reinterpreted in the language of continuum mechanics. This is done by developing continuum notions for atomistic systems. Work on this dates back at least to Cauchy in the 1820s with his aim to define stress in crystalline solids. Later, Irving and Kirkwood [IK50] derived continuum fields for an atomistic system that is probabilistic in nature using principles of non-equilibrium classical statistical mechanics. More recently, Hardy [Har82, HRS02] and Murdoch [Mur82] defined continuum fields for an atomistic model using spatial averaging.

Of all the continuum fields, the atomistic stress tensor has been debated the most because of its non-uniqueness. The most commonly used atomistic stress definitions are the virial [Max70, Max74], Tsai [Tsa79], Irving–Kirkwood [IK50] and Murdoch–Hardy [Mur03] stress tensors. In recent work [AT10, AT11], the authors extensively studied the definition for the stress tensor within a unified framework based on a generalization of the Irving–Kirkwood procedure to arbitrary multi-body potentials. Through this unified framework it is shown that all existing definitions follow as special cases of a single stress expression. One of the sources of non-uniqueness of the atomistic stress tensor is identified to be the

non-uniqueness of force decomposition, which is in turn related to the non-uniqueness of the potential energy representation used in the calculation. The term "representation" reflects the fact that the potential energy, which is a function of distances between atoms, must be extended in a non-unique fashion off the subspace corresponding to real physical distances in order to compute the derivatives appearing in the stress expression.

In the absence of a sound quantum mechanical origin for potential energy representations, we focus our attention on characterizing the non-uniqueness of force decomposition. Our analysis is based on rigidity theory, which results in a decomposition of the distribution associated with the potential part of the atomistic stress tensor in the Murdoch–Hardy procedure into an irrotational part that is independent of the potential energy representation, and a traction-free solenoidal part. This decomposition has a potential application in systematic reduction of noise in atomistic fields. A similar decomposition of the Cauchy stress tensor can be constructed in continuum mechanics using the generalized Beltrami representation, which is a version of vector Helmholtz decomposition for symmetric tensors. We identify analogies between the two decompositions, and in the process obtain a strain tensor equivalent in atomistics. Finally, we compare the two decompositions through a numerical test, and demonstrate their equivalence.

The paper is organized as follows. In Section 3.2, we review the derivation of the atomistic stress tensor in the Murdoch–Hardy procedure. In Section 3.3, we identify the non-uniqueness of the force decomposition that results in the non-uniqueness of atomistic the stress tensor, and give it a geometric interpretation. In Section 3.4, we decompose the potential part of the atomistic stress tensor into a solenoidal part and an irrotational part, and identify the properties of the decomposition. In Section 3.5, we review the generalized Beltrami representation for symmetric tensor fields, and obtain an orthogonal decomposition of a symmetric tensor field into a traction-free solenoidal part and an irrotational part. In Section 3.6, we demonstrate the equivalence of the decompositions proposed in Sections 3.4 and 3.5 using a numerical test. We conclude with a summary in Section 3.7.

3.2 The atomistic stress tensor in the Murdoch–Hardy procedure

An atomistic system is modeled as a collection of N interacting point particles in the Euclidean[1] space $\mathbb{R}^3$. The positions and velocities of the point particles at time t are given by the functions $\boldsymbol{x}_\alpha(t)$ and $\boldsymbol{v}_\alpha(t)$ ($\alpha = 1, \ldots, N, t \geq 0$), respectively. We also use the expressions $\boldsymbol{x}_\alpha$ and $\boldsymbol{v}_\alpha$ to denote the value of the functions $\boldsymbol{x}_\alpha(\cdot)$ and $\boldsymbol{v}_\alpha(\cdot)$ at a particular instant

[1] All real coordinate vector spaces appearing in this paper are equipped with the standard inner product.

of time. The system is assumed to be conservative, which means that there exists a potential energy function $\widehat{\mathcal{V}}(\boldsymbol{x}_1, \boldsymbol{x}_2, \ldots, \boldsymbol{x}_N)$ for the interaction of the particles. This function is taken to be differentiable, so that the force on particle α follows as the negative gradient of the potential energy with respect to its position,

$$\boldsymbol{f}_\alpha = -\nabla_{\boldsymbol{x}_\alpha} \widehat{\mathcal{V}}. \tag{3.2.1}$$

We assume a finite range of interaction for $\widehat{\mathcal{V}}$. This means that there exists a cutoff radius $r_{\text{cut}} > 0$ such that $\widehat{\mathcal{V}}$ can be decomposed as a finite sum of particle potential energies,[2]

$$\widehat{\mathcal{V}} = \sum_{\alpha=1}^{M} \widehat{\mathcal{V}}_\alpha, \tag{3.2.2}$$

where each $\mathcal{V}_\alpha$ in (3.2.2) is a conservative potential function of the positions of particles within a cluster of size r_{cut}. No restrictions are placed on the form of $\mathcal{V}_\alpha$, which can be a general many-body potential.

The atomistic stress can be derived using the Murdoch–Hardy (MH) or Irving–Kirkwood (IK) procedures. For the purpose of this paper, we discuss the atomistic stress tensor and its uniqueness using the MH procedure, although a similar description can be carried out using IK. Under the MH procedure, continuum fields are defined as direct spatial averages of microscopic variables. The spacial averaging is performed using a weighting function $w : \mathbb{R}^3 \to \mathbb{R}^+$ with a compact support. The weighting function must satisfy the normalization condition

$$\int_{\mathbb{R}^3} w(\boldsymbol{r})\, d\boldsymbol{r} = 1. \tag{3.2.3}$$

The derivation of the atomistic stress begins with the definition of the mass density, momentum density, and velocity fields:

$$\rho_w(\boldsymbol{x}, t) := \sum_\alpha m_\alpha w(\boldsymbol{x}_\alpha - \boldsymbol{x}), \tag{3.2.4a}$$

$$\boldsymbol{p}_w(\boldsymbol{x}, t) := \sum_\alpha m_\alpha \boldsymbol{v}_\alpha w(\boldsymbol{x}_\alpha - \boldsymbol{x}), \tag{3.2.4b}$$

$$\boldsymbol{v}_w(\boldsymbol{x}, t) := \boldsymbol{p}_w / \rho_w, \tag{3.2.4c}$$

where $\boldsymbol{x} \in \mathbb{R}^3$, and the subscript w indicates the role of the weighting function. In order

[2]Note that the decomposition given in (3.2.2) is not unique. No physical meaning is attached to the particle energies $\mathcal{V}_\alpha$. For more on the non-uniqueness of the energy decomposition, see [AT11].

to arrive at an expression for the atomistic stress tensor, denoted by $\boldsymbol{\sigma}_w$, it is postulated that the fields ρ_w, $\boldsymbol{v}_w$ and $\boldsymbol{\sigma}_w$, satisfy the equation of motion from continuum mechanics [TME12]. For simplicity, we assume that there are no body forces acting on the system. We therefore have

$$\frac{\partial(\rho_w \boldsymbol{v}_w)}{\partial t} + \operatorname{div}_{\boldsymbol{x}}(\rho_w \boldsymbol{v}_w \otimes \boldsymbol{v}_w) = \operatorname{div}_{\boldsymbol{x}} \boldsymbol{\sigma}_w. \tag{3.2.5}$$

Substituting the definitions for ρ_w and $\boldsymbol{v}_w$ given in (3.2.4) into (3.2.5), with some additional algebra (see [AT10] for the full derivation), we arrive at an expression for the divergence of the atomistic stress tensor given by

$$\operatorname{div}_{\boldsymbol{x}} \boldsymbol{\sigma}_w(\boldsymbol{x}, t) = \sum_{\alpha} \boldsymbol{f}_\alpha(t) w(\boldsymbol{x}_\alpha(t) - \boldsymbol{x}) - \operatorname{div}_{\boldsymbol{x}} \sum_{\alpha} m_\alpha (\boldsymbol{v}_\alpha^{\mathrm{rel}} \otimes \boldsymbol{v}_\alpha^{\mathrm{rel}}) w(\boldsymbol{x}_\alpha - \boldsymbol{x}), \tag{3.2.6}$$

where $\boldsymbol{f}_\alpha(t)$ is defined in (3.2.1), and $\boldsymbol{v}_\alpha^{\mathrm{rel}}(\boldsymbol{x}, t) := \boldsymbol{v}_\alpha(t) - \boldsymbol{v}_w(\boldsymbol{x}, t)$. From (3.2.6), it is clear that the stress tensor has two contributions, commonly referred to as the potential and kinetic parts of the stress tensor. The kinetic part, denoted by $\boldsymbol{\sigma}_{w,\mathrm{k}}$, is given by

$$\boldsymbol{\sigma}_{w,\mathrm{k}}(\boldsymbol{x}, t) = -\sum_{\alpha} m_\alpha (\boldsymbol{v}_\alpha^{\mathrm{rel}} \otimes \boldsymbol{v}_\alpha^{\mathrm{rel}}) w(\boldsymbol{x}_\alpha - \boldsymbol{x}), \tag{3.2.7}$$

and the potential part of the stress tensor, denoted by $\boldsymbol{\sigma}_{w,\mathrm{v}}$, satisfies the equation

$$\operatorname{div}_{\boldsymbol{x}} \boldsymbol{\sigma}_{w,\mathrm{v}}(\boldsymbol{x}, t) = \sum_{\alpha} \boldsymbol{f}_\alpha(t) w(\boldsymbol{x}_\alpha(t) - \boldsymbol{x}). \tag{3.2.8}$$

It is clear that there are many candidates for $\boldsymbol{\sigma}_{w,\mathrm{v}}$ that satisfy (3.2.8). Examples include the Hardy [Har82], Murdoch [Mur07] and the Tsai [Tsa79] stress tensors. The procedure to arrive at these stress tensors involves the following two steps:

1. The force $\boldsymbol{f}_\alpha$ in (3.2.8) is decomposed as

$$\boldsymbol{f}_\alpha = \sum_{\substack{\beta \\ \beta \neq \alpha}} \boldsymbol{f}_{\alpha\beta}, \tag{3.2.9}$$

   where $\boldsymbol{f}_{\alpha\beta} = -\boldsymbol{f}_{\beta\alpha}$. We call a decomposition *central force* if $\boldsymbol{f}_{\alpha\beta}$ is parallel to the line joining particles α and β, and *non-central force* otherwise. Substituting (3.2.9)

into (3.2.8), we obtain[3]

$$\operatorname{div}_{\boldsymbol{x}} \boldsymbol{\sigma}_{w,\mathrm{v}}(\boldsymbol{x},t) = \sum_{\substack{\alpha,\beta \\ \alpha\neq\beta}} \boldsymbol{f}_{\alpha\beta} w(\boldsymbol{x}_\alpha(t) - \boldsymbol{x}). \tag{3.2.10}$$

2. The sum in (3.2.10) is written as an integral of a generating function $\boldsymbol{g}(\boldsymbol{x},\boldsymbol{y})$ that is anti-symmetric in its arguments, with certain decay properties [AT10]:

$$\operatorname{div}_{\boldsymbol{x}} \boldsymbol{\sigma}_{w,\mathrm{v}}(\boldsymbol{x},t) = \int_{\mathbb{R}^3} \boldsymbol{g}(\boldsymbol{x},\boldsymbol{y},t)\, d\boldsymbol{y}. \tag{3.2.11}$$

Different choices of the generating function result in different stress tensors. For instance, the generating function for the Hardy stress is given by

$$\boldsymbol{g}^{\mathrm{H}}(\boldsymbol{x},\boldsymbol{y},t) = \sum_{\substack{\alpha,\beta \\ \alpha\neq\beta}} \boldsymbol{f}_{\alpha\beta} w(\boldsymbol{x}_\alpha - \boldsymbol{x}) \delta(\boldsymbol{x}_\beta - \boldsymbol{x}_\alpha + \boldsymbol{x} - \boldsymbol{y}), \tag{3.2.12}$$

where δ is the Dirac delta distribution in $\mathbb{R}^3$.

Finally, Noll's lemma [Nol55] is invoked to express the right-hand-side of (3.2.11) in divergence form, from which an expression for the stress tensor follows. The stress tensor proposed by Hardy [Har82, HRS02] is obtained using the kernel $\boldsymbol{g}^{\mathrm{H}}$:

$$\boldsymbol{\sigma}_{w,\mathrm{v}} = \frac{1}{2} \sum_{\substack{\alpha,\beta \\ \alpha\neq\beta}} \int_{s=0}^{1} [-\boldsymbol{f}_{\alpha\beta}\, w((1-s)\boldsymbol{x}_\alpha + s\boldsymbol{x}_\beta - \boldsymbol{x}) \otimes (\boldsymbol{x}_\alpha - \boldsymbol{x}_\beta)]\, ds. \tag{3.2.13}$$

If $\boldsymbol{f}_{\alpha\beta}$ is parallel to the line joining particles α and β, the Hardy stress $\boldsymbol{\sigma}_{w,\mathrm{v}}$ is symmetric. We also note that the fields ρ_w, $\boldsymbol{p}_w$, and $\boldsymbol{\sigma}_{w,\mathrm{v}}$ obtained in the MH procedure can be written as a convolution[4] of the weighting function w with a corresponding distribution[5]. In other

[3]The following notation is used: $\sum_{\substack{\alpha,\beta \\ \alpha\neq\beta}} = \sum_\alpha \sum_{\substack{\beta \\ \beta\neq\alpha}}$.

[4]See [Hör90] for the formal definition of a convolution of a function with a distribution. Here, we do not require such a general definition since algebra on a Dirac-delta distribution can be carried out as if it were a function. Therefore we use the following definition for the convolution of two smooth functions u and v that have a compact support in $\mathbb{R}^3$,

$$u \star v(\boldsymbol{x}) := \int_{\mathbb{R}^3} u(\boldsymbol{x}-\boldsymbol{y}) v(\boldsymbol{y})\, d\boldsymbol{y},$$

where v is replaced by the Dirac-delta distribution.

[5]A distribution is a linear map from the space of smooth functions with compact support to the real line $\mathbb{R}$.

words,

$$\rho_w(\boldsymbol{x},t) = w \star \rho, \quad \boldsymbol{p}_w(\boldsymbol{x},t) = w \star \boldsymbol{p}, \quad \boldsymbol{\sigma}_{w,\mathrm{v}}(\boldsymbol{x},t) = w \star \boldsymbol{\sigma}_{\mathrm{v}}, \tag{3.2.14}$$

where $\star$ denotes the convolution operator, and the distributions ρ, $\boldsymbol{p}$, and $\boldsymbol{\sigma}_{\mathrm{v}}$ are given by

$$\rho(\boldsymbol{x},t) = \sum_{\alpha} m_\alpha \delta(\boldsymbol{x} - \boldsymbol{x}_\alpha), \tag{3.2.15}$$

$$\boldsymbol{p}(\boldsymbol{x},t) = \sum_{\alpha} m_\alpha \boldsymbol{v}_\alpha \delta(\boldsymbol{x} - \boldsymbol{x}_\alpha), \tag{3.2.16}$$

$$\boldsymbol{\sigma}_{\mathrm{v}}(\boldsymbol{x},t) = \sum_{\substack{\alpha,\beta \\ \alpha<\beta}} -\boldsymbol{f}_{\alpha\beta} \otimes (\boldsymbol{x}_\alpha - \boldsymbol{x}_\beta) \int_{s=0}^{1} \delta((1-s)\boldsymbol{x}_\alpha + s\boldsymbol{x}_\beta - \boldsymbol{x})\, ds. \tag{3.2.17}$$

By writing the spatially-averaged fields ρ_w, $\boldsymbol{p}_w$ and $\boldsymbol{\sigma}_{w,\mathrm{v}}$ in convolution form, we are able to separate out the role of the weighting function, and thereby arrive at distributions ρ, $\boldsymbol{p}$ and $\boldsymbol{\sigma}_{\mathrm{v}}$ that are independent of it.

Let us now discuss the various sources of non-uniqueness of the potential part of the atomistic stress tensor $\boldsymbol{\sigma}_{w,\mathrm{v}} = w \star \boldsymbol{\sigma}_{\mathrm{v}}$ resulting from the MH procedure described above. The first source of non-uniqueness is the choice of the weighting function w. See for example [UMP13] for a discussion on the optimal choice of w based on the correlation length of the potential energy function. The second source of non-uniqueness is the choice of the force decomposition mentioned above in step 1 which affects σ_{v}. A recent article by Arroyo et al. [VTSA14] discusses the significance of the force decomposition on the atomistic stress in lipid bilayers used to evaluate the material constants of the bilayer membrane. The third source of non-uniqueness is the choice of the kernel function mentioned above in step 2. See [AT10] for kernel functions that result in various atomistic stress tensors.

The main focus of this paper is the non-uniqueness of $\boldsymbol{\sigma}_{\mathrm{v}}$ resulting due to the non-uniqueness of the force decomposition and the derivation of a decomposition that separates $\boldsymbol{\sigma}_{\mathrm{v}}$ into unique and non-unique parts. In the next section, we present some general properties of the decomposition given in (3.2.9), demonstrate its non-uniqueness, and set up a discussion for its interpretation.

3.3 Non-uniqueness of the force decomposition

It is clear that the force decomposition in (3.2.9) represents an over-determined system of $3N$ equations with $3N(N-1)$ unknowns.[6] This implies that there are can be many solutions for $\boldsymbol{f}_{\alpha\beta}$. Thus in order to arrive at a reasonable force decomposition, additional conditions are required. Two such conditions are obtained if we interpret $\boldsymbol{f}_{\alpha\beta}$ as the force on particle α due to the presence of particle β, and enforce the condition of momentum balance and angular momentum balance for any subset of particles within the body. These conditions are referred to in [AT10] as the "strong" and "weak law of action and reaction" respectively, and are given by

$$\boldsymbol{f}_{\alpha\beta} = -\boldsymbol{f}_{\beta\alpha} \tag{3.3.1}$$

$$\boldsymbol{f}_{\alpha\beta} \parallel \boldsymbol{x}_\alpha - \boldsymbol{x}_\beta. \tag{3.3.2}$$

Equations (3.3.1) and (3.3.2) reduce the number of unknowns in (3.2.9) from $3N(N-1)$ to $N(N-1)/2$, where the unknowns are now represented as a set of scalars $\{f_{\alpha\beta} : \alpha, \beta = 1, \ldots, N, \text{and } \alpha \neq \beta\}$. Note that for $N > 4$, in spite of the reduction in the number of unknowns, the system of equations remains over-determined. We will now give a geometric interpretation of the non-uniqueness of a force decomposition satisfying (3.3.1) and (3.3.2). In order to do so, we will need the following definitions.

An *edge* is defined as a two-element subset $\{\alpha, \beta\}$ of $\{1, \ldots, N\}$. We use the shorthand notation $\alpha\beta$ to denote an edge. Let E denote the ordered set of all edges, with a strict order given by

$$\alpha\beta < \gamma\delta \iff \begin{cases} \min(\alpha,\beta) < \min(\gamma,\delta) \text{ or} \\ \min(\alpha,\beta) = \min(\gamma,\delta), \max(\alpha,\beta) < \max(\gamma,\delta). \end{cases} \tag{3.3.3}$$

In other words, the edges are ordered as $\{1,2\} < \{1,3\} < \cdots < \{1,N\} < \{2,3\} < \cdots < \{N-1,N\}$. Let $\boldsymbol{x} = (\boldsymbol{x}_1, \ldots, \boldsymbol{x}_N) \in \mathbb{R}^{3N}$ denote the configuration of interest, and $E_{\boldsymbol{x}}$ denote the ordered subset of edges in E falling within the range of interaction,

$$E_{\boldsymbol{x}} := \{\alpha\beta : \|\boldsymbol{x}_\alpha - \boldsymbol{x}_\beta\| < r_{\text{cut}}\}. \tag{3.3.4}$$

In particular, let $E_{\boldsymbol{x}}(k)$ denote the k-th edge in $E_{\boldsymbol{x}}$. Denote the cardinality (i.e. number of elements) of $E_{\boldsymbol{x}}$ as e. It can be easily shown that there exists a neighborhood $\mathcal{N}_{\boldsymbol{x}}$ of $\boldsymbol{x}$

[6] There are $N(N-1)$ forces since in general $\boldsymbol{f}_{\alpha\beta}$ can be different from $\boldsymbol{f}_{\beta\alpha}$. The factor 3 is included because force is a 3-dimensional vector

in $\mathbb{R}^{3N}$ such that for every $\boldsymbol{y} \in \mathcal{N}_{\boldsymbol{x}}$, $E_{\boldsymbol{y}} = E_{\boldsymbol{x}}$. In other words, for every configuration $\boldsymbol{y} \in \mathcal{N}_{\boldsymbol{x}}$, the lengths of edges present in $E_{\boldsymbol{x}}$ and its complement, remain less than and greater than r_{cut}, respectively. We refer to $\mathcal{N}_{\boldsymbol{x}}$ as the *local configuration space* at $\boldsymbol{x}$.

The local configuration space can be described in terms of "local distances" using a *local rigidity map*[7] $\boldsymbol{R} : \mathcal{N}_{\boldsymbol{x}} \to \mathbb{R}^e$ defined as

$$\boldsymbol{R}(\boldsymbol{y}) = (r_{E_{\boldsymbol{x}}(1)}, \ldots, r_{E_{\boldsymbol{x}}(e)}), \quad \boldsymbol{y} \in \mathcal{N}_{\boldsymbol{x}}, \tag{3.3.5}$$

with $r_{E_{\boldsymbol{x}}}(k) = \|\boldsymbol{y}_\alpha - \boldsymbol{y}_\beta\|$, if $E_{\boldsymbol{x}}(k) = \alpha\beta$. We define the *local shape space* $\mathcal{S}_{\boldsymbol{x}}$ as the image of the local rigidity map:

$$\mathcal{S}_{\boldsymbol{x}} := \operatorname{Im} \boldsymbol{R}. \tag{3.3.6}$$

The term "local" is being used because each e-tuple in $\mathcal{S}_{\boldsymbol{x}}$ contains only those distances that are less than r_{cut}, as opposed to the shape space defined in [AT10] which includes all distances. We adopt the definition in (3.3.6) to make use of the finite range of interaction assumption implicit in (3.2.2) which renders itself useful in our study of the force decomposition in Section 3.4. In addition, we note that since the local distances are not independent of each other, the local shape space may be viewed as a lower-dimensional surface in $\mathbb{R}^e$. It can be shown that each $\widehat{\mathcal{V}}_\alpha$ in (3.2.2), viewed as a function on $\mathbb{R}^{3N}$, and restricted to $\mathcal{N}_{\boldsymbol{x}}$, can be represented uniquely[8] by a function $\breve{\mathcal{V}}_\alpha : \mathcal{S}_{\boldsymbol{x}} \to \mathbb{R}$. In other words,

$$\widehat{\mathcal{V}}_\alpha(\boldsymbol{y}) = \breve{\mathcal{V}}(\boldsymbol{R}(\boldsymbol{y})), \quad \forall \boldsymbol{y} \in \mathcal{N}_{\boldsymbol{x}}. \tag{3.3.7}$$

Therefore, from (3.2.2) it follows that $\widehat{\mathcal{V}}$ restricted to $\mathcal{N}_{\boldsymbol{x}}$, can be represented as a new function[9], $\breve{\mathcal{V}} := \sum_\alpha \breve{\mathcal{V}}_\alpha : \mathcal{S}_{\boldsymbol{x}} \to \mathbb{R}$.

In order to obtain a force decomposition, we now assume that there exists an extension $\mathcal{V}$ of the function $\breve{\mathcal{V}}$ defined on $\mathcal{S}_{\boldsymbol{x}}$ to a neighborhood of $\mathcal{S}_{\boldsymbol{x}} \in \mathbb{R}^e$, i.e

$$\mathcal{V} \mid_{\mathcal{S}_{\boldsymbol{x}}} \equiv \breve{\mathcal{V}}, \tag{3.3.8}$$

[7] Such maps are used in rigidity theory which studies the rigidity of structures formed as an ensemble of rigid elements. See [CW96] for an introduction to rigidity theory.

[8] See [Adm10] for a proof of uniqueness.

[9] Note that in the absence of a finite range of interaction, it may not be possible to represent $\widehat{\mathcal{V}}$ as a new function on $\mathcal{S}_{\boldsymbol{x}}$.

and define the force $\boldsymbol{f}_{\alpha\beta}$ for any configuration $\boldsymbol{y} \in \mathcal{N}_{\boldsymbol{x}}$ as

$$\boldsymbol{f}_{\alpha\beta} := \begin{cases} -\dfrac{\partial \mathcal{V}}{\partial r_{\alpha\beta}}(\boldsymbol{R}(\boldsymbol{y}))\dfrac{\boldsymbol{y}_\alpha - \boldsymbol{y}_\beta}{r_{\alpha\beta}}, & \text{if } \alpha\beta \in E_{\boldsymbol{x}}, \\ \boldsymbol{0}, & \text{otherwise.} \end{cases} \tag{3.3.9}$$

We refer to $\mathcal{V}$ in (3.3.8) as a *potential energy extension*. Note that the derivatives of $\mathcal{V}$ in (3.3.9) with respect to $r_{\alpha\beta}$ for each $\alpha\beta \in E_{\boldsymbol{x}}$ are well-defined because $\mathcal{V}$ is defined in a neighborhood of $\boldsymbol{R}(\boldsymbol{y})$. This is not true of $\breve{\mathcal{V}}$ since $\partial\breve{\mathcal{V}}/\partial r_{\alpha\beta}$ is undefined.[10]

It is easy to verify that (3.3.9) satisfies equations (3.2.9), (3.3.1) and (3.3.2), thus qualifying to be a force decomposition that satisfies the weak and strong law of action-reaction. Moreover, the stress tensor obtained using (3.3.9) and (3.2.13) is always symmetric. However, it is clear from the above definition that $\boldsymbol{f}_{\alpha\beta}$ is not unique as it depends on the potential energy extension. (Note that different extensions of the potential energy result in the same forces $\boldsymbol{f}_\alpha$, but different force decompositions.) In practice, the choice of the potential energy extension is made by the choice of the empirical interatomic potential, which is normally already represented as an extension. For example, pair potentials, embedded atom method potentials, three–body potentials, and so on, are potential energy extensions. On the other hand, we could in principle, take any extension and modify it, thus changing the force decomposition. Consider for example a pair potential extension with a range of interaction defined by r_{cut} at a configuration $\boldsymbol{x} \in \mathbb{R}^{3N}$,

$$\mathcal{V}_2(\boldsymbol{\zeta}) = \sum_{\alpha\beta \in E_{\boldsymbol{x}}} \phi(\zeta_{\alpha\beta}), \tag{3.3.10}$$

where ϕ is a pair potential function which satisfies $\phi(r) = 0$ for $r \geq r_{\text{cut}}$, and the set of arguments $\boldsymbol{\zeta} = \{\zeta_{\alpha\beta}\} \in \mathbb{R}^e$ are arbitrary numbers corresponding to the bonds in $E_{\boldsymbol{x}}$. The value of $\mathcal{V}_2$ only corresponds to a physical prediction when $\zeta_{\alpha\beta} = r_{\alpha\beta} = \|\boldsymbol{x}_\alpha - \boldsymbol{x}_\beta\|$. To create an alternate extension with the same cutoff radius, we can add to $\mathcal{V}_2$ a function of distance arguments which is identically zero for all sets of arguments that correspond to actual physical local distances between particles. This is satisfied by the so-called *Cayley–Menger (CM) determinant* [AT10]. The CM determinant, $\chi_k(r_{12}, \ldots, r_{(k-1)k})$ of a set of k particles represents the volume of a simplex formed by k particles in a $(k-1)$–dimensional space. For example, χ_5 represents the volume of a 5-simplex in four dimensions. If the five particles are embedded in 3-dimensions, then this volume is zero by construction.[11]

[10] See Section II.B of [AT11] for a concise discussion of extensions of potential energy functions and an explanation of why $\partial\breve{\mathcal{V}}/\partial r_{\alpha\beta}$ is undefined.

[11] As a simple example, consider 3 particles constrained to move on a line. Assume the particles interact

Returning to (3.3.10), we construct the following alternate potential. Without loss of generality, we assume that in the present configuration $\boldsymbol{x}$, particles $1, \ldots, 5$ form a local cluster of size less than $r_{\rm cut}$, or in other words all the edges connecting particles $1, \ldots, 5$ are in $E_{\boldsymbol{x}}$. We define an alternate extension as

$$\mathcal{V}_{\rm alt}(\boldsymbol{\zeta}) = \sum_{\alpha\beta \in E_{\boldsymbol{x}}} \phi(\zeta_{\alpha\beta}) + \chi_5(\zeta_{12}, \zeta_{13}, \ldots, \zeta_{45}), \tag{3.3.11}$$

where χ_5 is the CM determinant for a cluster of 5 particles. Thus, $\chi_{5|\mathcal{S}_{\boldsymbol{x}}} = 0$, and so $\mathcal{V}_{\rm alt}$ and $\mathcal{V}_2$ agree on $\mathcal{S}_{\boldsymbol{x}}$. By choosing a cluster of size less than $r_{\rm cut}$, we ensure that the cutoff radius of $\mathcal{V}_{\rm alt}$ remains $r_{\rm cut}$. It can be easily shown (see [AT10]) that the force decomposition resulting from $\mathcal{V}_{\rm alt}$ differs from that obtained from $\mathcal{V}_2$. This leads us to the question:

> Are the potential energy extensions used in practice the appropriate ones to be used for calculating the stress tensor?

In order to explore the above question, we next consider the possible quantum mechanical origins of potential energy extensions. In practice, potential energy extensions are obtained by a priori choosing a functional form for $\mathcal{V}$. The parameters in the functional form are evaluated by fitting $\mathcal{V}$ to the Born-Oppenheimer potential energy $\widehat{\mathcal{V}}$ which is obtained as an eigenvalue in the solution to the Schödinger wave equation under the Born–Oppenheimer approximation [TM11]. It is clear from (3.3.11) that a fitted functional form can be altered using a CM determinant without affecting the fit. To our knowledge, there is no rigorous method of choosing a single functional form for $\mathcal{V}$ from the wave function obtained by solving the Schrödinger wave equation. Therefore, it is not clear how the non-uniqueness of the potential energy extension can be avoided using the quantum mechanical model.[12]

---

via a pair potential, $\mathcal{V}_2 = \phi(\zeta_{12}) + \phi(\zeta_{13}) + \phi(\zeta_{23})$. This function gives the energy of the particles when $(\zeta_{12}, \zeta_{13}, \zeta_{23}) = (r_{12}, r_{13}, r_{23})$, where r_{12}, r_{13} and r_{23} are the distances between the particles. An alternate extension is constructed as

$$\mathcal{V}_{\rm alt} = \mathcal{V}_2(\zeta_{12}, \zeta_{13}, \zeta_{23}) + \chi(\zeta_{12}, \zeta_{13}, \zeta_{23}),$$

where χ is the one-dimensional CM determinant for 3 particles:

$$\chi(\zeta_{12}, \zeta_{13}, \zeta_{23}) = (\zeta_{13} - \zeta_{23} - \zeta_{12})(\zeta_{12} - \zeta_{13} - \zeta_{23})(\zeta_{23} - \zeta_{12} - \zeta_{13})(\zeta_{12} + \zeta_{13} + \zeta_{23}).$$

It is clear that χ simply reflects the geometric constraint on the particle distances. For example if the particles are ordered $x_1 < x_2 < x_3$, then the distances must satisfy $r_{12} + r_{23} = r_{13}$, this is enforced by the first term on the right-hand side above. The other terms correspond to other orderings of the particles. Thus $\chi(\zeta_{12}, \zeta_{13}, \zeta_{23})$ is identically zero whenever the arguments $\zeta_{\alpha\beta}$ correspond to actual distances between particles, e.g. $\chi(1, 2, 1)$ is zero, but $\chi(1, 1, 1)$ (which is not physical) is non-zero.

[12] Recently, Murdoch in his book [Mur12] has addressed some of the issues we have raised [AT10] regarding the force decomposition and its relationship to quantum mechanics. According to Murdoch, $\boldsymbol{f}_{\alpha\beta}$

In the absence of a physically-motivated unique force decomposition, we now focus our attention on characterizing the non-uniqueness of the atomistic stress tensor by decomposing it into an extension-dependent part and an extension-independent part. We will then see in Section 3.5 that this decomposition has an interesting analog in continuum mechanics.

3.4 Decomposition of the atomistic stress into an irrotational and a solenoidal part

In this section, we propose a decomposition for the potential part of the atomistic stress tensor $\boldsymbol{\sigma}_{\mathrm{v}}$ into an extension-independent part $\boldsymbol{\sigma}_{\mathrm{v}}^{\parallel}$, and an extension-dependent part $\boldsymbol{\sigma}_{\mathrm{v}}^{\perp}$. In other words, altering the potential energy extension does not affect $\boldsymbol{\sigma}_{\mathrm{v}}^{\parallel}$.

3.4.1 Theoretical derivation of the atomistic stress decomposition

Let $\boldsymbol{x} \in \mathbb{R}^{3N}$ denote the configuration of interest, and let $\boldsymbol{p} = \boldsymbol{R}(\boldsymbol{x}) \in \mathcal{S}_{\boldsymbol{x}}$ denote a point on the local shape space corresponding to $\boldsymbol{x}$. This is depicted schematically in Fig. 3.1 with $\mathcal{S}_{\boldsymbol{x}}$ shown as a surface in $\mathbb{R}^e$, where e is the cardinality of $E_{\boldsymbol{x}}$. Recall that the atomistic stress tensor depends on the choice of the force decomposition which depends on the choice of potential energy extension. For a given extension $\mathcal{V}$, a candidate for the central force decomposition of the forces $\boldsymbol{f}_\alpha \, (\alpha = 1, \dots, N)$ is given in (3.3.9), where the magnitude of force $\boldsymbol{f}_{\alpha\beta}$ is given by

$$f_{\alpha\beta} = \begin{cases} -\left.\dfrac{\partial \mathcal{V}}{\partial r_{\alpha\beta}}\right|_{\boldsymbol{R}(\boldsymbol{x})} & \text{if } \alpha\beta \in E_{\boldsymbol{x}}, \\ 0 & \text{otherwise.} \end{cases} \tag{3.4.1}$$

Let $(f_{\alpha\beta})$ denote the ordered e-tuple given by the set $\{f_{\alpha\beta} : \alpha\beta \in E_{\boldsymbol{x}}\}$ with the ordering given in (3.3.3).[13] The vector $(f_{\alpha\beta}) \in \mathbb{R}^e$ is shown in Fig. 3.1. Let $\mathscr{T}_{\boldsymbol{p}}\mathcal{S}_{\boldsymbol{x}}$ denote the "tangent space" to the surface $\mathcal{S}_{\boldsymbol{x}}$ at the point $\boldsymbol{p}$, as shown in Fig. 3.1.[14] In order to arrive

is the net force on the subatomic particles of atom α due to the subatomic particles of atom β. Although this viewpoint treats the subatomic particles as classical particles, Murdoch argues that this approach can be extended to a quantum mechanical system. We remain skeptical of this interpretation since the only forces that can be obtained from a quantum mechanical model are the net forces on the particles α and β, under the Born–Oppenheimer approximation using the Hellman–Feynman theorem [TM11].

[13] We will use the shorthand notation $(\square_{\alpha\beta})$ for the ordered tuple given by the set $\{\square_{\alpha\beta} : \alpha\beta \in E_{\boldsymbol{x}}\}$ with the ordering given by (3.3.3).

[14] In mathematics, a tangent space is normally defined for a manifold (see for example [Lee12] for definitions of manifolds and tangent spaces). Note that the surface $\mathcal{S}_{\boldsymbol{x}}$ is not a manifold due to the presence of singular configurations, such as all particles lying on a plane or a line. Thus, $\mathscr{T}_{\boldsymbol{p}}\mathcal{S}_{\boldsymbol{x}}$ is not strictly a tangent

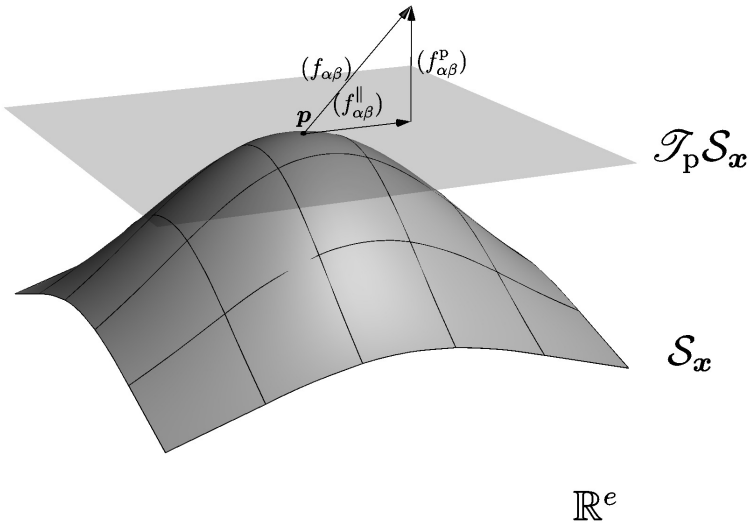

Figure 3.1: Schematic representation of the local shape space at a configuration $\boldsymbol{x} \in \mathbb{R}^{3N}$ as a surface embedded in $\mathbb{R}^e$. In addition, the tangent space $\mathscr{T}_{\boldsymbol{p}}\mathcal{S}_{\boldsymbol{x}}$ of the local shape space at the point $\boldsymbol{p} = \boldsymbol{R}(\boldsymbol{x})$ is shown. The vectors $(f^{\parallel}_{\alpha\beta}) \in \mathscr{T}_{\boldsymbol{p}}\mathcal{S}_{\boldsymbol{x}}$ and $(f^{\perp}_{\alpha\beta}) \in \mathscr{T}_{\boldsymbol{p}}\mathcal{S}^{\perp}_{\boldsymbol{x}}$.

at a decomposition for the atomistic stress tensor, we split the vector $(f_{\alpha\beta})$ by projecting it onto the tangent space, and its orthogonal complement[15] $\mathscr{T}_{\boldsymbol{p}}\mathcal{S}^{\perp}_{\boldsymbol{x}}$ in $\mathbb{R}^e$, as shown in Fig. 3.1. In other words,

$$(f_{\alpha\beta}) = (f^{\parallel}_{\alpha\beta}) + (f^{\perp}_{\alpha\beta}), \tag{3.4.2}$$

where $(f^{\parallel}_{\alpha\beta}) \in \mathscr{T}_{\boldsymbol{p}}\mathcal{S}_{\boldsymbol{x}}$, and $(f^{\perp}_{\alpha\beta}) \in \mathscr{T}_{\boldsymbol{p}}\mathcal{S}^{\perp}_{\boldsymbol{x}}$. We can now define sets of interatomic forces:

$$\boldsymbol{f}_{\alpha\beta} = f_{\alpha\beta}\frac{\boldsymbol{x}_\alpha - \boldsymbol{x}_\beta}{r_{\alpha\beta}}, \quad \boldsymbol{f}^{\parallel}_{\alpha\beta} = f^{\parallel}_{\alpha\beta}\frac{\boldsymbol{x}_\alpha - \boldsymbol{x}_\beta}{r_{\alpha\beta}}, \quad \boldsymbol{f}^{\perp}_{\alpha\beta} = f^{\perp}_{\alpha\beta}\frac{\boldsymbol{x}_\alpha - \boldsymbol{x}_\beta}{r_{\alpha\beta}}. \tag{3.4.3}$$

From (3.4.2) and (3.4.3), the vector $\boldsymbol{f}_{\alpha\beta}$ splits as

$$\boldsymbol{f}_{\alpha\beta} = \boldsymbol{f}^{\parallel}_{\alpha\beta} + \boldsymbol{f}^{\perp}_{\alpha\beta}. \tag{3.4.4}$$

space. Nevertheless, we use this terminology, because the definition we adopt (given below in (3.4.6)) is equivalent to the conventional definition at non-singular points.

[15] An orthogonal complement $V^{\perp}$ of a vector subspace V of $\mathbb{R}^e$ is defined as

$$V^{\perp} := \{\boldsymbol{w} \in \mathbb{R}^e : \boldsymbol{w} \cdot \boldsymbol{v} = 0 \text{ for all } \boldsymbol{v} \in V\}.$$

Since the atomistic stress tensor given in (3.2.14) depends linearly on $\boldsymbol{f}_{\alpha\beta}$, (3.4.4) results in the following decomposition of the atomistic stress tensor:

$$\boldsymbol{\sigma}_{\mathrm{v}} = \boldsymbol{\sigma}_{\mathrm{v}}^{\parallel} + \boldsymbol{\sigma}_{\mathrm{v}}^{\perp}. \tag{3.4.5}$$

In order to formalize the geometric idea described above, we rigorously define the vector spaces $\mathscr{T}_{\boldsymbol{p}}\mathcal{S}_{\boldsymbol{x}}$ and $\mathscr{T}_{\boldsymbol{p}}\mathcal{S}_{\boldsymbol{x}}^{\perp}$ using the local rigidity map defined in (3.3.5). For each point $\boldsymbol{y} \in \mathcal{N}_{\boldsymbol{x}}$, there exists a *tangent map* $T_{\boldsymbol{x}}\boldsymbol{R} : \mathbb{R}^{3N} \mapsto \mathbb{R}^{e}$, which maps the tangent space of $\mathcal{N}_{\boldsymbol{x}}$ at $\boldsymbol{y}$ to the tangent space of $\mathbb{R}^{e}$ at $\boldsymbol{R}(\boldsymbol{x}) \in \mathcal{S}_{\boldsymbol{x}}$.[16] We define the vector space $\mathscr{T}_{\boldsymbol{p}}\mathcal{S}_{\boldsymbol{x}}$ as the image of the map $T_{\boldsymbol{x}}\boldsymbol{R}$:

$$\mathscr{T}_{\boldsymbol{p}}\mathcal{S}_{\boldsymbol{x}} := \operatorname{Im} T_{\boldsymbol{x}}\boldsymbol{R} \subset \mathbb{R}^{e}. \tag{3.4.6}$$

Intuitively, the tangent map at $\boldsymbol{x}$ is a linear map that maps a "perturbation" of $\boldsymbol{x}$ in $\mathcal{N}_{\boldsymbol{x}}$ to a perturbation of $\boldsymbol{R}(\boldsymbol{x})$ in $\mathbb{R}^{e}$. A perturbation in $\boldsymbol{x}$ can be described as a vector in $\mathbb{R}^{3N}$, while a perturbation in $\boldsymbol{R}(\boldsymbol{x})$ is described as a vector in $\mathscr{T}_{\boldsymbol{p}}\mathcal{S}_{\boldsymbol{x}}$.

We now give an explicit construction of $\mathscr{T}_{\boldsymbol{p}}\mathcal{S}_{\boldsymbol{x}}$ defined in (3.4.6). A coordinate representation of $T_{\boldsymbol{x}}\boldsymbol{R}$, in the Cartesian coordinate system of $\mathbb{R}^{3N}$ and $\mathbb{R}^{e}$ is given by the Jacobian matrix $\mathfrak{R}_{\boldsymbol{x}}$ evaluated at the point $\boldsymbol{x}$ for the map $\boldsymbol{R}$. $\mathfrak{R}_{\boldsymbol{x}}$ is a matrix of size $e \times 3N$, with the following form. For each bond $i \in \{1, 2, \ldots, e\}$, which refers to a bond, say $\alpha\beta$,

$$(\mathfrak{R}_{\boldsymbol{x}})_{ij} = \begin{cases} (\boldsymbol{x}_{\alpha} - \boldsymbol{x}_{\beta})_k / r_{\alpha\beta}, & j \in \{3(\alpha-1)+k : k = 1,2,3\}, \\ (\boldsymbol{x}_{\beta} - \boldsymbol{x}_{\alpha})_k / r_{\alpha\beta}, & j \in \{3(\beta-1)+k : k = 1,2,3\}, \\ 0, & \text{otherwise.} \end{cases} \tag{3.4.7}$$

From the definition of the Jacobian in (3.4.7), the action of $\mathfrak{R}_{\boldsymbol{x}}$ on $\boldsymbol{u} = (\boldsymbol{u}_1, \ldots, \boldsymbol{u}_N) \in \mathbb{R}^{3N}$ is given by

$$(\mathfrak{R}_{\boldsymbol{x}}\boldsymbol{u})_{\alpha\beta} = \frac{(\boldsymbol{u}_{\alpha} - \boldsymbol{u}_{\beta}) \cdot (\boldsymbol{x}_{\alpha} - \boldsymbol{x}_{\beta})}{r_{\alpha\beta}}, \tag{3.4.8}$$

where $\boldsymbol{u}$ can be viewed as a first-order approximation to a perturbation of $\boldsymbol{x}$, and $\mathfrak{R}_{\boldsymbol{x}}\boldsymbol{u}$ can be viewed as a first-order approximation to the corresponding perturbation of the interatomic distances. Since $\mathfrak{R}_{\boldsymbol{x}}$ is a representation of $T_{\boldsymbol{x}}\boldsymbol{R}$, from (3.4.6) we have the following

[16] Since $\mathcal{N}_{\boldsymbol{x}}$ is an open subset of $\mathbb{R}^{3N}$, the tangent space of $\mathcal{N}_{\boldsymbol{x}}$ at any point $\boldsymbol{y} \in \mathcal{N}_{\boldsymbol{x}}$ is isomorphic to $\mathbb{R}^{3N}$.

explicit construction of $\mathscr{T}_{\boldsymbol{p}}\mathcal{S}_{\boldsymbol{x}}$:

$$\mathscr{T}_{\boldsymbol{p}}\mathcal{S}_{\boldsymbol{x}} = \operatorname{Im}\mathfrak{R}_{\boldsymbol{x}}, \tag{3.4.9}$$

$$= \operatorname{span}\{\mathfrak{R}_{\boldsymbol{x}}|\{\boldsymbol{u}_i : i = 1, \ldots, N\} \text{ form a basis of } \mathbb{R}^{3N}\}. \tag{3.4.10}$$

Note that the vectors $T_{\boldsymbol{x}}\boldsymbol{R}(\boldsymbol{u}_i)$ in (3.4.10) *do not* form a basis for $\mathscr{T}_{\boldsymbol{p}}\mathcal{S}_{\boldsymbol{x}}$ because the Jacobian maps the perturbation vectors $\boldsymbol{u}$ corresponding to translations and rotations to the zero vector.[17] Since $(\operatorname{Im}\mathfrak{R}_{\boldsymbol{x}})^{\perp} = \operatorname{Ker}\mathfrak{R}_{\boldsymbol{x}}^{\mathrm{T}}$, from (3.4.9) we have

$$\mathscr{T}_{\boldsymbol{p}}\mathcal{S}_{\boldsymbol{x}}^{\perp} = \operatorname{Ker}\mathfrak{R}_{\boldsymbol{x}}^{\mathrm{T}}, \tag{3.4.11}$$

where

$$\operatorname{Ker}\mathfrak{R}_{\boldsymbol{x}}^{\mathrm{T}} := \{\boldsymbol{v} \in \mathbb{R}^e | \mathfrak{R}_{\boldsymbol{x}}^{\mathrm{T}}\boldsymbol{v} = \boldsymbol{0}\}. \tag{3.4.12}$$

We now have the following characterization of $\mathscr{T}_{\boldsymbol{p}}\mathcal{S}_{\boldsymbol{x}}^{\perp}$. From the definition of $\mathfrak{R}_{\boldsymbol{x}}$ given in (3.4.7), the action of $\mathfrak{R}_{\boldsymbol{x}}^{\mathrm{T}}$ on an arbitrary $(v_{\alpha\beta}) \in \mathbb{R}^e$, is given by[18]

$$(\mathfrak{R}_{\boldsymbol{x}}^{\mathrm{T}}\boldsymbol{v})_{\alpha} = \sum_{\substack{\beta \\ \alpha\beta \in E_{\boldsymbol{x}}}} v_{\alpha\beta}\frac{\boldsymbol{x}_{\alpha} - \boldsymbol{x}_{\beta}}{r_{\alpha\beta}}, \quad \alpha = 1, \ldots, N. \tag{3.4.13}$$

From (3.4.11), (3.4.12) and (3.4.13), it is clear that $\mathscr{T}_{\boldsymbol{p}}\mathcal{S}_{\boldsymbol{x}}^{\perp}$ consists of all $(g_{\alpha\beta})$ which result in zero force on each particle. In other words

$$(g_{\alpha\beta}) \in \ker\mathfrak{R}_{\boldsymbol{x}}^{\mathrm{T}} \iff \boldsymbol{0} = \sum_{\alpha\beta \in E_{\boldsymbol{x}}} \boldsymbol{g}_{\alpha\beta}. \tag{3.4.14}$$

We collect the above results in the following theorem.

Theorem 3. *Let $\boldsymbol{R} : \mathcal{N}_{\boldsymbol{x}} \to \mathcal{S}_{\boldsymbol{x}}$ be a mapping of the local configuration space onto the local shape space at $\boldsymbol{x}$. Let $(\boldsymbol{u}_i : i = 1, \ldots, N)$ be an ordered basis of $\mathbb{R}^{3N}$. For any $\boldsymbol{x} \in \mathbb{R}^{3N}$, the vector space $\mathscr{T}_{\boldsymbol{p}}\mathcal{S}_{\boldsymbol{x}}$, and its complimentary space $\mathscr{T}_{\boldsymbol{p}}\mathcal{S}_{\boldsymbol{x}}^{\perp}$ are described by the*

[17] A perturbation $\boldsymbol{u}$ of the form $(\boldsymbol{c}, \ldots, \boldsymbol{c})$, where $\boldsymbol{c}$ is an arbitrary vector in $\mathbb{R}^3$ corresponds to translations, and a perturbation vector of the form $\boldsymbol{u} = (\boldsymbol{u}_1, \ldots, \boldsymbol{u}_N)$, where $\boldsymbol{u}_{\alpha} = \boldsymbol{W}\boldsymbol{x}_{\alpha}$, and W is an arbitrary skew symmetric tensor, corresponds to an infinitesimal rotation.

[18] $\boldsymbol{v}$ can be viewed as a first-order approximation to a perturbation of $(f_{\alpha\beta}) \in \mathbb{R}^e$, and $\mathfrak{R}_{\boldsymbol{x}}^{\mathrm{T}}\boldsymbol{v}$ can be viewed as a first-order approximation to the corresponding perturbation in the net forces on the particles.

Jacobian $\mathfrak{R}_{\boldsymbol{x}}$ of the rigidity map $\boldsymbol{R}$ as

$$\mathscr{T}_{\boldsymbol{p}}\mathcal{S}_{\boldsymbol{x}} = \operatorname{span}\{\mathfrak{R}_{\boldsymbol{x}}\boldsymbol{u}_i : i = 1, \dots, N\}, \tag{3.4.15}$$

$$\mathscr{T}_{\boldsymbol{p}}\mathcal{S}_{\boldsymbol{x}}^{\perp} = \{(g_{\alpha\beta}) \in \mathbb{R}^e : \sum_{\substack{\beta \\ \alpha\beta \in E_{\boldsymbol{x}}}} \boldsymbol{g}_{\alpha\beta} = \boldsymbol{0} \text{ for each } \alpha = 1, \dots, N\}. \tag{3.4.16}$$

Moreover, the vectors space $\mathbb{R}^e$ splits as

$$\mathbb{R}^e = \operatorname{im}\mathfrak{R}_{\boldsymbol{x}} \oplus \ker\mathfrak{R}_{\boldsymbol{x}}^{\mathrm{T}}, \tag{3.4.17}$$

where $\oplus$ denotes direct sum between vector spaces.

In the following corollary, we deduce some properties of $(f_{\alpha\beta}^{\parallel}) \in \mathscr{T}_{\boldsymbol{p}}\mathcal{S}_{\boldsymbol{x}}$ and $(f_{\alpha\beta}^{\perp}) \in \mathscr{T}_{\boldsymbol{p}}\mathcal{S}_{\boldsymbol{x}}^{\perp}$ and the associated $\mathbb{R}^{3e}$-dimensional vectors $(\boldsymbol{f}_{\alpha\beta}^{\parallel})$ and $(\boldsymbol{f}_{\alpha\beta}^{\perp})$, defined in (3.4.3), where we use the notation in footnote 13.

Corollary 2. *For a given potential energy extension, there exist unique vectors $(f_{\alpha\beta}^{\parallel}) \in \mathscr{T}_{\boldsymbol{p}}\mathcal{S}_{\boldsymbol{x}}$, and $(f_{\alpha\beta}^{\perp}) \in \mathscr{T}_{\boldsymbol{p}}\mathcal{S}_{\boldsymbol{x}}^{\perp}$, such that the $\mathbb{R}^{3e}$-dimensional vectors formed from them satisfy,*

$$(\boldsymbol{f}_{\alpha\beta}) = (\boldsymbol{f}_{\alpha\beta}^{\parallel}) + (\boldsymbol{f}_{\alpha\beta}^{\perp}). \tag{3.4.18}$$

Moreover, $(\boldsymbol{f}_{\alpha\beta}^{\parallel})$ decomposes the forces $\boldsymbol{f}_\alpha$ $(\alpha = 1, \dots, N)$, and $(\boldsymbol{f}_{\alpha\beta}^{\perp})$ decomposes a null force on each particle, i.e.

$$\boldsymbol{f}_\alpha = \sum_{\substack{\beta \\ \beta \neq \alpha}} \boldsymbol{f}_{\alpha\beta}^{\parallel}, \tag{3.4.19}$$

$$\boldsymbol{0} = \sum_{\substack{\beta \\ \beta \neq \alpha}} \boldsymbol{f}_{\alpha\beta}^{\perp}. \tag{3.4.20}$$

Additionally, $(\boldsymbol{f}_{\alpha\beta}^{\parallel})$ is independent of the choice of the potential extension.

Proof. Equation (3.4.18) follows from (3.4.17) and definitions given in (3.4.3). From the definition of $\boldsymbol{f}_{\alpha\beta}$ in (3.3.9), we know that

$$\boldsymbol{f}_\alpha = \sum_{\substack{\beta \\ \beta \neq \alpha}} \boldsymbol{f}_{\alpha\beta}.$$

From (3.4.18), since each $\boldsymbol{f}_{\alpha\beta}$ is decomposed as $\boldsymbol{f}^{\parallel}_{\alpha\beta} + \boldsymbol{f}^{\perp}_{\alpha\beta}$, we obtain

$$\boldsymbol{f}_\alpha = \sum_{\substack{\beta \\ \beta\neq\alpha}} \left(\boldsymbol{f}^{\parallel}_{\alpha\beta} + \boldsymbol{f}^{\perp}_{\alpha\beta} \right).$$

Since $(f^{\perp}_{\alpha\beta}) \in \mathscr{T}_{\boldsymbol{p}}\mathcal{S}^{\perp}_{\boldsymbol{x}}$, from (3.4.16) it follows that $\sum_{\substack{\beta \\ \beta\neq\alpha}} \boldsymbol{f}^{\perp}_{\alpha\beta} = \boldsymbol{0}$. Therefore,

$$\boldsymbol{f}_\alpha = \sum_{\substack{\beta \\ \beta\neq\alpha}} \boldsymbol{f}^{\parallel}_{\alpha\beta}. \tag{3.4.21}$$

Finally, we show that $(\boldsymbol{f}^{\parallel}_{\alpha\beta})$ is independent of the choice of extension. Suppose that we have an alternate extension, that results in

$$\boldsymbol{f}_\alpha = \sum_{\substack{\beta \\ \beta\neq\alpha}} \tilde{\boldsymbol{f}}^{\parallel}_{\alpha\beta}, \tag{3.4.22}$$

which is an analog of (3.4.21) for the alternate extension. Subtracting (3.4.22) from (3.4.21), we obtain

$$\boldsymbol{0} = \sum_{\substack{\beta \\ \beta\neq\alpha}} \boldsymbol{f}^{\parallel}_{\alpha\beta} - \tilde{\boldsymbol{f}}^{\parallel}_{\alpha\beta}. \tag{3.4.23}$$

Since $(f^{\parallel}_{\alpha\beta})$ and $(\tilde{f}^{\parallel}_{\alpha\beta})$ belong to $\operatorname{Im}\mathfrak{R}_{\boldsymbol{x}}$, it follows that $(f^{\parallel}_{\alpha\beta} - \tilde{f}^{\parallel}_{\alpha\beta}) \in \operatorname{Im}\mathfrak{R}_{\boldsymbol{x}}$. On the other hand, from (3.4.16) and (3.4.23), we conclude that $(f^{\parallel}_{\alpha\beta} - \tilde{f}^{\parallel}_{\alpha\beta}) \in \operatorname{Ker}\mathfrak{R}^{\mathrm{T}}_{\boldsymbol{x}}$. Since $\operatorname{Im}\mathfrak{R} \cap \operatorname{Ker}\mathfrak{R}^{\mathrm{T}}_{\boldsymbol{x}} = \{\boldsymbol{0}\}$, it follows that for each bond, $f^{\parallel}_{\alpha\beta} - \tilde{f}^{\parallel}_{\alpha\beta} = 0$, which is the desired result. □

We now define $\boldsymbol{\sigma}^{\parallel}_{\mathrm{v}}$ and $\boldsymbol{\sigma}^{\perp}_{\mathrm{v}}$ as the distributions obtained by substituting in $\boldsymbol{f}^{\parallel}_{\alpha\beta}$ and $\boldsymbol{f}^{\perp}_{\alpha\beta}$, respectively, in place of $\boldsymbol{f}_{\alpha\beta}$ in the right-hand side of (3.2.17). Since $\boldsymbol{\sigma}_{\mathrm{v}}$ defined in (3.2.17) depends linearly on the forces $\boldsymbol{f}_{\alpha\beta}$, it follows that

$$\boldsymbol{\sigma}_{\mathrm{v}} = \boldsymbol{\sigma}^{\parallel}_{\mathrm{v}} + \boldsymbol{\sigma}^{\perp}_{\mathrm{v}}. \tag{3.4.24}$$

We define the stress tensor fields corresponding to the distributions $\boldsymbol{\sigma}^{\parallel}_{\mathrm{v}}$ and $\boldsymbol{\sigma}^{\perp}_{\mathrm{v}}$ as

$$\boldsymbol{\sigma}^{\parallel}_{w,\mathrm{v}} := w \star \boldsymbol{\sigma}^{\parallel}_{\mathrm{v}}, \tag{3.4.25a}$$

$$\boldsymbol{\sigma}^{\perp}_{w,\mathrm{v}} := w \star \boldsymbol{\sigma}^{\perp}_{\mathrm{v}}. \tag{3.4.25b}$$

In the following two corollaries, we obtain properties of $\boldsymbol{\sigma}^{\parallel}_{w,\mathrm{v}}$ and $\boldsymbol{\sigma}^{\perp}_{w,\mathrm{v}}$.

Corollary 3. *The tensors $\boldsymbol{\sigma}_{w,\mathrm{v}}$, $\boldsymbol{\sigma}^{\parallel}_{w,\mathrm{v}}$ and $\boldsymbol{\sigma}^{\perp}_{w,\mathrm{v}}$, satisfy the equations*

$$\operatorname{div}_{\boldsymbol{x}} \boldsymbol{\sigma}_{w,\mathrm{v}}(\boldsymbol{x},t) = \operatorname{div}_{\boldsymbol{x}} \boldsymbol{\sigma}^{\parallel}_{w,\mathrm{v}}(\boldsymbol{x},t) = \sum_{\alpha} \boldsymbol{f}_{\alpha} w(\boldsymbol{x}_{\alpha}(t) - \boldsymbol{x}), \tag{3.4.26a}$$

$$\operatorname{div}_{\boldsymbol{x}} \boldsymbol{\sigma}^{\perp}_{w,\mathrm{v}}(\boldsymbol{x},t) = \boldsymbol{0}. \tag{3.4.26b}$$

Moreover, $\boldsymbol{\sigma}^{\parallel}_{w,\mathrm{v}}$ is independent of the potential energy extension.

Proof. From (3.4.25) we see that expressions $\boldsymbol{\sigma}^{\parallel}_{w,\mathrm{v}}$ and $\boldsymbol{\sigma}^{\perp}_{w,\mathrm{v}}$ are obtained from (3.2.13) by replacing the forces $\boldsymbol{f}_{\alpha\beta}$ with $\boldsymbol{f}^{\parallel}_{\alpha\beta}$ and $\boldsymbol{f}^{\perp}_{\alpha\beta}$, respectively. Therefore, from Corollary 2, $\boldsymbol{\sigma}^{\parallel}_{w,\mathrm{v}}$ is independent of the potential energy extension. Moreover, since $\boldsymbol{\sigma}_{w,\mathrm{v}}$ satisfies (3.2.10), we have

$$\operatorname{div}_{\boldsymbol{x}} \boldsymbol{\sigma}^{\parallel}_{w,\mathrm{v}}(\boldsymbol{x},t) = \sum_{\substack{\alpha,\beta \\ \alpha<\beta}} \boldsymbol{f}^{\parallel}_{\alpha\beta} w(\boldsymbol{x}_{\alpha} - \boldsymbol{x}) \tag{3.4.27}$$

$$\operatorname{div}_{\boldsymbol{x}} \boldsymbol{\sigma}^{\perp}_{w,\mathrm{v}}(\boldsymbol{x},t) = \sum_{\substack{\alpha,\beta \\ \alpha<\beta}} \boldsymbol{f}^{\perp}_{\alpha\beta} w(\boldsymbol{x}_{\alpha} - \boldsymbol{x}). \tag{3.4.28}$$

Using (3.4.19) and (3.4.20), equation (3.4.26) follows from the above equalities. □

Corollary 4. *Let $\boldsymbol{x} \in \mathbb{R}^{3N}$ be a configuration for which $\boldsymbol{f}_{\alpha} = \boldsymbol{0}$ for each particle α. For such a configuration, $\boldsymbol{\sigma}_{\mathrm{v}}$ has the following trivial decomposition: $\boldsymbol{\sigma}^{\perp}_{\mathrm{v}} = \boldsymbol{\sigma}_{\mathrm{v}}$ and $\boldsymbol{\sigma}^{\parallel}_{\mathrm{v}} = \boldsymbol{0}$.*

Proof. Since the net force on each particle is zero, we have $\sum_{\substack{\beta \\ \beta\neq\alpha}} \boldsymbol{f}_{\alpha\beta} = \boldsymbol{0}$. Therefore, it follows from (3.4.16) that $(f_{\alpha\beta}) \in \mathscr{T}_{\boldsymbol{p}}\mathcal{S}^{\perp}_{\boldsymbol{x}}$. Moreover, from (3.4.17) in Theorem 3, we have $(f^{\parallel}_{\alpha\beta}) = (f_{\alpha\beta})$ and $(f^{\perp}_{\alpha\beta}) = \boldsymbol{0}$. Therefore, $\boldsymbol{\sigma}^{\parallel}_{w,\mathrm{v}} = \boldsymbol{0}$ and $\boldsymbol{\sigma}^{\perp}_{w,\mathrm{v}} = \boldsymbol{\sigma}_{w,\mathrm{v}}$. □

From Corollaries 3 and 4, we see that $\boldsymbol{\sigma}^{\perp}_{w,\mathrm{v}}$ is always divergence-free and $\boldsymbol{\sigma}^{\parallel}_{w,\mathrm{v}}$ is zero in the absence of external loading. Therefore, we refer to $\boldsymbol{\sigma}^{\perp}_{w,\mathrm{v}}$ as the *solenoidal part* of the atomistic stress and $\boldsymbol{\sigma}^{\parallel}_{w,\mathrm{v}}$ as the *irrotational part* of the atomistic stress. The solenoidal part $\boldsymbol{\sigma}^{\perp}_{w,\mathrm{v}}$ is extension-dependent and thus non-unique, whereas the irrotational part $\boldsymbol{\sigma}^{\parallel}_{w,\mathrm{v}}$ is uniquely defined. The terms irrotational and solenoidal are borrowed from the Helmholtz decomposition of vector fields. The choice of this terminology is made clear in the next section where we discuss the Beltrami representation of the continuum Cauchy stress tensor, which is a Helmholtz-like decomposition for symmetric tensor fields.

The decomposition derived in this section has a potential application in the systematic reduction of noise in atomistic fields. Recall from Section 3.2 that one of the sources of non-uniqueness in the Murdoch–Hardy procedure is the choice of the weighting function. The size of the weighting function is chosen to average out the noise which exists due to the discrete nature of the atomistic system, and at the same time preserve the macroscopic feature of the continuum field. A recent article by Ulz et al. [UMP13] proposes an optimal size for the support of the weighting function based on the correlation length of the potential energy function.

We observe in our numerical tests that a large proportion of noise in the atomistic stress exists in the solenoidal part, and a large proportion of its macroscopic features exist in the irrotational part. This suggests using two weighting functions with different-sized supports to obtain the atomistic stress. The weighting function with the larger support will be used to obtain the solenoidal part so that most of the noise is averaged out, and a weighting function with the smaller support will be used to obtain the irrotational part to best preserve the macroscopic features. This results in a systematic reduction of noise which may not be accessible using a single weighting function.

3.4.2 A practical algorithm of the atomistic stress decomposition

We now describe a practical algorithm for decomposing the atomistic stress tensor into its solenoidal and irrotational parts. This requires as to decompose the forces $(\boldsymbol{f}_{\alpha\beta})$ according to (3.4.18).

The input to algorithm is the configuration of the system $\boldsymbol{x}$, the cutoff radius r_{cut}, the potential energy function $\mathcal{V}$, and the weighting function w. The cutoff radius and the configuration are used collect the edges in $E_{\boldsymbol{x}}$. Using $E_{\boldsymbol{x}}$ and $\boldsymbol{x}$, the $e \times 3N$ sparse matrix $\mathfrak{R}_{\boldsymbol{x}}$ defined in (3.4.7) is assembled in sparse format. Each component of $(f_{\alpha\beta})$ defined in (3.4.1) is calculated using the given potential energy extension and assembled as an $e \times 1$ array. The vector $(f^{\parallel}_{\alpha\beta})$ is obtained by projecting it onto the tangent space $\mathscr{T}_{\boldsymbol{p}}\mathcal{S}_{\boldsymbol{x}}$. The projection is implemented as a minimization problem:

$$(f^{\parallel}_{\alpha\beta}) = \operatorname*{argmin}_{\boldsymbol{y}\in\mathscr{T}_{\boldsymbol{p}}\mathcal{S}_{\boldsymbol{x}}} \|\boldsymbol{y} - (f_{\alpha\beta})\|. \tag{3.4.29}$$

Referring to (3.4.15), we see that this is equivalent to setting

$$(f^{\parallel}_{\alpha\beta}) = \mathfrak{R}_{\boldsymbol{x}} u_*, \tag{3.4.30}$$

where u_* is the solution to the following least-squares problem:

$$\boldsymbol{u}_* = \operatorname*{argmin}_{\boldsymbol{u}\in\mathbb{R}^{3N}} \|\mathfrak{R}_{\boldsymbol{x}}\boldsymbol{u} - (f_{\alpha\beta})\|. \tag{3.4.31}$$

In order to solve (3.4.31), we use a linear least squares solver based on the Golub–Kahan bi-diagonalization process [PS82]. Once $(f^{\parallel}_{\alpha\beta})$ are computed, The orthogonal forces follow as $f^{\perp}_{\alpha\beta} = f_{\alpha\beta} - f^{\parallel}_{\alpha\beta}$. The vectors $\boldsymbol{f}_{\alpha\beta}$, $\boldsymbol{f}^{\parallel}_{\alpha\beta}$ and $\boldsymbol{f}^{\perp}_{\alpha\beta}$ are then computed from (3.4.3), and the stress fields $\boldsymbol{\sigma}_{w,\mathrm{v}}$, $\boldsymbol{\sigma}^{\parallel}_{w,\mathrm{v}}$ and $\boldsymbol{\sigma}^{\perp}_{w,\mathrm{v}}$ follow using the weighting function w. The above procedure is summarized in Algorithm 1.

Algorithm 1 Decomposition $\boldsymbol{\sigma}_{w,\mathrm{v}} = \boldsymbol{\sigma}^{\parallel}_{w,\mathrm{v}} + \boldsymbol{\sigma}^{\perp}_{w,\mathrm{v}}$

1: Read the configuration $\boldsymbol{x} = (\boldsymbol{x}_1, \ldots, \boldsymbol{x}_N)$ and the cutoff radius r_{cut} of the potential
2: Using r_{cut} and $\boldsymbol{x}$, collect the edges $E_{\boldsymbol{x}}$ defined in (3.3.4)
3: $e :=$ cardinality of $E_{\boldsymbol{x}}$
4: Construct the sparse $e \times 3N$ rigidity matrix $\mathfrak{R}_{\boldsymbol{x}}$ using (3.4.7)
5: Compute the $e \times 1$ vector $(f_{\alpha\beta})$ using (3.4.1)
6: Solve the minimization problem $\boldsymbol{u}_* = \operatorname{argmin}_{\boldsymbol{u}\in\mathbb{R}^{3N}} \|\mathfrak{R}_{\boldsymbol{x}}\boldsymbol{u} - (f_{\alpha\beta})\|$
7: Compute the $e \times 1$ vectors $(f^{\parallel}_{\alpha\beta}) := \mathfrak{R}_{\boldsymbol{x}}\boldsymbol{u}^*$ and $(f^{\perp}_{\alpha\beta}) = (f_{\alpha\beta}) - (f^{\parallel}_{\alpha\beta})$
8: Compute the vectors $\boldsymbol{f}_{\alpha\beta}$, $\boldsymbol{f}^{\parallel}_{\alpha\beta}$ and $\boldsymbol{f}^{\perp}_{\alpha\beta}$.
9: Using the weighting function w, compute $\boldsymbol{\sigma}_{w,\mathrm{v}}$ given in (3.2.13), and $\boldsymbol{\sigma}^{\parallel}_{w,\mathrm{v}}$, $\boldsymbol{\sigma}^{\perp}_{w,\mathrm{v}}$ given in (3.4.25)

A KIM-compliant Fortran program for performing the decomposition is available as part of the supporting material.[19]

In the next section, we discuss an analogous decomposition of the Cauchy stress tensor in continuum mechanics using the generalized Beltrami representation.

3.5 A Generalized Beltrami representation for the continuum Cauchy stress tensor

Let $\Omega \subset \mathbb{R}^3$ be a bounded open subset with a smooth boundary, and let $\mathscr{V}$ and SYM denote the space of smooth vector fields and smooth symmetric tensor fields on Ω, respectively.

[19]The Knowledgebase of Interatomic Models (KIM) [TES+11, TEPS13] is a project focused on creating standards for atomistic simulations including an application programming interface (API) for information exchange between atomistic simulation codes and interatomic potentials. The Fortran program accompanying this paper works with all interatomic potentials stored in the KIM Repository at `https://openkim.org`, which are compatible with the KIM API standard.

It is well-known from Helmholtz decomposition of vector fields that any $\boldsymbol{u} \in \mathscr{V}$ can be represented in terms of a smooth scalar field ϕ, and a vector field $\boldsymbol{\psi} \in \mathscr{V}$:

$$\boldsymbol{u}(\boldsymbol{x}) = \nabla\phi(\boldsymbol{x}) + \operatorname{curl}\boldsymbol{\psi}(\boldsymbol{x}), \quad \boldsymbol{x} \in \Omega. \tag{3.5.1}$$

The above decomposition is commonly referred to as a "Helmholtz decomposition." A representation similar to (3.5.1) exists for a tensor field $\boldsymbol{T} \in$ SYM, given by

$$\boldsymbol{T}(\boldsymbol{x}) = \operatorname{curl}(\operatorname{curl}\boldsymbol{\Psi}(\boldsymbol{x})) + \frac{1}{2}(\nabla\boldsymbol{v}(\boldsymbol{x}) + \nabla\boldsymbol{v}^{\mathrm{T}}(\boldsymbol{x})), \quad \boldsymbol{x} \in \Omega, \tag{3.5.2}$$

where $\boldsymbol{\Psi} \in$ SYM and $\boldsymbol{v} \in \mathscr{V}$. The representation given in (3.5.2) is commonly referred to as a "generalized Beltrami representation" [Gur63, FS03, FRC05]. Within elasticity theory, Beltrami [Bel92] discovered that in the absence of body force field, a continuum Cauchy stress tensor $\boldsymbol{\sigma}_{\mathrm{c}}$ of the form

$$\boldsymbol{\sigma}_{\mathrm{c}}(\boldsymbol{x}) = \operatorname{curl}(\operatorname{curl}\boldsymbol{\Psi})(\boldsymbol{x}), \tag{3.5.3}$$

identically satisfies the equilibrium equation, $\operatorname{div}_{\boldsymbol{x}}\boldsymbol{\sigma}_{\mathrm{c}} = \boldsymbol{0}$. The representation given in (3.5.3) is commonly referred to as a "Beltrami representation." A question then arose regarding the validity of the converse statement: Does $\operatorname{div}_{\boldsymbol{x}}\boldsymbol{T} = \boldsymbol{0}, \boldsymbol{T} \in$ SYM imply that $\boldsymbol{T}$ has the Beltrami representation given in (3.5.3)? In 1963, Gurtin [Gur63] showed that there exist symmetric tensor fields satisfying $\operatorname{div}_{\boldsymbol{x}}\boldsymbol{T} = \boldsymbol{0}$, which *do not* have a Beltrami representation. In particular, it was shown that a symmetric tensor field $\boldsymbol{T}$ has a Beltrami representation if and only if either of the following two conditions are satisfied:

1. $\operatorname{div}_{\boldsymbol{x}}\boldsymbol{T} = \boldsymbol{0}$ in Ω, and Ω is *non-periphractic*[20].
2. For every closed surface $\mathcal{S} \subset \partial\Omega$,

$$\int_{\mathcal{S}} \boldsymbol{T}(\boldsymbol{x})\boldsymbol{n}(\boldsymbol{x})\, da = \boldsymbol{0} \tag{3.5.4}$$

$$\int_{\mathcal{S}} \boldsymbol{x} \wedge \boldsymbol{T}(\boldsymbol{x})\boldsymbol{n}(\boldsymbol{x})\, da = \boldsymbol{0}, \tag{3.5.5}$$

where $\boldsymbol{n}(\boldsymbol{x})$ is a unit normal field on $\mathcal{S}$, and $\wedge$ denotes the vector cross product.

For an example in which conditions (1) and (2) are not satisfied, consider a periphractic domain such as a hollow sphere of positive thickness. Construct a boundary-value problem

[20] A periphractic domain refers to domains which have holes, but not holes that pierce completely through it.

on this domain by specifying non-zero tractions on the inner and outer surfaces, such that the integrals of tractions on the inner and outer surfaces are non-zero, while the net traction on the body is zero. A linear elastic solution for the given boundary-value problem results in a stress tensor field that does not have a Beltrami representation. Since (3.5.2) "completes" the Beltrami representation, it is a generalization of the Beltrami representation.

Note that for an unbounded domain, the Helmholtz decomposition given in (3.5.1) applies to only smooth functions with a decay property at infinity given by

$$\boldsymbol{u}(\boldsymbol{x}) = \boldsymbol{c} + \boldsymbol{o}(\|\boldsymbol{x}\|^{-\delta}), \tag{3.5.6}$$

for some $\delta > 0$ and $c \in \mathbb{R}^3$. (See [Gur62] for a proof of the Helmholtz decomposition for unbounded domains.) For a given $\boldsymbol{u}$ that decays at infinity, the fields $\nabla\phi$ and $\operatorname{curl}\boldsymbol{\psi}$ are uniquely defined.[21] This follows from the following argument. Assume that there exists an alternate decomposition of $\boldsymbol{u}$ given by $\boldsymbol{u} = \nabla\tilde{\phi} + \operatorname{curl}\tilde{\boldsymbol{\psi}}$, for some scalar and vector fields $\tilde{\phi}$ and $\tilde{\boldsymbol{\psi}}$ respectively, such that $\nabla\phi \not\equiv \nabla\tilde{\phi}$. This implies $\triangle(\phi - \tilde{\phi}) = 0$, and since ϕ and $\tilde{\phi}$ satisfy the decay property given in (3.5.6), $\phi - \tilde{\phi}$ is bounded. From the maximum principle [RR04] for harmonic functions, we know that the only harmonic function on $\mathbb{R}^3$ that is bounded is a constant function. Therefore, ϕ and $\tilde{\phi}$ differ by a constant, which implies $\nabla\phi \equiv \nabla\tilde{\phi}$, a contradiction. On the other hand, the decomposition given in (3.5.1) is *not* unique for bounded domains. This can be easily seen by altering an existing decomposition $\boldsymbol{u} = \nabla\phi + \operatorname{curl}\boldsymbol{\psi}$ to $\boldsymbol{u} = \nabla(\phi + h) + \operatorname{curl}(\boldsymbol{\psi} - \widehat{\boldsymbol{\psi}})$, where h is a harmonic potential on Ω, and $\widehat{\boldsymbol{\psi}}$ is a vector field such that[22] $\operatorname{curl}\widehat{\boldsymbol{\psi}} = \nabla h$. A unique decomposition can be obtained for bounded domains, if an additional condition

$$\operatorname{curl}\boldsymbol{\psi}(\boldsymbol{x}) \cdot \boldsymbol{n}(\boldsymbol{x}) = 0, \quad \boldsymbol{x} \in \partial\Omega, \tag{3.5.7}$$

is imposed on $\boldsymbol{\psi}$. We therefore have the following orthogonal decomposition of $\mathscr{V}$, equipped with the L^2 inner product for bounded domains:

$$\mathscr{V} = \{\nabla\phi : \phi \in \mathscr{S}\} \oplus^{\perp} \{\operatorname{curl}\boldsymbol{\psi} : \operatorname{curl}\boldsymbol{\psi} \cdot \boldsymbol{n} = 0 \text{ on } \partial\Omega, \boldsymbol{\psi} \in \mathscr{V}\}. \tag{3.5.8}$$

See [Ghi10] for a discussion on various other Helmholtz orthogonal decompositions of square-integrable vector fields.

[21] Note that this does not mean that ϕ and $\boldsymbol{\psi}$ are unique.

[22] Since $\operatorname{div}(\nabla h) = 0$, there exists a vector field $\widehat{\boldsymbol{\psi}}$ such that $\operatorname{curl}\widehat{\boldsymbol{\psi}} = \nabla h$. For a proof, see [GR79].

Similar to the above discussion on vector fields, the decomposition for tensor fields given in (3.5.2) is not unique. This can be seen from the following example. Consider a solution for the displacement field $\widehat{\boldsymbol{v}}$ for a linear elastic boundary-value problem on a non-periphractic domain with the elasticity tensor $\mathbb{C}$ equal to identity tensor.[23] Then the resulting continuum stress tensor field is given by

$$\widehat{\boldsymbol{\sigma}} = \frac{1}{2}(\nabla\widehat{\boldsymbol{v}} + \nabla\widehat{\boldsymbol{v}}^{\mathrm{T}}). \tag{3.5.9}$$

On the other hand, since $\operatorname{div}\widehat{\boldsymbol{\sigma}} = \boldsymbol{0}$, and the domain is non-periphractic, from condition 1 we know that there exists a $\widehat{\boldsymbol{\Psi}} \in \mathrm{SYM}$, such that

$$\widehat{\boldsymbol{\sigma}} = \operatorname{curl}(\operatorname{curl}\widehat{\boldsymbol{\Psi}}). \tag{3.5.10}$$

Using (3.5.9) and (3.5.10), we can now alter an existing decomposition for a tensor field $\boldsymbol{T} \in \mathrm{SYM}$, given in (3.5.2), by changing $\boldsymbol{\Psi}$ and $\boldsymbol{v}$ to $\boldsymbol{\Psi} + \widehat{\boldsymbol{\Psi}}$ and $\boldsymbol{v} - \widehat{\boldsymbol{v}}$, respectively. A unique decomposition of a tensor field is obtained if we impose the following additional condition on $\boldsymbol{\Psi}$:

$$\operatorname{curl}(\operatorname{curl}\boldsymbol{\Psi}(\boldsymbol{x}))\boldsymbol{n}(\boldsymbol{x}) = \boldsymbol{0}, \quad \boldsymbol{x} \in \partial\Omega. \tag{3.5.11}$$

Equation (3.5.11) is an analog of (3.5.7) for tensor fields. Therefore, the continuum Cauchy stress can be uniquely decomposed as

$$\boldsymbol{\sigma}_{\mathrm{c}} = \boldsymbol{\sigma}_{\mathrm{c}}^{\parallel} + \boldsymbol{\sigma}_{\mathrm{c}}^{\perp}, \tag{3.5.12}$$

where for some $\boldsymbol{v} \in \mathscr{V}$ and $\boldsymbol{\Psi} \in \mathrm{SYM}$,

$$\boldsymbol{\sigma}_{\mathrm{c}}^{\parallel}(\boldsymbol{x}) = \frac{1}{2}(\nabla\boldsymbol{v}(\boldsymbol{x}) + \nabla\boldsymbol{v}^{\mathrm{T}}(\boldsymbol{x})), \qquad \boldsymbol{x} \in \Omega, \tag{3.5.13a}$$

$$\boldsymbol{\sigma}_{\mathrm{c}}^{\perp}(\boldsymbol{x}) = \operatorname{curl}(\operatorname{curl}\boldsymbol{\Psi}(\boldsymbol{x})), \qquad \boldsymbol{x} \in \Omega, \tag{3.5.13b}$$

$$(\boldsymbol{\sigma}_{\mathrm{c}}^{\perp}\boldsymbol{n})(\boldsymbol{x}) = \boldsymbol{0}, \qquad \boldsymbol{x} \in \partial\Omega. \tag{3.5.13c}$$

In other words, we have the following orthogonal decomposition of SYM, equipped with the L^2 inner product:

$$\begin{aligned}\mathrm{SYM} =& \{\nabla\boldsymbol{v} + \nabla\boldsymbol{v}^{\mathrm{T}} : \boldsymbol{v} \in \mathscr{V}\}\oplus^{\perp} \\ & \{\operatorname{curl}\operatorname{curl}\boldsymbol{\Psi} : \operatorname{curl}(\operatorname{curl}\boldsymbol{\psi})\boldsymbol{n} = \boldsymbol{0} \text{ on } \partial\Omega, \boldsymbol{\Psi} \in \mathrm{SYM}\}.\end{aligned} \tag{3.5.14}$$

[23] Since the fourth-order identity tensor is strongly elliptic, it follows that a unique solution $\widehat{\boldsymbol{v}}$ exists.

It is clear from (3.5.13) that $\boldsymbol{\sigma}_{\mathrm{c}}^{\parallel}$ is the "irrotational" part, and $\boldsymbol{\sigma}_{\mathrm{c}}^{\perp}$ is the traction-free "solenoidal part" of $\boldsymbol{\sigma}_{\mathrm{c}}$.

We now identify and motivate the following analogies between the atomistic entities defined in Section 3.4 and the continuum entities.

1. Local shape space and strain analogy:

$$\begin{array}{l}\text{Tangent space of the}\\ \text{local shape space}\end{array} \quad \leftrightarrow \quad \begin{array}{l}\text{Set of compatible}\\ \text{strain fields}\end{array}. \tag{3.5.15}$$

   A vector in the tangent space may be viewed as a compatible perturbation of distances. At the same time, we know that a compatible strain field is a first-order approximation of the left and right Cauchy–Green strain tensor fields, which describe the changes in the length of infinitesimal material vectors. This motivates the analogy given in (3.5.15).

2. Atomistic and continuum stress analogy:

$$\boldsymbol{\sigma}_{w,\mathrm{v}}^{\parallel} \quad \leftrightarrow \quad \boldsymbol{\sigma}_{\mathrm{c}}^{\parallel}, \tag{3.5.16}$$

$$\boldsymbol{\sigma}_{w,\mathrm{v}}^{\perp} \quad \leftrightarrow \quad \boldsymbol{\sigma}_{\mathrm{c}}^{\perp}. \tag{3.5.17}$$

   Recall that $\boldsymbol{\sigma}_{w,\mathrm{v}}^{\parallel}$ is defined using $(f_{\alpha\beta}^{\parallel})$, which is the projection of $(f_{\alpha\beta})$ onto the tangent space of $\mathcal{S}_{\boldsymbol{x}}$ (see Theorem 3). At the same time, from (3.5.14), (3.5.12) and the following identities,

$$\mathrm{curl}(\mathrm{curl}(\nabla \boldsymbol{v} + \nabla \boldsymbol{v}^{\mathrm{T}})) \equiv \mathbf{0}, \qquad \mathrm{div}(\mathrm{curl}(\mathrm{curl}\, \boldsymbol{\Psi})) \equiv \mathbf{0}, \tag{3.5.18}$$

   it follows that $\boldsymbol{\sigma}_{\mathrm{c}}^{\parallel}$ is the projection of $\boldsymbol{\sigma}_{\mathrm{c}}$ onto the space of compatible strain fields on Ω. This motivates the analogies given in (3.5.16) and (3.5.17).

In this paper, we do not subject the above analogies to further rigorous treatment. Instead, we check their validity using a numerical test in the next section.

3.6 Numerical test

In this section, we use a numerical example to compare the decompositions of the atomistic and continuum stress tensors given in Sections 3.4 and 3.5. We consider the linear elastic problem of an anisotropic infinite plate with a hole subjected to a uniaxial loading

at infinity. For the sake of comparison, the plate material is taken to be single crystal Ar in the face-centered cubic (fcc) structure.

3.6.1 Decomposition of the continuum stress

The continuum linear elastic constitutive law is given by

$$\boldsymbol{\sigma}_{\mathrm{c}} = \mathbb{C}\frac{\nabla \boldsymbol{u}_{\mathrm{c}} + \nabla \boldsymbol{u}_{\mathrm{c}}^{\mathrm{T}}}{2}, \tag{3.6.1}$$

where $\mathbb{C}$ is the fourth-order elasticity tensor. The continuum boundary-value problem is

$$\operatorname{div} \boldsymbol{\sigma}_{\mathrm{c}}(\boldsymbol{x}) = \boldsymbol{0} \quad \text{for} \quad \boldsymbol{x} \in \Omega, \tag{3.6.2a}$$

$$\boldsymbol{\sigma}_{\mathrm{c}}(\boldsymbol{x}) \to \boldsymbol{\sigma}_{\infty} \text{ as } \|\boldsymbol{x}\| \to \infty, \tag{3.6.2b}$$

where $\boldsymbol{\sigma}_{\infty} = \sigma_{\infty}(\boldsymbol{e}_1 \otimes \boldsymbol{e}_1)$ is a constant uniaxial stress tensor. This problem is commonly referred to as the *Kirsch problem*, and the exact analytical solution $\boldsymbol{u}_{\mathrm{c}}$ can be found in [Lek63]. For this numerical test, we assume that the loading at infinity and the hole axes are parallel to the crystallographic axes of the plate. The continuum stress $\boldsymbol{\sigma}_{\mathrm{c}}$ can then be evaluated from $\boldsymbol{u}_{\mathrm{c}}$ using (3.6.1). We now decompose $\boldsymbol{\sigma}_{\mathrm{c}}$ into $\boldsymbol{\sigma}_{\mathrm{c}}^{\parallel}$ and $\boldsymbol{\sigma}_{\mathrm{c}}^{\perp}$.

Since $\boldsymbol{\sigma}_{\mathrm{c}}^{\perp}$ is divergence-free and traction-free (see (3.5.13)), it follows that $\boldsymbol{\sigma}_{\mathrm{c}}^{\parallel}$ also satisfies (3.6.2). Moreover, since the expression for $\boldsymbol{\sigma}_{\mathrm{c}}^{\parallel}$ in (3.5.13), is identical to the right-hand side of (3.6.1) with $\mathbb{C}$ replaced with the fourth-order identity tensor, $\boldsymbol{\sigma}_{\mathrm{c}}^{\parallel}$ can be obtained from the analytical solution given in [Lek63] by replacing the elastic constants corresponding to $\mathbb{C}$ in the solution, with elastic constants corresponding to the identity tensor. Then $\boldsymbol{\sigma}_{\mathrm{c}}^{\perp}$ follows as $\boldsymbol{\sigma}_{\mathrm{c}}^{\perp} = \boldsymbol{\sigma}_{\mathrm{c}} - \boldsymbol{\sigma}_{\mathrm{c}}^{\parallel}$.

3.6.2 Decomposition of the atomistic stress

In the atomistic simulation, the Kirsch problem is modeled using a collection of Ar atoms in the fcc structure at zero temperature. The atomic interactions are modeled using a modified Lennard–Jones (LJ) pair potential [TM11] with Ar parameters from [Ber58] archived in OpenKIM [Adm, TES$^+$11].[24] The LJ parameters are $\epsilon = 10.4$ meV and $\sigma = 3.4$ Å. The cutoff radius is $r_{\mathrm{cut}} = 8.5$ Å. The equilibrium fcc lattice parameter at zero temperature ($T = 0$ K) calculated for this potential is $a_0 = 5.29216$ Å. The reference (unloaded) configuration of the plate is obtained by stacking $100 \times 100 \times 5$ unit cells, and removing all

[24] In a modified LJ potential, the standard LJ potential is modified by the addition of a quadratic function to bring the potential and its first and second derivatives to zero at the cutoff radius.

atoms that fall inside a circle of radius 50 Å positioned at the center of the stack, with its out-of-plane axis parallel to the [001] crystallographic axis. The resulting system consists of 194415 atoms. The system is loaded at infinity in the x-direction with $\sigma_\infty = 2.5 \times 10^{-5}\,\mathrm{eV/\AA}^3$, and initially displacing the atoms according to the exact solution $\boldsymbol{u}_\mathrm{c}$ described in Section 3.6.1. Following the initial displacement, the atoms on the boundary are held fixed and the interior of the system is allowed to relax using a conjugate gradient algorithm to remove any unbalanced loads [TM11].

The atomistic stress field $\boldsymbol{\sigma}_{w,\mathrm{v}}$ is obtained using the expression given in (3.2.13). The forces $\boldsymbol{f}_{\alpha\beta}$ appearing in this expression are given by

$$\boldsymbol{f}_{\alpha\beta} = -\frac{\partial \mathcal{V}_{\mathrm{MLJ}}}{\partial r_{\alpha\beta}} \frac{\boldsymbol{x}_\alpha - \boldsymbol{x}_\beta}{r_{\alpha\beta}}, \tag{3.6.3}$$

where $\mathcal{V}_{\mathrm{MLJ}}$ is the modified LJ potential energy which is a function of the distances between atoms, $r_{\alpha\beta} = \|\boldsymbol{x}_\alpha - \boldsymbol{x}_\beta\|$, and $\boldsymbol{x}_\alpha$ and $\boldsymbol{x}_\beta$ are the positions of atoms α and β at the end of the atomistic simulation. The weighting function in (3.2.13) is taken to be a constant with a trigonometric mollifying function:

$$w(\boldsymbol{r}) = \widehat{w}(\|\boldsymbol{r}\|) = \begin{cases} c_R & \text{if } \|\boldsymbol{r}\| < R - \epsilon, \\ \frac{1}{2} c_R \left[1 - \cos\left(\frac{R - \|\boldsymbol{r}\|}{\epsilon}\pi\right)\right] & \text{if } R - \epsilon < \|\boldsymbol{r}\| < R, \\ 0 & \text{otherwise,} \end{cases} \tag{3.6.4}$$

where c_R is chosen such that w is a normalized function. We set $R = 12$ Å and $\epsilon = 1.44$ Å. The atomistic stress tensor can now be decomposed using the algorithm described in Section 3.4.2.

3.6.3 Comparison of the continuum and atomistic decompositions

In this section, we compare results of the continuum and atomistic decompositions of the stress tensor for the Kirsch problem. Figs. 3.2 and 3.3 show plots of the decomposition of the xx, yy and xy components of the normalized continuum stress, and the normalized atomistic stress respectively, into an irrotational part and a traction-free solenoidal part. We make the following observations based on the plots.

1. The total atomistic stress tensor $\boldsymbol{\sigma}_{w,\mathrm{v}}$ is in good agreement in form and magnitude with the continuum stress tensor $\boldsymbol{\sigma}_\mathrm{c}$.

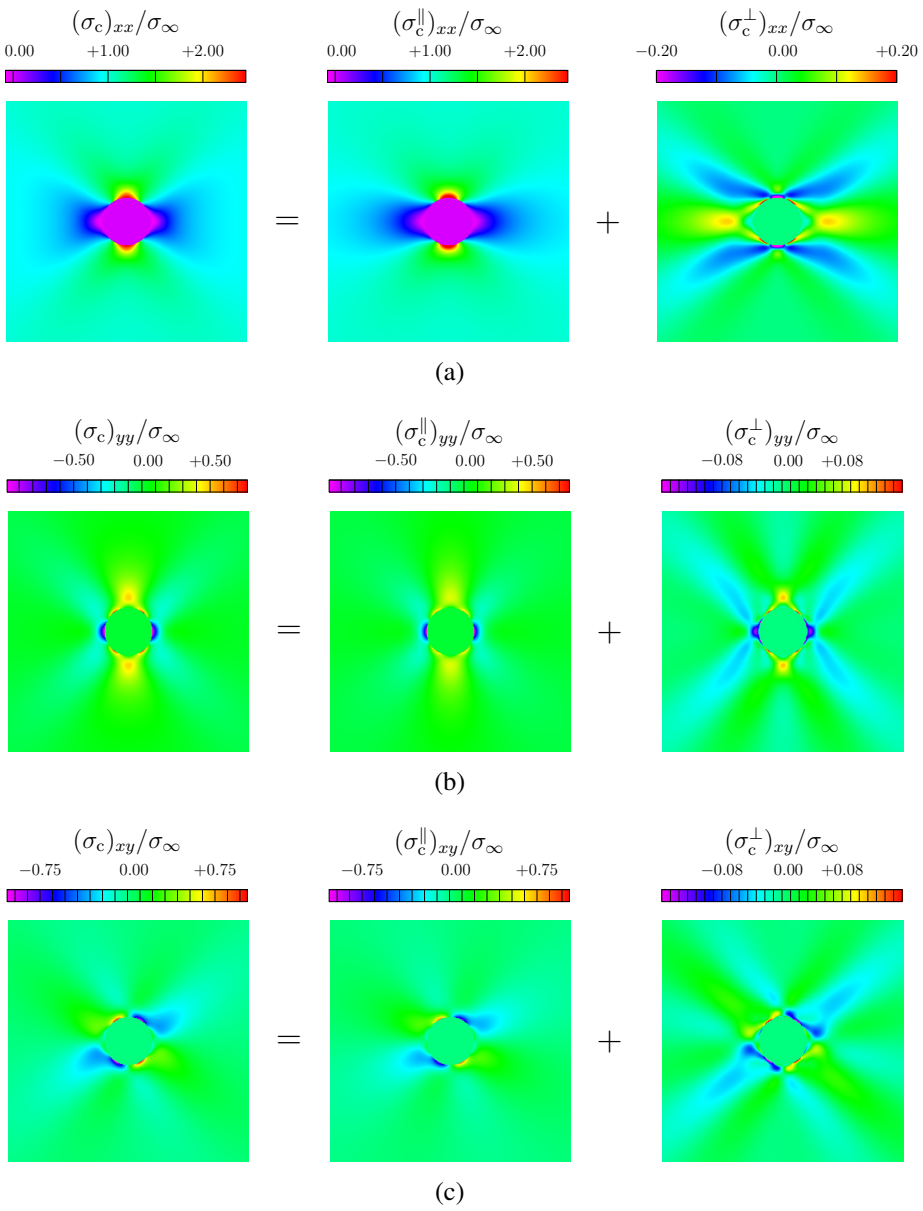

Figure 3.2: A plot showing the decomposition of the normalized continuum stress into an irrotational part $\boldsymbol{\sigma}_{\mathrm{c}}^{\parallel}/\sigma_\infty$, and a traction-free solenoidal part $\boldsymbol{\sigma}_{\mathrm{c}}^{\perp}/\sigma_\infty$. Parts (a), (b), and (c) show the decomposition of the xx, yy and xy components of $\boldsymbol{\sigma}_{\mathrm{c}}/\sigma_\infty$, respectively.

2. The qualitative forms of $\boldsymbol{\sigma}_{\mathrm{c}}^{\perp}$ and $\boldsymbol{\sigma}_{w,\mathrm{v}}^{\perp}$ are in good agreement with each other.

3. The magnitudes of $\boldsymbol{\sigma}_{\mathrm{c}}^{\perp}$ is less than the magnitude of $\boldsymbol{\sigma}_{w,\mathrm{v}}^{\perp}$. The reason for this is that decomposition of $\boldsymbol{\sigma}_{\mathrm{c}}$ is for an infinite domain, whereas the decomposition of $\boldsymbol{\sigma}_{w,\mathrm{v}}$ is for a finite atomistic body. We find that $\boldsymbol{\sigma}_{w,\mathrm{v}}^{\perp}$ tends to $\boldsymbol{\sigma}_{\mathrm{c}}^{\perp}$ as we increase the size of the atomistic body.

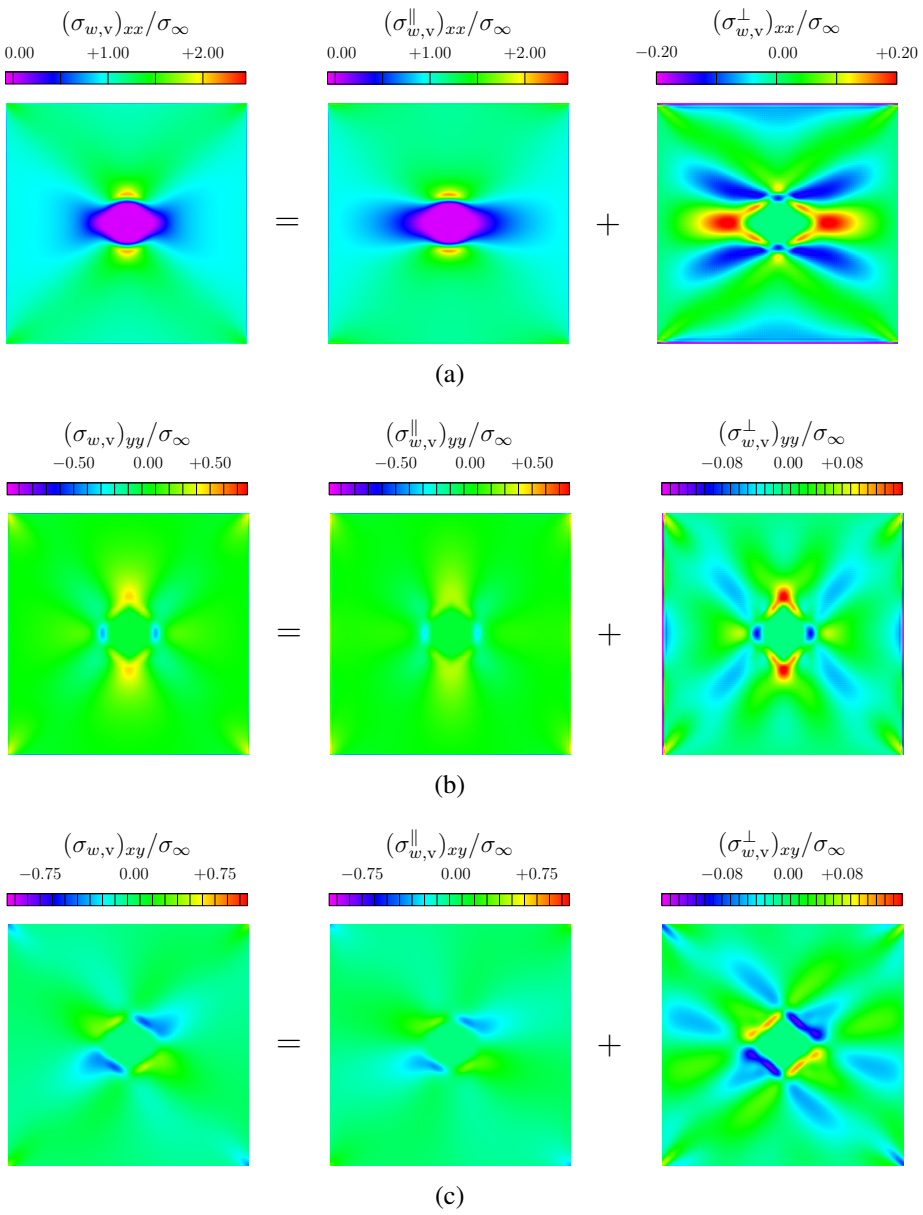

Figure 3.3: A plot showing the decomposition of the normalized atomistic stress into an irrotational part $\boldsymbol{\sigma}^{\parallel}_{w,\mathrm{v}}/\sigma_\infty$, and a solenoidal part $\boldsymbol{\sigma}^{\perp}_{w,\mathrm{v}}/\sigma_\infty$. Parts (a), (b), and (c) show the decomposition of the xx, yy and xy components of $\boldsymbol{\sigma}_{w,\mathrm{v}}/\sigma_\infty$, respectively.

The above observations suggest that the decomposition of the atomistic stress proposed in Section 3.4 is in good agreement with the decomposition of the continuum stress obtained using the Beltrami representation in Section 3.5.

3.7 Summary

In this paper, we study the non-uniqueness of the atomistic stress tensor arising from the non-uniqueness of the force decomposition, which in turn is due to the choice of the potential energy representation. A geometric interpretation of force decomposition is given using rigidity theory and its non-uniqueness is characterized. This analysis results in a decomposition of the atomistic stress into an irrotational part that depends on the choice of potential energy representation, and a solenoidal part that is independent of it. A similar decomposition is constructed in continuum mechanics using the generalized Beltrami representation, which is a version of Helmholtz decomposition for symmetric tensor fields. We identify various analogies between the two decompositions and obtain an atomistic equivalent to the continuum strain tensor. We numerically compare the two decompositions and demonstrate their equivalence for a linear elasticity boundary-value problem of an anisotropic infinite plate with a hole under uniaxial stress at infinity.

Chapter 4

Stress and heat flux for arbitrary multibody potentials: A unified framework

4.1 Introduction

The idea of defining continuum fields from particle mechanics (for the special case of pair potential interactions) was pioneered in the landmark paper of Irving and Kirkwood [IK50]. Irving and Kirkwood derived the equations of hydrodynamics from the principles of non-equilibrium classical statistical mechanics and in the process established pointwise definitions for various continuum fields. Under this procedure, basic continuum fields including the mass density, momentum density and the specific internal energy are defined *a priori* using a probability density function. Using these definitions, expressions for the stress tensor and the heat flux vector fields are obtained that identically satisfy the balance laws of continuum mechanics. The continuum fields obtained in Irving and Kirkwood's original paper [IK50] involved a series expansion of the Dirac delta distribution, which is not mathematically rigorous.[1] In a follow-up study, Noll [Nol55, LVLT10] proved two lemmas, which allowed him to avoid the use of the delta distribution and to obtain closed-form analytical expressions for the continuum fields.

Since the Irving–Kirkwood procedure is stochastic in nature, many problems arise when

[1] The derivation is non-rigorous in the sense that expressing the stress tensor as a series expansion is only possible when the probability density function, which is used in the derivation, is an analytic function of the spatial variables (see [Nol55]).

one tries to use the resulting expressions for a practical calculation — a key one being our lack of knowledge of the probability density function. To avoid these difficulties Hardy [Har82], and independently Murdoch [MB93, MB94, Mur03, Mur07] developed a simpler spatial averaging procedure that avoids the mathematical complexity of the Irving–Kirkwood procedure. We refer to the procedure due to Hardy as the *Hardy procedure* and that due to Murdoch as the *Murdoch procedure*.[2] In these procedures, continuum fields are defined as direct spatial averages of the discrete equations of motion using a normalized weighting function. This approach also leads to a set of definitions that identically satisfy the balance equations. Therefore, we have three different approaches for defining the continuum fields from particle mechanics — although originally developed for pair potentials only.

Of the continuum fields, the stress tensor has been studied most extensively. In addition to the definitions for the stress tensor obtained from the systematic approaches described above, a number of other definitions have been proposed in the past dating back to the work of Cauchy [Cau28a, Cau28b] on the stress vector and Clausius [Cla70] on the virial stress.[3] Efforts at obtaining microscopic definitions for the stress tensor (as well as other continuum variables) are ongoing; see for example [Tsa79, WAD95, CRD01, ZIH$^+$04, HPB05, Del05, MRT06, Che06, MJP09b, MJP09a, TPM09, RT10] for some important contributions. A recent article [AT10] by the authors extensively studies the definition for the stress tensor within a unified framework based on a generalization of the Irving–Kirkwood procedure to arbitrary multi-body potentials followed by a process of spatial averaging. Through this unified framework it is shown that all existing definitions, including the virial stress tensor [Cla70], Hardy stress tensor [Har82], and Cauchy/Tsai stress tensor [Cau28a, Cau28b, Tsa79], which all seem to be derived from disparate approaches, follow as special cases from a single stress expression. Furthermore, the derivation in [AT10] reveals the subtle (and hitherto unrecognized issue) that interatomic potentials constitute *continuously differentiable extensions* to functions defined over a more limited domain. This is a vital part of the derivation with important implications for the uniqueness of the microscopic stress tensor — an issue which is widely discussed in the literature cited above. Although there have been a number of attempts to generalize the Irving–Kirkwood procedure and the Hardy procedure to multi-body potentials (see [ZWS08, Che06, ZT04, HPB05]), these attempts are either restricted to specific potentials (see [Che06, ZT04]) or the source of non-uniqueness of the stress tensor is not explicitly identified. In contrast, the unified

[2] Although the Hardy and Murdoch procedures seem similar, they are notably different in the derivation of the energy balance equation, and the resulting expressions for energy density and the heat flux vector.

[3] See [AT10] for a more detailed historical review.

framework developed in [AT10] applies to *arbitrary* multi-body potentials and rigorously characterizes the non-uniqueness of the stress tensor.

The aim of this paper is to continue to use this unified framework to study the energy balance equation of continuum mechanics in the context of multi-body potentials. As noted earlier, in the original Irving–Kirkwood and the Hardy procedure, the definition for the potential part of the specific internal energy (for the special case of pair potentials in a mono-atomic system) is assumed *a priori* and the expression for the heat flux vector is then derived to ensure that the energy balance equation is identically satisfied. Unfortunately, this approach does not generalize to arbitrary multi-body potentials (or even pair potentials with multiple species types) since it involves an ambiguous definition for the "energy of an atom". To the best of the authors' knowledge, all the existing works (see [ZWS08, Che06, ZT04, MR83, TNO08]) which attempt to derive a microscopic definition for the heat flux in the case of multi-body potentials by generalizing the Irving–Kirkwood procedure or the Hardy procedure suffer from this ambiguity. For example, in [Che06] it was assumed that the energy corresponding to a cluster of three particles interacting through a three-body potential is evenly distributed among the particles. However, there is no symmetry argument to justify this assumption.[4] Furthermore, even for the case of pair potential interactions, the original Irving–Kirkwood approach leads to an expression for the heat flux vector which is not invariant with respect to the addition of a constant to the potential energy of the system, which is not physically reasonable. In contrast, in the Murdoch procedure, the specific internal energy and heat flux vector are obtained together as part of the derivation and the resulting expressions are consistent with physical expectations. Motivated by this, in this paper, we reformulate the Irving–Kirkwood procedure using the method followed by Murdoch [MB94]. This approach leads to physically-acceptable expressions for the internal energy density and heat flux vector which are grounded in rigorous statistical mechanics principles and which does not require any energy decomposition between the particles. Furthermore, as noted above, our derivation extends those of Irving–Kirkwood and Murdoch to arbitrary multi-body potentials. Finally, the application of the spatial averaging step in the unified procedure leads to expressions suitable for use in molecular dynamics simulations. These expressions are compared with those from the original Irving–Kirkwood formulation through a number of simple numerical experiments.

[4]The symmetry argument for equally dividing the energy among particles only holds for identical atoms interacting via a pair potential. It is lost for multi-species systems and for all higher-order potentials. For example, for a three-body potential (even in the case of a single-species system), the symmetry between atoms is lost in all clusters of three particles which do not form an equilateral triangle. The same reasoning applies for potentials of higher order.

The following notation is used in this paper. Vectors are denoted by lower case letters in bold font, while tensors of higher order are denoted by capital letters in bold font. The inner product of two vectors is given by a dot "$\cdot$", and their tensor product is given by the symbol "$\otimes$". The inner product of two second-order tensors is denoted by ":". The gradient of a vector field, $\boldsymbol{v}(\boldsymbol{x})$, is denoted by $\nabla_{\boldsymbol{x}}\boldsymbol{v}(\boldsymbol{x})$. A second-order tensor, $\boldsymbol{T}$, operating on a vector, $\boldsymbol{v}$, is denoted by $\boldsymbol{T}\boldsymbol{v}$. The divergence of a tensor field, $\boldsymbol{T}(\boldsymbol{x})$, is denoted by $\mathrm{div}_{\boldsymbol{x}}\,\boldsymbol{T}(\boldsymbol{x})$, which corresponds to $\partial \boldsymbol{T}_{ij}/\partial \boldsymbol{x}_j$ in indicial notation (with Einstein's summation convention).

4.2 Continuum fields as phase averages

Consider a system modeled as a collection of N point particles, each particle identified by an index α ($\alpha = 1, 2, \ldots, N$). The position, mass, and velocity of particle α are denoted by $\boldsymbol{x}_\alpha$, m_α and $\boldsymbol{v}_\alpha$, respectively. We assume that the particles interact through a continuously differentiable function $\mathcal{V}(\boldsymbol{x}_1, \ldots, \boldsymbol{x}_N)$, which is called the *potential energy* of the system. The complete microscopic state of the system at any instant of time is known from the knowledge of position and velocity of each particle in $\mathbb{R}^3$. Hence, the state of the system at time t may be represented by a point in a $6N$-dimensional phase space.[5] Let Γ denote the phase space. Therefore any point in Γ, can be represented as,

$$(\boldsymbol{x}(t); \boldsymbol{v}(t)) := (\boldsymbol{x}_1(t), \ldots, \boldsymbol{x}_N(t); \boldsymbol{v}_1(t), \ldots, \boldsymbol{v}_N(t)). \tag{4.2.1}$$

In reality, the microscopic state of the system is never known to us and the only observables identified are the macroscopic fields as defined in continuum mechanics. We identify the continuum fields with macroscopic observables obtained in a two-step process: (1) a pointwise field is obtained as a statistical mechanics phase average; (2) a macroscopic field is obtained as a spatial average over the pointwise field. The phase averaging in step (1) is done with respect to a continuously differentiable[6] probability density function $W : \Gamma \times \mathbb{R}^+ \to \mathbb{R}^+$ defined on all phase space for all t. The explicit dependence of W on time t, indicates that our system need not be in thermodynamic equilibrium.

The basic idea behind the original Irving and Kirkwood procedure is to prescribe the mass

[5] The usual convention is to represent the phase space via positions and momenta of the particles. For convenience, in this section, we instead use positions and velocities.

[6] The assumption that the probability density function exists and it is continuously differentiable can be considerably weakened by viewing W as a generalized function/distribution in the sense of Schwartz. For the sake of brevity we do not take this approach, however, we later use a generalized function/distribution as a candidate for W to arrive at expressions for continuum fields that can be used in a molecular dynamics simulation. See Section 4.3 for details.

density, velocity and the specific internal energy fields, which we call the input fields, and derive the body force vector, stress tensor and the heat flux vector fields, which we call the output fields, such that all the definitions are consistent with the balance laws of mass, momentum and energy:

$$\begin{array}{cc} \textbf{Input fields} & \textbf{Output fields} \\ \left\{ \begin{array}{l} \text{mass density} \\ \text{velocity} \\ \text{specific internal energy} \end{array} \right\} & \rightarrow \left\{ \begin{array}{l} \text{body force} \\ \text{stress} \\ \text{heat flux} \end{array} \right\}. \end{array} \tag{4.2.2}$$

To arrive at these definitions, we repeatedly use the following result of Liouville's theorem, which describes the evolution of the probability density function:

$$\frac{\partial W}{\partial t} + \sum_{\alpha=1}^{N} [\boldsymbol{v}_\alpha \cdot \nabla_{\boldsymbol{x}_\alpha} W + \dot{\boldsymbol{v}}_\alpha \cdot \nabla_{\boldsymbol{v}_\alpha} W] = 0. \tag{4.2.3}$$

Since the force on a particle α is given by

$$\boldsymbol{f}_\alpha := -\nabla_{\boldsymbol{x}_\alpha} \mathcal{V}, \tag{4.2.4}$$

equation (4.2.3) can be rewritten as

$$\frac{\partial W}{\partial t} + \sum_{\alpha=1}^{N} \left[\boldsymbol{v}_\alpha \cdot \nabla_{\boldsymbol{x}_\alpha} W - \frac{\nabla_{\boldsymbol{x}_\alpha} \mathcal{V}}{m_\alpha} \cdot \nabla_{\boldsymbol{v}_\alpha} W \right] = 0, \tag{4.2.5}$$

where, as stated before, $\mathcal{V}(\boldsymbol{x}_1, \boldsymbol{x}_2, \ldots, \boldsymbol{x}_N)$ denotes the potential energy of the system. Equation (4.2.5) is called *Liouville's equation*.

To proceed, we divide the potential energy into two parts:

1. An *external* part, $\mathcal{V}_{\text{ext}}$, associated with long-range interactions such as gravity or electromagnetic fields,

2. An *internal* part, $\mathcal{V}_{\text{int}}$, associated with short-range particle interactions. In general, the internal part of the potential energy is also called the *interatomic potential energy*.

We next define the input fields used in the Irving–Kirkwood procedure.

4.2.1 Phase averaging

Under the Irving–Kirkwood procedure, pointwise fields are defined as phase averages. For example, the pointwise mass density field is defined as

$$\rho(\boldsymbol{x},t) := \sum_{\alpha} m_\alpha \int_{\mathbb{R}^{3N}\times\mathbb{R}^{3N}} W\delta(\boldsymbol{x}_\alpha - \boldsymbol{x})\, d\boldsymbol{x}d\boldsymbol{v}, \tag{4.2.6}$$

δ denotes the Dirac delta distribution, and $\sum_\alpha$ denotes summation from $\alpha = 1$ to N. To avoid the Dirac delta distribution and for greater clarity we adopt the notation introduced by Noll. Hence (4.2.6) can be rewritten as

$$\begin{aligned}\rho(\boldsymbol{x},t) &= \sum_{\alpha} m_\alpha \int W\, d\boldsymbol{x}_1 \dots d\boldsymbol{x}_{\alpha-1} d\boldsymbol{x}_{\alpha+1} \dots d\boldsymbol{x}_N d\boldsymbol{v} \\ &=: \sum_{\alpha} m_\alpha \left\langle W \mid \boldsymbol{x}_\alpha = \boldsymbol{x} \right\rangle, \end{aligned} \tag{4.2.7}$$

where $\langle W \mid \boldsymbol{x}_\alpha = \boldsymbol{x}\rangle$ denotes an integral of W over all its arguments except $\boldsymbol{x}_\alpha$, and $\boldsymbol{x}_\alpha$ is substituted with $\boldsymbol{x}$.

The second input field, which is the pointwise velocity field, is defined via the momentum density field, $\boldsymbol{p}(\boldsymbol{x},t)$, as follows:

$$\boldsymbol{p}(\boldsymbol{x},t) := \sum_{\alpha} m_\alpha \left\langle W\boldsymbol{v}_\alpha \mid \boldsymbol{x}_\alpha = \boldsymbol{x} \right\rangle, \tag{4.2.8}$$

$$\boldsymbol{v}(\boldsymbol{x},t) := \frac{\boldsymbol{p}(\boldsymbol{x},t)}{\rho(\boldsymbol{x},t)}. \tag{4.2.9}$$

The third input field, which is the specific internal energy, depends on the interatomic potential. At this point, it must be noted that the original Irving–Kirkwood procedure was limited to systems interacting through a pair potential function:

$$\begin{aligned}\mathcal{V}_{\text{int}} &= \mathcal{V}_{\text{int}}(r_{12},\dots,r_{1N},r_{23},\dots,r_{(N-1)N}) \\ &= \sum_{\alpha} \mathcal{V}_\alpha, \end{aligned} \tag{4.2.10}$$

where $\mathcal{V}_\alpha$ is the energy of particle α, defined as

$$\mathcal{V}_\alpha := \frac{1}{2}\left[\sum_{\substack{\beta \\ \beta<\alpha}} \phi_{\beta\alpha}(r_{\beta\alpha}) + \sum_{\substack{\beta \\ \beta>\alpha}} \phi_{\alpha\beta}(r_{\alpha\beta})\right]. \tag{4.2.11}$$

and $\phi_{\alpha\beta}$ ($\alpha < \beta$) is the energy corresponding to the interaction of the pair (α, β). In this case, the specific internal energy is defined as

$$\epsilon(\boldsymbol{x}, t) := \epsilon_{\mathrm{k}}(\boldsymbol{x}, t) + \epsilon_{\mathrm{v}}(\boldsymbol{x}, t), \tag{4.2.12}$$

where

$$\rho\epsilon_{\mathrm{k}}(\boldsymbol{x}, t) := \frac{1}{2}\sum_{\alpha} m_\alpha \langle \|\boldsymbol{v}_\alpha\|^2 W \mid \boldsymbol{x}_\alpha = \boldsymbol{x}\rangle, \tag{4.2.13}$$

is the kinetic contribution to the specific internal energy , and

$$\rho\epsilon_{\mathrm{v}}(\boldsymbol{x}, t) := \sum_{\alpha} \langle \mathcal{V}_\alpha W \mid \boldsymbol{x}_\alpha = \boldsymbol{x}\rangle, \tag{4.2.14}$$

is the potential contribution to the specific internal energy. According to the definition given in (4.2.12), the specific internal energy at $(\boldsymbol{x}, t)$ is the weighted sum of the energy of each particle with the probability that it is at $\boldsymbol{x}$ at time t. It is clear from the definition in (4.2.11) that the interaction energy $\phi_{\alpha\beta}$, between any two particles α and β, is shared equally between the particles α and β. This is plausible for systems with identical particles interacting with pair potential, but there is no *a priori* physically motivated way of deciding how to distribute the energy for systems interacting through a multi-body potential. This is one of the primary reasons why the definition for the specific internal energy and the energy balance equation has to be re-examined as we do later in Section 4.2.4.

It is clear from the definitions in (4.2.7), (4.2.8), (4.2.13) and (4.2.14) that the integrals in these equations converge only under appropriate decay conditions [AT10] on W. Under these condition, any continuously differentiable vector or tensor-valued function defined on the phase space for all t (and satisfying certain additional decay conditions described in [AT10]), we have[7]

$$\int_{\mathbb{R}^3} \boldsymbol{G} \cdot \nabla_{\boldsymbol{x}_\alpha} W \, d\boldsymbol{x}_\alpha = -\int_{\mathbb{R}^3} W \operatorname{div}_{\boldsymbol{x}_\alpha} \boldsymbol{G} \, d\boldsymbol{x}_\alpha, \tag{4.2.15a}$$

$$\int_{\mathbb{R}^3} \boldsymbol{G} \cdot \nabla_{\boldsymbol{v}_\alpha} W \, d\boldsymbol{v}_\alpha = -\int_{\mathbb{R}^3} W \operatorname{div}_{\boldsymbol{v}_\alpha} \boldsymbol{G} \, d\boldsymbol{v}_\alpha. \tag{4.2.15b}$$

The above identities are repeatedly used in deriving the equation of continuity, the equation of motion, and the energy balance equation in the Irving–Kirkwood procedure.

[7] If $\boldsymbol{G}$ is a second-order tensor or higher, then the dot product indicates tensor operating on a vector. Note that in (4.2.15), in the interest of brevity, we are breaking our notation of denoting a second-order tensor operating on a vector by juxtaposition.

4.2.2 General interatomic potentials

In this section, we describe some properties of interatomic potentials, which play a crucial role in extending the original Irving–Kirkwood procedure to multi-body potentials. In addition, it gives new new insights into the original procedure which was limited to pair potentials. This section is largely based on [AT10], and is briefly summarized here for completeness and to define the necessary notation and terminology.

In general, the internal part of the potential energy, also called the *interatomic potential energy*, depends on the positions of all particles in the system:

$$\mathcal{V}_{\text{int}} = \widehat{\mathcal{V}}_{\text{int}}(\boldsymbol{x}_1, \boldsymbol{x}_2, \ldots, \boldsymbol{x}_N), \tag{4.2.16}$$

where the "hat" indicates that the functional dependence is on absolute particle positions (as opposed to distances later on). We assume that $\widehat{\mathcal{V}}_{\text{int}} : \mathbb{R}^{3N} \to \mathbb{R}$ is a continuously differentiable function.[8] Due to the invariance of the potential energy with respect to rigid-body motions and reflections, it can be shown that $\mathcal{V}_{\text{int}}$ in (4.2.16) can be expressed as a new function [**?**]

$$\mathcal{V}_{\text{int}} = \breve{\mathcal{V}}_{\text{int}}(\cdot), \tag{4.2.17}$$

where the argument of $\breve{\mathcal{V}}_{\text{int}}$ is an $N(N-1)/2$ tuple of "physically-realizable distances". Before we describe what this means, we note that the $N(N-1)/2$ distances between the N particles embedded in $\mathbb{R}^3$ are not independent. This can be easily seen for any collection of 5 particles or more. Therefore, the set of all $N(N-1)/2$ tuples of physically realizable distances is a proper subset of $\mathbb{R}^{N(N-1)/2}$. In fact, it is a $(3N-6)$-dimensional manifold called the *shape space* of the system which is defined as

$$\begin{aligned}\mathcal{S} := \{(r_{12}, r_{13}, \ldots, r_{1N}, r_{23}, \ldots, r_{(N-1)N}) \mid \\ r_{\alpha\beta} = \|\boldsymbol{x}_\alpha - \boldsymbol{x}_\beta\|, (\boldsymbol{x}_1, \ldots, \boldsymbol{x}_N) \in \mathbb{R}^{3N}\}.\end{aligned} \tag{4.2.18}$$

For example, for a chain of 3 particles in one dimension, with positions $x_1 < x_2 < x_3$, the three distances (r_{12}, r_{13}, r_{23}) must satisfy $r_{12} + r_{23} = r_{13}$. Values of (r_{12}, r_{13}, r_{23}) that do not satisfy this constraint are not "physically realizable" and are therefore outside the shape space manifold.

From the above discussion it is clear that the potential energy is only defined on the shape

[8] Note that this assumption may fail in systems undergoing first-order magnetic or electronic phase transformations.

space of the system. We will soon see that in order to derive the stress tensor, we need to evaluate partial derivatives like the following:

$$\frac{\partial \mathcal{V}_{\text{int}}}{\partial r_{12}} = \lim_{\epsilon \to 0} \frac{\mathcal{V}_{\text{int}}(r_{12} + \epsilon, \ldots, r_{N(N-1)}) - \mathcal{V}_{\text{int}}(r_{12}, \ldots, r_{N(N-1)})}{\epsilon}. \tag{4.2.19}$$

It is clear that this relation requires us to evaluate the potential energy outside the shape space since if $(r_{12}, \ldots, r_{N(N-1)})$ is on $\mathcal{S}$ then by adding ϵ to one of the distances, we move off it. Thus, the expression in (4.2.19) makes sense only when we extend the function to the neighborhood of the shape space manifold (see Section 3.4 in [AT10] for a more detailed discussion).

This is the reason we now restrict our discussion to those systems for which there exists a continuously differentiable extension of $\breve{\mathcal{V}}_{\text{int}}$, defined on the shape space, to $\mathbb{R}^{N(N-1)/2}$. This is a reasonable assumption because all interatomic potentials used in practice, for a system of N particles, are either continuously differentiable functions on $\mathbb{R}^{N(N-1)/2}$, or can easily be extended to one. For example, the pair potential and the embedded-atom method (EAM) potential [DB84] are continuously differentiable functions on $\mathbb{R}^{N(N-1)/2}$, while the Stillinger-Weber [SW85] and the Tersoff [Ter88] potentials which depend on the angles between relative position vectors, can be easily extended to $\mathbb{R}^{N(N-1)/2}$ by expressing these angles as a function of distances between particles. Therefore, we assume that there exists a continuously differentiable function $\mathcal{V}_{\text{int}} : \mathbb{R}^{N(N-1)/2} \to \mathbb{R}$, such that the restriction of $\mathcal{V}_{\text{int}}$ to $\mathcal{S}$ is equal to $\breve{\mathcal{V}}_{\text{int}}$:

$$\mathcal{V}_{\text{int}}(\boldsymbol{s}) = \breve{\mathcal{V}}_{\text{int}}(\boldsymbol{s}) \quad \forall \boldsymbol{s} = (r_{12}, \ldots, r_{(N-1)N}) \in \mathcal{S}. \tag{4.2.20}$$

An immediate question that arises is whether this extension is unique in a neighborhood of $\boldsymbol{s} \in \mathcal{S}$. Note that for $2 \leq N \leq 4$, $3N - 6 = N(N-1)/2$. Therefore, for $2 \leq N \leq 4$, for every point $\boldsymbol{s} \in \mathcal{S}$, there exists a neighborhood in $\mathbb{R}^{N(N-1)/2}$ which lies in $\mathcal{S}$. However, for $N > 4$, there may be multiple extensions of $\breve{\mathcal{V}}_{\text{int}}$.

We will soon see that the quantity evaluated in (4.2.19) may differ for different extensions. On the other hand, the *internal* force on any particle α,

$$\begin{aligned} \boldsymbol{f}_{\alpha}^{\text{int}} &:= -\nabla_{\boldsymbol{x}_\alpha} \mathcal{V}_{\text{int}} \\ &= -\nabla_{\boldsymbol{x}_\alpha} \widehat{\mathcal{V}}_{\text{int}} \end{aligned} \tag{4.2.21}$$

is uniquely defined for any extension. We next address the possibility of having multiple extensions for the potential energy by studying the various constraints that the distances between particles must satisfy in order to be embeddable in $\mathbb{R}^3$. We demonstrate, through a simple example, how multiple extensions for the potential energy lead to a non-unique decomposition of the force on a particle, which in turn leads to a non-unique pointwise stress tensor.

Central-force decomposition and the possibility of alternate extensions

We first show that the force on a particle can always be decomposed as a sum of central forces regardless of the nature of the interatomic potential. The force on a particle due to internal interactions is defined in (4.2.21). This can also be evaluated using the continuously differentiable extension $\mathcal{V}_{\text{int}}$ and the chain rule as

$$\begin{aligned} \boldsymbol{f}_\alpha^{\text{int}}(r_{12},\dots,r_{(N-1)N}) &= -\nabla_{\boldsymbol{x}_\alpha}\mathcal{V}_{\text{int}}(r_{12},\dots,r_{(N-1)N}) \\ &= \sum_{\substack{\beta \\ \beta\neq\alpha}} \boldsymbol{f}_{\alpha\beta}, \end{aligned} \tag{4.2.22}$$

where

$$\boldsymbol{f}_{\alpha\beta} := \begin{cases} \frac{\partial \mathcal{V}_{\text{int}}}{\partial r_{\alpha\beta}} \frac{\boldsymbol{x}_\beta - \boldsymbol{x}_\alpha}{r_{\alpha\beta}} & \text{if } \alpha < \beta, \\ \frac{\partial \mathcal{V}_{\text{int}}}{\partial r_{\beta\alpha}} \frac{\boldsymbol{x}_\beta - \boldsymbol{x}_\alpha}{r_{\alpha\beta}} & \text{if } \alpha > \beta, \end{cases} \tag{4.2.23}$$

is the contribution to the force on particle α due to the presence of particle β.

Note that $\boldsymbol{f}_{\alpha\beta}$ is parallel to the direction $\boldsymbol{x}_\beta - \boldsymbol{x}_\alpha$ and satisfies $\boldsymbol{f}_{\alpha\beta} = -\boldsymbol{f}_{\beta\alpha}$. This leads us to the important result that the *internal force on a particle, for any interatomic potential that has a continuously differentiable extension, can always be decomposed as a sum of central forces, i.e., forces parallel to directions connecting the particle to its neighbors*. This may seem strange to some readers due to the common confusion in the literature of using the term "central-force model" to refer exclusively to simple pair potentials. In fact, we see that due to the invariance requirement stated above, *all* interatomic potentials (including those with explicit bond angle dependence) that can be expressed as a continuously differentiable function of distance coordinates, are central-force models. By this we mean that the force on any particle (say α) can be decomposed as a sum (over β) of terms, $\boldsymbol{f}_{\alpha\beta}$, aligned with the vectors joining particle α with its neighbors and satisfying action and reaction. The difference between a pair potential and a many-body potential is that in the former $\boldsymbol{f}_{\alpha\beta}$ only depends on $r_{\alpha\beta}$ whereas in the latter $\boldsymbol{f}_{\alpha\beta}$ can depend on the distances between all particles.

The next question is how different potential energy extensions affect the force decomposition in (4.2.22). We have already seen through (4.2.21) that the force $\boldsymbol{f}_\alpha^{\text{int}}$ is independent of the particular extension used. However, we show below that the individual terms in the decomposition, $\boldsymbol{f}_{\alpha\beta}$, are *not* unique. These terms depend on the manner in which the potential energy, defined on the shape space, is extended to its neighborhood in $\mathbb{R}^{N(N-1)/2}$.

In order to construct different extensions, we use the geometric constraints that the distances have to satisfy in order for them to be embeddable in $\mathbb{R}^3$.[9] The nature of these constraints is studied in the field of *distance geometry*, which describes the geometry of sets of points in terms of the distances between them. One of the main results of this theory, is that the constraints are given by *Cayley-Menger determinants*, which are related to the volume of a simplex formed by N points in an $N-1$ dimensional space. The Cayley–Menger determinant corresponding to N particles is given by

$$\begin{aligned}\chi(&\zeta_{12},\ldots,\zeta_{1N},\zeta_{23},\ldots,\zeta_{(N-1)N}\big)\\ &= \det\begin{bmatrix} 0 & s_{12} & s_{13} & \cdots & s_{1N} & 1\\ s_{12} & 0 & s_{23} & \cdots & s_{2N} & 1\\ s_{13} & s_{23} & 0 & \cdots & s_{3N} & 1\\ \vdots & \vdots & \vdots & & \vdots & \vdots\\ s_{1N} & s_{2N} & s_{3N} & \cdots & 0 & 1\\ 1 & 1 & 1 & \cdots & 1 & 0\end{bmatrix},\end{aligned} \tag{4.2.24}$$

where $s_{\alpha\beta} = \zeta_{\alpha\beta}^2$.

In the following example we restrict ourselves to one dimension since the resulting expressions are short and easy to manipulate, although this example can be readily extended to any dimension. It is easy to see that in one dimension the number of independent coordinates are $N-1$ and for $N>2$ the number of interatomic distances exceeds the number of independent coordinates. Therefore, for simplicity, consider as before a system consisting of three particles interacting in one dimension. The standard pair potential representation for this system, which is defined for all ζ_{12}, ζ_{13} and ζ_{23} is given by

$$\mathcal{V}_{\text{int}}(\zeta_{12},\zeta_{13},\zeta_{23}) = \phi_{12}(\zeta_{12}) + \phi_{13}(\zeta_{13}) + \phi_{23}(\zeta_{23}). \tag{4.2.25}$$

We noted earlier that the distances between particles are geometrically constrained by the requirement that one of the distance is equal to the sum of the other two. In spite of this

[9] We thank Ryan Elliott for suggesting this line of thinking.

constraint, $\mathcal{V}_{\text{int}}$ is defined for all values of $(\zeta_{12}, \zeta_{13}, \zeta_{23})$. This clearly shows that the pair potential is already an extension. Since the calculation gets unwieldy, let us again consider the special case where the particles are arranged to satisfy $x_1 < x_2 < x_3$, for which $r_{13} = r_{12} + r_{23}$. Using (4.2.22), the internal force, f_1^{int}, evaluated at this configuration, is decomposed as

$$\begin{aligned} f_1^{\text{int}}(r_{12}, r_{13}, r_{23}) = -\frac{d\mathcal{V}_{\text{int}}}{dx_1} &= -\frac{d\phi_{12}}{dx_1} - \frac{d\phi_{13}}{dx_1} \\ &= \phi'_{12}(r_{12}) + \phi'_{13}(r_{13}) \\ &=: f_{12} + f_{13}. \end{aligned} \tag{4.2.26}$$

We now construct an alternate extension to the standard pair potential representation given in (4.2.25). This is done through the Cayley-Menger determinant corresponding to a cluster of three points, which follows from (4.2.24) as

$$\begin{aligned} \chi(\zeta_{12}, \zeta_{13}, \zeta_{23}) = (\zeta_{12} - \zeta_{13} - \zeta_{23})(\zeta_{23} - \zeta_{12} - \zeta_{13}) \\ \times (\zeta_{13} - \zeta_{23} - \zeta_{12})(\zeta_{12} + \zeta_{13} + \zeta_{23}). \end{aligned}$$

Since the Cayley–Menger determinant is related to the area formed by the three particles, and the three particles are restricted to be in one-dimension, it follows that

$$\chi(r_{12}, r_{13}, r_{23}) = 0. \tag{4.2.27}$$

Using the identity in (4.2.27), an alternate extension $\mathcal{V}_{\text{int}}^{\mathcal{A}}$ is constructed:

$$\mathcal{V}_{\text{int}}^{\mathcal{A}}(\zeta_{12}, \zeta_{13}, \zeta_{23}) = \mathcal{V}_{\text{int}}(\zeta_{12}, \zeta_{13}, \zeta_{23}) + \chi(\zeta_{12}, \zeta_{13}, \zeta_{23}). \tag{4.2.28}$$

Note that $\mathcal{V}_{\text{int}}^{\mathcal{A}}$ is indeed an extension because from (4.2.27) it is clear that $\mathcal{V}_{\text{int}}^{\mathcal{A}}$ is equal to $\mathcal{V}_{\text{int}}$ at every point on the shape space of the system and it is continuously differentiable because $\chi(\zeta_{12}, \zeta_{13}, \zeta_{23})$, being a polynomial, is infinitely differentiable. Let us now see how the internal force, f_1^{int}, for the special configuration considered in this example, is

decomposed using the new extension:

$$\begin{aligned} f_1^{\text{int}} = -\frac{d\mathcal{V}_{\text{int}}^{\mathcal{A}}}{dx_1} &= -\frac{d\mathcal{V}_{\text{int}}}{dx_1} - \frac{d\chi}{dx_1} \\ &= \left(\phi'_{12} - \frac{\partial\chi}{\partial\zeta_{12}}(\boldsymbol{s})\frac{\partial\zeta_{12}}{\partial x_1}(\boldsymbol{s})\right) + \left(\phi'_{13} - \frac{\partial\chi}{\partial\zeta_{13}}(\boldsymbol{s})\frac{\partial\zeta_{13}}{\partial x_1}(\boldsymbol{s})\right) \\ &= (f_{12} - 8r_{12}r_{23}(r_{12}+r_{23})) + (f_{13} + 8r_{12}r_{23}(r_{12}+r_{23})) \\ &=: \tilde{f}_{12} + \tilde{f}_{13}, \end{aligned} \tag{4.2.29}$$

where in the above equation $\boldsymbol{s} = (r_{12}, r_{13}, r_{23})$ is a point in the shape space $\mathcal{S}$. It is clear from (4.2.26) and (4.2.29) that the central-force decomposition is not the same for the two representations, i.e., $f_{12} \neq \tilde{f}_{12}$ and $f_{13} \neq \tilde{f}_{13}$, however the force on particle 1, f_1^{int}, is the same in both cases as expected.

4.2.3 Equation of Motion and the stress tensor

The equation of motion and the stress tensor for multi-body potentials has been extensively studied in the authors' previous work [AT10]. We now present those parts of the derivation which are necessary to derive the energy equation in Section 4.2.4. The equation of motion from continuum mechanics is given by [Mal69]

$$\frac{\partial(\rho\boldsymbol{v})}{\partial t} + \operatorname{div}_{\boldsymbol{x}}(\rho\boldsymbol{v}\otimes\boldsymbol{v}) = \operatorname{div}_{\boldsymbol{x}}\boldsymbol{\sigma} + \boldsymbol{b}, \tag{4.2.30}$$

where $\boldsymbol{\sigma}$ is the Cauchy stress tensor and $\boldsymbol{b}$ is the body force field. Using Liouville's equation and substituting in the definitions for mass density and the velocity fields defined in (4.2.7) and (4.2.9), respectively, into (4.2.30), it can be shown that the stress tensor and the body force field must satisfy

$$\begin{aligned} \operatorname{div}_{\boldsymbol{x}}\boldsymbol{\sigma} + \boldsymbol{b} = &-\sum_\alpha m_\alpha \operatorname{div}_{\boldsymbol{x}}\left\langle(\boldsymbol{v}_\alpha^{\text{rel}}\otimes\boldsymbol{v}_\alpha^{\text{rel}})W \mid \boldsymbol{x}_\alpha = \boldsymbol{x}\right\rangle \\ &-\sum_\alpha \left\langle W\nabla_{\boldsymbol{x}_\alpha}\mathcal{V}_{\text{int}} \mid \boldsymbol{x}_\alpha = \boldsymbol{x}\right\rangle \\ &-\sum_\alpha \left\langle W\nabla_{\boldsymbol{x}_\alpha}\mathcal{V}_{\text{ext}} \mid \boldsymbol{x}_\alpha = \boldsymbol{x}\right\rangle, \end{aligned} \tag{4.2.31}$$

where

$$\boldsymbol{v}_\alpha^{\text{rel}} := \boldsymbol{v}_\alpha - \boldsymbol{v} \tag{4.2.32}$$

is the velocity of particle α relative to the pointwise velocity field. It is natural to associate $\mathcal{V}_{\text{ext}}$ with the body force field $\boldsymbol{b}$ in (4.2.31). We therefore define $\boldsymbol{b}(\boldsymbol{x}, t)$ as

$$\boldsymbol{b}(\boldsymbol{x}, t) := -\sum_{\alpha} \langle W \nabla_{\boldsymbol{x}_\alpha} \mathcal{V}_{\text{ext}} \mid \boldsymbol{x}_\alpha = \boldsymbol{x} \rangle \,. \tag{4.2.33}$$

Substituting (4.2.33) into (4.2.31), we have

$$\begin{aligned} \operatorname{div}_{\boldsymbol{x}} \boldsymbol{\sigma} = &-\sum_{\alpha} m_\alpha \operatorname{div}_{\boldsymbol{x}} \left\langle (\boldsymbol{v}_\alpha^{\text{rel}} \otimes \boldsymbol{v}_\alpha^{\text{rel}}) W \mid \boldsymbol{x}_\alpha = \boldsymbol{x} \right\rangle \\ &-\sum_{\alpha} \langle W \nabla_{\boldsymbol{x}_\alpha} \mathcal{V}_{\text{int}} \mid \boldsymbol{x}_\alpha = \boldsymbol{x} \rangle \,. \end{aligned} \tag{4.2.34}$$

From (4.2.34), we see that the pointwise stress tensor has two contributions:

$$\boldsymbol{\sigma}(\boldsymbol{x}, t) = \boldsymbol{\sigma}_{\text{k}}(\boldsymbol{x}, t) + \boldsymbol{\sigma}_{\text{v}}(\boldsymbol{x}, t), \tag{4.2.35}$$

where $\boldsymbol{\sigma}_{\text{k}}$ and $\boldsymbol{\sigma}_{\text{v}}$ are, respectively, the *kinetic* and *potential* parts of the pointwise stress. The kinetic part is given by

$$\boldsymbol{\sigma}_{\text{k}}(\boldsymbol{x}, t) = -\sum_{\alpha} m_\alpha \left\langle (\boldsymbol{v}_\alpha^{\text{rel}} \otimes \boldsymbol{v}_\alpha^{\text{rel}}) W \mid \boldsymbol{x}_\alpha = \boldsymbol{x} \right\rangle . \tag{4.2.36}$$

It is evident that the kinetic part of the stress tensor is symmetric. The kinetic stress reflects the momentum flux associated with the vibrational kinetic energy portion of the internal energy.

Continuing with (4.2.34), the potential part of the stress must satisfy the following differential equation:

$$\operatorname{div}_{\boldsymbol{x}} \boldsymbol{\sigma}_{\text{v}}(\boldsymbol{x}, t) = \sum_{\alpha} \left\langle W \boldsymbol{f}_\alpha^{\text{int}} \mid \boldsymbol{x}_\alpha = \boldsymbol{x} \right\rangle , \tag{4.2.37}$$

Equation (4.2.37) needs to be solved in order to obtain an explicit form for $\boldsymbol{\sigma}_{\text{v}}$. In the original paper of Irving and Kirkwood [IK50], a solution to (4.2.37) was obtained for the special case of pair potential interactions by applying a Taylor expansion to the Dirac delta distribution. In contrast, Noll showed that a closed-form solution for $\boldsymbol{\sigma}_{\text{v}}$ can be obtained by recasting the right-hand side in a different form and applying a lemma proved in [Nol55]. We proceed with Noll's approach, except we place no restriction on the nature of the interatomic potential energy $\mathcal{V}_{\text{int}}$.

Derivation of the pointwise stress tensor

We substitute the force decomposition given in (4.2.22) corresponding to a continuously differentiable extension into the potential part of the pointwise stress tensor in (4.2.37) to obtain

$$\operatorname{div}_{\boldsymbol{x}} \boldsymbol{\sigma}_{\mathrm{v}}(\boldsymbol{x}, t) = \sum_{\substack{\alpha,\beta \\ \alpha \neq \beta}} \langle W \boldsymbol{f}_{\alpha\beta} \mid \boldsymbol{x}_\alpha = \boldsymbol{x} \rangle. \tag{4.2.38}$$

On using the identity

$$\langle \boldsymbol{f}_{\alpha\beta} W \mid \boldsymbol{x}_\alpha = \boldsymbol{x} \rangle = \int_{\mathbb{R}^3} \langle \boldsymbol{f}_{\alpha\beta} W \mid \boldsymbol{x}_\alpha = \boldsymbol{x}, \boldsymbol{x}_\beta = \boldsymbol{y} \rangle \, d\boldsymbol{y}, \tag{4.2.39}$$

equation (4.2.38) takes the form

$$\operatorname{div}_{\boldsymbol{x}} \boldsymbol{\sigma}_{\mathrm{v}}(\boldsymbol{x}, t) = \int_{\mathbb{R}^3} \sum_{\substack{\alpha,\beta \\ \alpha \neq \beta}} \langle W \boldsymbol{f}_{\alpha\beta} \mid \boldsymbol{x}_\alpha = \boldsymbol{x}, \boldsymbol{x}_\beta = \boldsymbol{y} \rangle \, d\boldsymbol{y}. \tag{4.2.40}$$

We now note the following lemma due to Noll, which will be used to obtain a closed-form solution to the output fields derived in the Irving–Kirkwood procedure.

Lemma 1. *Let $\boldsymbol{f}(\boldsymbol{v}, \boldsymbol{w})$ be a tensor-valued function of two vectors $\boldsymbol{v}$ and $\boldsymbol{w}$, which satisfies the following three conditions:*

1. *$\boldsymbol{f}(\boldsymbol{v}, \boldsymbol{w})$ is defined for all $\boldsymbol{v}$ and $\boldsymbol{w}$ and is continuously differentiable .*
2. *There exists a $\delta > 0$, such that the auxiliary function $\boldsymbol{g}(\boldsymbol{v}, \boldsymbol{w})$, defined through*

$$\boldsymbol{g}(\boldsymbol{v}, \boldsymbol{w}) := \boldsymbol{f}(\boldsymbol{v}, \boldsymbol{w}) \|\boldsymbol{v}\|^{3+\delta} \|w\|^{3+\delta}, \tag{4.2.41}$$

   and its gradients $\nabla_{\boldsymbol{v}} \boldsymbol{g}$ and $\nabla_{\boldsymbol{w}} \boldsymbol{g}$ are bounded.

3. *$\boldsymbol{f}(\boldsymbol{v}, \boldsymbol{w})$ is antisymmetric, i.e.,*

$$\boldsymbol{f}(\boldsymbol{v}, \boldsymbol{w}) = -\boldsymbol{f}(\boldsymbol{w}, \boldsymbol{v}). \tag{4.2.42}$$

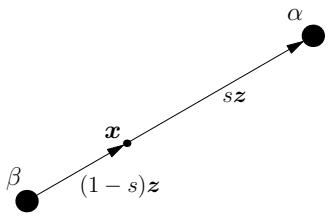

Figure 4.1: A schematic diagram helping to explain the vectors appearing in the pointwise potential stress expression in (4.2.44). The bond α–β is defined by the vector $\boldsymbol{z}$. When $s = 0$, atom α is located at point $\boldsymbol{x}$, and when $s = 1$, atom β is located at $\boldsymbol{x}$.

Under the above conditions, the following equation holds:[10]

$$\int_{\boldsymbol{y}\in\mathbb{R}^3} \boldsymbol{f}(\boldsymbol{x},\boldsymbol{y})\, d\boldsymbol{y} = \\ -\frac{1}{2}\,\mathrm{div}_{\boldsymbol{x}} \int_{\boldsymbol{z}\in\mathbb{R}^3} \left[\int_{s=0}^{1} \boldsymbol{f}(\boldsymbol{x}+s\boldsymbol{z}, \boldsymbol{x}-(1-s)\boldsymbol{z})\, ds\right] \otimes \boldsymbol{z}\, d\boldsymbol{z}. \quad (4.2.43)$$

It is clear that being anti-symmetric, the integrand in the right-hand side of (4.2.40) satisfies all the necessary conditions for the application of Lemma 1. Conditions (1) and (2) are satisfied through the regularity conditions on W. Therefore, using Lemma 1, we have

$$\boldsymbol{\sigma}_{\mathrm{v}}(\boldsymbol{x},t) = \quad (4.2.44)$$
$$\frac{1}{2}\sum_{\substack{\alpha,\beta \\ \alpha\neq\beta}} \int_{\mathbb{R}^3} \int_{s=0}^{1} \langle -\boldsymbol{f}_{\alpha\beta} W \mid \boldsymbol{x}_\alpha = \boldsymbol{x}+s\boldsymbol{z}, \boldsymbol{x}_\beta = \boldsymbol{x}-(1-s)\boldsymbol{z}\rangle\, ds \otimes \boldsymbol{z}\, d\boldsymbol{z}.$$

The expression for the potential part of the pointwise stress tensor in (4.2.44) is a general result applicable to all interatomic potentials. We make some important observations regarding this expressions below:

1. The expression for $\boldsymbol{\sigma}_{\mathrm{v}}$ given in (4.2.44) has an easy interpretation. $\boldsymbol{\sigma}_{\mathrm{v}}$ at a point $\boldsymbol{x}$ is the superposition of the expectation values of the forces in all possible bonds passing through $\boldsymbol{x}$. The variable $\boldsymbol{z}$ selects a bond length and direction and the variable s slides the bond through $\boldsymbol{x}$ from end to end (see Fig. 4.1).

2. $\boldsymbol{\sigma}_{\mathrm{v}}$ is symmetric. This is clear because $\boldsymbol{f}_{\alpha\beta}$ is parallel to $\boldsymbol{z}$ and $\boldsymbol{z}\otimes\boldsymbol{z}$ is symmetric.

[10]The expression in Noll's paper appears transposed relative to (4.2.43). This is because the gradient and divergence operations used by Noll are the transpose of our definitions.

Since the kinetic part of the stress in (4.2.36) is also symmetric, we can conclude that the *pointwise stress tensor is symmetric for all interatomic potentials*.

3. Since $\boldsymbol{\sigma}_{\mathrm{v}}$ depends on the nature of the force decomposition and different extensions of a given potential energy can result in different force decompositions, we conclude that the pointwise stress tensor is *non-unique* for all interatomic potentials (including the pair potential).

The non-uniqueness of the pointwise stress tensor also plays an important role in the energy equation, derived in the next section, since the stress appears in it.

4.2.4 Equation of energy balance

The energy balance equation from continuum mechanics is given by

$$\frac{\partial \rho\epsilon}{\partial t} + \operatorname{div}_{\boldsymbol{x}}(\boldsymbol{q} - \boldsymbol{\sigma}\boldsymbol{v} + \rho\epsilon\boldsymbol{v}) = \boldsymbol{0}, \tag{4.2.45}$$

where ϵ is the specific internal energy and $\boldsymbol{q}$ is the heat flux vector. We saw in the previous section that the Irving–Kirkwood procedure extended to general interatomic potentials yields various possible definitions for the stress tensor. In a similar vein, we hope to use this extended procedure to derive possible definitions for the heat flux vector for arbitrary multi-body potentials. Before that, let us look at the definition for the heat flux vector given by the original Irving–Kirkwood procedure for the case of a pair potential. The heat flux vector in this case is decomposed as

$$\boldsymbol{q} := \boldsymbol{q}_{\mathrm{k}} + \boldsymbol{q}_{\mathrm{T}} + \boldsymbol{q}_{\mathrm{v}}, \tag{4.2.46}$$

where

$$\boldsymbol{q}_{\mathrm{k}} := \frac{1}{2}\sum_{\alpha} m_\alpha \langle \|\boldsymbol{v}_\alpha^{\mathrm{rel}}\|^2 \boldsymbol{v}_\alpha^{\mathrm{rel}} W \mid \boldsymbol{x}_\alpha = \boldsymbol{x}\rangle, \tag{4.2.47}$$

$$\boldsymbol{q}_{\mathrm{T}} := \frac{1}{2}\sum_{\alpha} \langle \boldsymbol{v}_\alpha^{\mathrm{rel}} \mathcal{V}_\alpha W \mid \boldsymbol{x}_\alpha = \boldsymbol{x}\rangle, \tag{4.2.48}$$

and

$$\boldsymbol{q}_{\mathrm{v}} := -\frac{1}{2}\sum_{\substack{\alpha,\beta \\ \alpha\neq\beta}} \int_{\boldsymbol{z}\in\mathbb{R}^3} \frac{\boldsymbol{z}}{\|\boldsymbol{z}\|}\boldsymbol{z}\cdot\phi'_{\alpha\beta} \quad \times \\ \int_{s=0}^{1} \left\langle \left(\frac{\boldsymbol{v}_\alpha + \boldsymbol{v}_\beta}{2} - \boldsymbol{v} \right) W \mid \boldsymbol{x}_\alpha = \boldsymbol{x} + s\boldsymbol{z}, \boldsymbol{x}_\beta = \boldsymbol{x} - (1-s)\boldsymbol{z} \right\rangle ds\, d\boldsymbol{z}, \tag{4.2.49}$$

represent the kinetic part, transport part, and the potential part of the heat flux vector respectively. It was shown by Noll [Nol55] that if the heat flux vector is defined according to (4.2.46), then along with the definition for the specific internal energy given in (4.2.12), and Lemma 1, the energy balance equation (4.2.45) is identically satisfied. We can now try to extend this procedure to arbitrary multi-body potentials by defining a potential energy extension and repeat the steps given in [Nol55]. But before we can do so, we must grapple with the ambiguity that arises in the definition for the potential part of the specific energy, ϵ_{v}, given in (4.2.14). As mentioned at the end of Section 4.2.1, in order to define ϵ_{v} for multi-body potentials we must give a precise definition for the energy of each particle $\mathcal{V}_\alpha$ as done in (4.2.11) for a pair potential. Even for the case of identical particles, it is not *a priori* clear how to distribute the energy between the particles for a multi-body potential. It is clear from (4.2.48) that this results in an ambiguous definition for $\boldsymbol{q}_{\mathrm{T}}$ which depends on the definition for $\mathcal{V}_\alpha$. Moreover, one would expect that the definitions for the pointwise fields should be invariant with respect to addition of any constant to the potential energy. It is clear that all the definitions discussed so far satisfy this invariance except for (4.2.48). Therefore a question that naturally arises is, whether the decomposition of energy is necessary to derive the energy balance equation. An alternate approach which we think is more reasonable comes from a paper by Murdoch [MB94] in his spatial averaging procedure. Here we adapt this approach to the Irving–Kirkwood procedure.

An alternate derivation of the energy balance equation

The alternate derivation for the energy balance equation in this section leads to an expression for the heat flux vector which does not contain the transport part. Moreover, this derivation applies to any multi-body potential with a continuously differentiable extension.

Under this alternate derivation we have the following input and output fields:

$$\begin{array}{cc} \textbf{Input} & \textbf{Output} \\ \left\{ \begin{array}{c} \rho \\ \boldsymbol{v} \\ \epsilon_{\mathrm{k}} \end{array} \right\} & \rightarrow \left\{ \begin{array}{c} \epsilon_{\mathrm{v}} \\ \boldsymbol{b} \\ \boldsymbol{\sigma} \\ \boldsymbol{q} = \boldsymbol{q}_{\mathrm{k}} + \boldsymbol{q}_{\mathrm{v}} \end{array} \right\} \end{array} \tag{4.2.50}$$

We consider the terms in (4.2.45), beginning with $\rho\epsilon_{\mathrm{k}}$ defined in (4.2.13). For simplicity, we assume $\mathcal{V}_{\mathrm{ext}} = 0$. We have

$$\frac{\partial E_{\mathrm{k}}}{\partial t} = \frac{1}{2}\sum_{\alpha} m_\alpha \left\langle \|\boldsymbol{v}_\alpha\|^2 \frac{\partial W}{\partial t} \mid \boldsymbol{x}_\alpha = \boldsymbol{x} \right\rangle, \tag{4.2.51}$$

where $E_{\mathrm{k}} := \rho\epsilon_{\mathrm{k}}$. Using Liouville's equation given in (4.2.3), we obtain

$$\begin{aligned} \frac{\partial E_{\mathrm{k}}}{\partial t} &= \frac{1}{2}\sum_{\alpha} m_\alpha \left\langle \|\boldsymbol{v}_\alpha\|^2 \sum_{\beta} \left(-\boldsymbol{v}_\beta \cdot \nabla_{\boldsymbol{x}_\beta} W + \frac{\nabla_{\boldsymbol{x}_\beta}\mathcal{V}}{m_\beta} \cdot \nabla_{\boldsymbol{v}_\beta} W \right) \mid \boldsymbol{x}_\alpha = \boldsymbol{x} \right\rangle \\ &= -\frac{1}{2}\sum_{\alpha} m_\alpha \left\langle \|\boldsymbol{v}_\alpha\|^2 \boldsymbol{v}_\alpha \cdot \nabla_{\boldsymbol{x}_\alpha} W \mid \boldsymbol{x}_\alpha = \boldsymbol{x} \right\rangle - \frac{1}{2}\sum_{\alpha} \left\langle \|\boldsymbol{v}_\alpha\|^2 \boldsymbol{f}_\alpha^{\mathrm{int}} \cdot \nabla_{\boldsymbol{v}_\alpha} W \mid \boldsymbol{x}_\alpha = \boldsymbol{x} \right\rangle, \\ &=: \boldsymbol{q}_1 + \boldsymbol{q}_2, \end{aligned} \tag{4.2.52}$$

where we have used the identities (4.2.15a) and (4.2.15b). Now note that the term $\|\boldsymbol{v}_\alpha\|^2\boldsymbol{v}_\alpha$ can be written as

$$\begin{aligned} \|\boldsymbol{v}_\alpha\|^2\boldsymbol{v}_\alpha = \|\boldsymbol{v}_\alpha^{\mathrm{rel}}\|^2\boldsymbol{v}_\alpha^{\mathrm{rel}} + 2(\boldsymbol{v}_\alpha^{\mathrm{rel}} \otimes \boldsymbol{v}_\alpha^{\mathrm{rel}})\boldsymbol{v} + \\ \boldsymbol{v}\|\boldsymbol{v}_\alpha\|^2 + \|\boldsymbol{v}\|^2\boldsymbol{v}_\alpha^{\mathrm{rel}}. \end{aligned} \tag{4.2.53}$$

Consider $\boldsymbol{q}_1$, the first term of (4.2.52). Using (4.2.53) and the definitions for $\boldsymbol{q}_{\mathrm{k}}$, $\boldsymbol{\sigma}_{\mathrm{k}}$ and E_{k} given in (4.2.47), (4.2.36) and (4.2.13) respectively, $\boldsymbol{q}_1$ can be expressed as

$$\begin{aligned} \boldsymbol{q}_1 &= -\operatorname{div}_{\boldsymbol{x}}(\boldsymbol{q}_{\mathrm{k}} - \boldsymbol{\sigma}_{\mathrm{k}}\boldsymbol{v} + E_{\mathrm{k}}\boldsymbol{v}) - \\ &\qquad \frac{1}{2}\|\boldsymbol{v}\|^2 \operatorname{div}_{\boldsymbol{x}} \sum_{\alpha} m_\alpha \left\langle \boldsymbol{v}_\alpha^{\mathrm{rel}} W \mid \boldsymbol{x}_\alpha = \boldsymbol{x} \right\rangle \\ &= -\operatorname{div}_{\boldsymbol{x}}(\boldsymbol{q}_{\mathrm{k}} - \boldsymbol{\sigma}_{\mathrm{k}}\boldsymbol{v} + E_{\mathrm{k}}\boldsymbol{v}), \end{aligned} \tag{4.2.54}$$

since $\sum_\alpha m_\alpha \langle \boldsymbol{v}_\alpha^{\mathrm{rel}} W \mid \boldsymbol{x}_\alpha = \boldsymbol{x} \rangle = \boldsymbol{0}$. Now consider $\boldsymbol{q}_2$, the second term of (4.2.52). Integrating by parts, and using the regularity conditions on W, $\boldsymbol{q}_2$ takes the form

$$\boldsymbol{q}_2 = \sum_\alpha \langle \boldsymbol{v}_\alpha \cdot \boldsymbol{f}_\alpha^{\mathrm{int}} W \mid \boldsymbol{x}_\alpha = \boldsymbol{x} \rangle. \tag{4.2.55}$$

Using (4.2.54) and (4.2.55), (4.2.52) becomes

$$\begin{aligned}
&\frac{\partial E_{\mathrm{k}}}{\partial t} \\
&= -\operatorname{div}_{\boldsymbol{x}}(\boldsymbol{q}_{\mathrm{k}} - \boldsymbol{\sigma}_{\mathrm{k}}\boldsymbol{v} + E_{\mathrm{k}}\boldsymbol{v}) + \sum_\alpha \langle \boldsymbol{v}_\alpha \cdot \boldsymbol{f}_\alpha^{\mathrm{int}} W \mid \boldsymbol{x}_\alpha = \boldsymbol{x} \rangle \\
&= -\operatorname{div}_{\boldsymbol{x}}(\boldsymbol{q}_{\mathrm{k}} - \boldsymbol{\sigma}_{\mathrm{k}}\boldsymbol{v} + E_{\mathrm{k}}\boldsymbol{v}) + \sum_\alpha \langle \boldsymbol{v}_\alpha^{\mathrm{rel}} \cdot \boldsymbol{f}_\alpha^{\mathrm{int}} W \mid \boldsymbol{x}_\alpha = \boldsymbol{x} \rangle \\
&\quad + \left[\sum_\alpha \langle \boldsymbol{f}_\alpha^{\mathrm{int}} W \mid \boldsymbol{x}_\alpha = \boldsymbol{x} \rangle \right] \cdot \boldsymbol{v}.
\end{aligned} \tag{4.2.56}$$

We know from the momentum balance equation (see (4.2.37)) that

$$\operatorname{div}_{\boldsymbol{x}} \boldsymbol{\sigma}_{\mathrm{v}} = \sum_\alpha \langle \boldsymbol{f}_\alpha^{\mathrm{int}} W \mid \boldsymbol{x}_\alpha = \boldsymbol{x} \rangle. \tag{4.2.57}$$

Using (4.2.57), together with the identity

$$\operatorname{div}_{\boldsymbol{x}}(\boldsymbol{T}\boldsymbol{b}) = \operatorname{div}(\boldsymbol{T}) \cdot \boldsymbol{b} + \boldsymbol{T} : \nabla_{\boldsymbol{x}} \boldsymbol{b},$$

where T and $\boldsymbol{b}$ are continuously differentiable tensor and vector-valued functions of $\boldsymbol{x}$ respectively, and noting that $\boldsymbol{\sigma} = \boldsymbol{\sigma}_{\mathrm{k}} + \boldsymbol{\sigma}_{\mathrm{v}}$, (4.2.56) can be rewritten as

$$\begin{aligned}
\frac{\partial E_{\mathrm{k}}}{\partial t} &= -\operatorname{div}_{\boldsymbol{x}}(\boldsymbol{q}_{\mathrm{k}} - \boldsymbol{\sigma}\boldsymbol{v} + E_{\mathrm{k}}\boldsymbol{v}) \\
&\quad + \sum_\alpha \langle \boldsymbol{v}_\alpha^{\mathrm{rel}} \cdot \boldsymbol{f}_\alpha^{\mathrm{int}} W \mid \boldsymbol{x}_\alpha = \boldsymbol{x} \rangle - \boldsymbol{\sigma} : \nabla_{\boldsymbol{x}} \boldsymbol{v}.
\end{aligned} \tag{4.2.58}$$

Now, consider the middle term on the right-hand side of (4.2.58) which is given by

$$\boldsymbol{q}_3 := \sum_\alpha \langle \boldsymbol{v}_\alpha^{\mathrm{rel}} \cdot \boldsymbol{f}_\alpha^{\mathrm{int}} W \mid \boldsymbol{x}_\alpha = \boldsymbol{x} \rangle. \tag{4.2.59}$$

Substituting the force decomposition given in (4.2.22) corresponding to a continuously differentiable extension, into (4.2.59), we obtain

$$\begin{aligned}\boldsymbol{q}_3 &= \sum_{\substack{\alpha,\beta \\ \alpha\neq\beta}} \langle \boldsymbol{v}_\alpha^{\mathrm{rel}} \cdot \boldsymbol{f}_{\alpha\beta} W \mid \boldsymbol{x}_\alpha = \boldsymbol{x} \rangle \\ &= \sum_{\substack{\alpha,\beta \\ \alpha\neq\beta}} \int_{\mathbb{R}^3} \langle \boldsymbol{v}_\alpha^{\mathrm{rel}} \cdot \boldsymbol{f}_{\alpha\beta} W \mid \boldsymbol{x}_\alpha = \boldsymbol{x}, \boldsymbol{x}_\beta = \boldsymbol{y} \rangle \, d\boldsymbol{y} \\ &= \int_{\mathbb{R}^3} \left[g_{\mathrm{S}}(\boldsymbol{x}, \boldsymbol{y}) + g_{\mathrm{AS}}(\boldsymbol{x}, \boldsymbol{y}) \right] \, d\boldsymbol{y}, \end{aligned} \tag{4.2.60}$$

where

$$g_{\mathrm{S}}(\boldsymbol{x}, \boldsymbol{y}) = \frac{1}{2} \sum_{\substack{\alpha,\beta \\ \alpha\neq\beta}} \langle (\boldsymbol{f}_{\alpha\beta} \cdot \boldsymbol{v}_\alpha^{\mathrm{rel}} + \boldsymbol{f}_{\beta\alpha} \cdot \boldsymbol{v}_\beta^{\mathrm{rel}}) W \mid \boldsymbol{x}_\alpha = \boldsymbol{x}, \boldsymbol{x}_\beta = \boldsymbol{y} \rangle, \tag{4.2.61}$$

$$g_{\mathrm{AS}}(\boldsymbol{x}, \boldsymbol{y}) = \frac{1}{2} \sum_{\substack{\alpha,\beta \\ \alpha\neq\beta}} \langle (\boldsymbol{f}_{\alpha\beta} \cdot \boldsymbol{v}_\alpha^{\mathrm{rel}} - \boldsymbol{f}_{\beta\alpha} \boldsymbol{v}_\beta^{\mathrm{rel}}) W \mid \boldsymbol{x}_\alpha = \boldsymbol{x}, \boldsymbol{x}_\beta = \boldsymbol{y} \rangle. \tag{4.2.62}$$

It is easy to check that $g_{\mathrm{AS}}(\boldsymbol{x}, \boldsymbol{y}) = -g_{\mathrm{AS}}(\boldsymbol{y}, \boldsymbol{x})$, i.e., it is antisymmetric with respect to its arguments. Moreover, the second integrand on the right-hand side of (4.2.60) satisfies all the necessary conditions for the applications of Lemma 1. Using Lemma 1, we can express the second integral in (4.2.60) as

$$\int_{\mathbb{R}^3} g_{\mathrm{AS}}(\boldsymbol{x}, \boldsymbol{y}) \, d\boldsymbol{y} = -\operatorname{div}_{\boldsymbol{x}} \boldsymbol{q}_{\mathrm{v}}. \tag{4.2.63}$$

where

$$\boldsymbol{q}_{\mathrm{v}} := \frac{1}{2} \sum_{\substack{\alpha,\beta \\ \alpha\neq\beta}} \int_{\boldsymbol{z}\in\mathbb{R}^3} \boldsymbol{z} \int_{s=0}^{1} \left\langle \boldsymbol{f}_{\alpha\beta} \cdot \left(\frac{\boldsymbol{v}_\alpha + \boldsymbol{v}_\beta}{2} - \boldsymbol{v} \right) W \mid \boldsymbol{x}_\alpha = \boldsymbol{x} + s\boldsymbol{z}, \boldsymbol{x}_\beta = \boldsymbol{x} - (1-s)\boldsymbol{z} \right\rangle \, ds \, d\boldsymbol{z}. \tag{4.2.64}$$

Substituting (4.2.63) into (4.2.60), and noting that

$$\int_{\mathbb{R}^3} g_{\mathrm{S}}(\boldsymbol{x},\boldsymbol{y})\,d\boldsymbol{y} = \frac{1}{2}\sum_{\substack{\alpha,\beta\\ \alpha\neq\beta}} \langle \boldsymbol{f}_{\alpha\beta}\cdot(\boldsymbol{v}_\alpha-\boldsymbol{v}_\beta)W \mid \boldsymbol{x}_\alpha=\boldsymbol{x}\rangle,$$
$$=: \bar{g}_{\mathrm{S}}(\boldsymbol{x},t) \tag{4.2.65}$$

we obtain

$$\frac{\partial E_{\mathrm{k}}}{\partial t} = -\operatorname{div}_{\boldsymbol{x}}[\boldsymbol{q}_{\mathrm{k}}+\boldsymbol{q}_{\mathrm{v}}-\boldsymbol{\sigma}\boldsymbol{v}+E_k\boldsymbol{v}] - \boldsymbol{\sigma}:\nabla_{\boldsymbol{x}}\boldsymbol{v}+\bar{g}_{\mathrm{S}}(\boldsymbol{x},t). \tag{4.2.66}$$

Now, recall the energy equation of continuum thermodynamics in (4.2.45). Subtracting (4.2.66) form (4.2.45), we obtain

$$\frac{\partial(\rho\epsilon_{\mathrm{v}})}{\partial t} = -\operatorname{div}_{\boldsymbol{x}}(\boldsymbol{q}-\boldsymbol{q}_{\mathrm{k}}-\boldsymbol{q}_{\mathrm{v}}+\rho\epsilon_{\mathrm{v}}\boldsymbol{v}) + \boldsymbol{\sigma}:\nabla_{\boldsymbol{x}}\boldsymbol{v}-\bar{g}_{\mathrm{S}}(\boldsymbol{x},t). \tag{4.2.67}$$

The following step is a crucial part of our derivation. Note that in contrast to the original Irving–Kirkwood derivation, the transport part of the heat flux, $\boldsymbol{q}_{\mathrm{T}}$, does not appear here. *We can therefore identify the heat flux vector* $\boldsymbol{q}$ *with* $\boldsymbol{q}_{\mathrm{k}}+\boldsymbol{q}_{\mathrm{v}}$, i.e.,

$$\boldsymbol{q} := \boldsymbol{q}_{\mathrm{k}}+\boldsymbol{q}_{\mathrm{v}}. \tag{4.2.68}$$

Thus, (4.2.67) reduces to

$$\frac{\partial(\rho\epsilon_{\mathrm{v}})}{\partial t} = -\operatorname{div}_{\boldsymbol{x}}(\rho\epsilon_{\mathrm{v}}\boldsymbol{v}) + \boldsymbol{\sigma}:\nabla_{\boldsymbol{x}}\boldsymbol{v}-\bar{g}_{\mathrm{S}}(\boldsymbol{x},t),$$

which implies that

$$\epsilon_{\mathrm{v}}\frac{\partial\rho}{\partial t}+\rho\frac{\partial\epsilon_{\mathrm{v}}}{\partial t} = \epsilon_{\mathrm{v}}\operatorname{div}_{\boldsymbol{x}}(\rho\boldsymbol{v}) - \rho\nabla\epsilon_{\mathrm{v}}\cdot\boldsymbol{v}$$
$$+\boldsymbol{\sigma}:\nabla_{\boldsymbol{x}}\boldsymbol{v}-\bar{g}_{\mathrm{S}}(\boldsymbol{x}). \tag{4.2.69}$$

Using the equation of continuity, (4.2.69) simplifies to

$$\rho\left(\frac{\partial\epsilon_{\mathrm{v}}}{\partial t}+\nabla\epsilon_{\boldsymbol{v}}\cdot\boldsymbol{v}\right) = \boldsymbol{\sigma}:\nabla_{\boldsymbol{x}}\boldsymbol{v}-\bar{g}_{\mathrm{S}}(\boldsymbol{x},t), \tag{4.2.70}$$

which implies that

$$\rho\dot{\epsilon}_{\mathrm{v}} = \boldsymbol{\sigma}:\nabla_{\boldsymbol{x}}\boldsymbol{v}-\bar{g}_{\mathrm{S}}(\boldsymbol{x},t). \tag{4.2.71}$$

It is clear from (4.2.71) that we now have a new definition for the specific internal energy (similar to the one obtained by Murdoch [MB94] in the Murdoch procedure) given by

$$\epsilon_{\mathrm{v}}(\boldsymbol{x},t) = \int_0^t \frac{1}{\rho}\left(\boldsymbol{\sigma} : \nabla_{\boldsymbol{x}}\boldsymbol{v} - \bar{g}_{\mathrm{S}}(\boldsymbol{x},t)\right)\, dt + c. \tag{4.2.72}$$

This definition does not require a decomposition of the total energy to individual atoms, i.e., it is independent of a particular choice for $\mathcal{V}_\alpha$, contrary to what is observed in the original Irving–Kirkwood procedure and its generalization to multi-body potentials found in the literature (see [Che06, ZT04, ZWS08, MR83, TNO08]).

In summary, we obtained new definitions for ϵ_{v} and $\boldsymbol{q}$, which are quite different from those obtained in the Irving–Kirkwood procedure. We believe that the new definitions for ϵ_{v} and $\boldsymbol{q}_{\mathrm{v}}$ given in (4.2.72) and (4.2.68) respectively are more physically reasonable as compared to those given in (4.2.14) and (4.2.46) due to the following features which are not observed in the Irving–Kirkwood procedure or any of its previous generalizations to multi-body potentials:

1. The definitions for $\boldsymbol{q}$ and ϵ_{v} given in (4.2.68) and (4.2.72) depend on the derivative of the potential thus making them invariant with respect to changes in the potential energy by a constant. This is a rather natural thing to expect.

2. The heat flux vector obtained in the alternate derivation does not have transport part. This suggests that we look for numerical experiments which yield a non-trivial transport part using the original Irving–Kirkwood procedure. Most of the numerical experiments found in the literature, which study the energy balance equation obtained though the Irving–Kirkwood procedure, lump the transport part into either the kinetic or potential parts of of the heat flux vector and do not observe it separately. Hence, there has been no extensive numerical study of the role of this term. If indeed the expression for the transport part of the heat flux vector found in the Irving–Kirkwood procedure always has a negligible contribution to the heat flux vector, then its existence can be questioned. Preliminary numerical simulations we conducted to explore this (which are not reported here) always yielded a negligible transport part.

3. From Section 4.2.3 and Section 4.2.4, it follows that the only ambiguity in the expressions obtained through this modified derivation is the non-uniqueness of the pointwise stress tensor, which is directly related to the force decomposition. It was shown in [AT10] that this non-uniqueness vanishes in the thermodynamic limit.

4.3 Expression for MD simulation

In the previous sections we saw that various pointwise fields can be obtained through the Irving–Kirkwood procedure. As noted in Section II, the pointwise field are not continuum fields. We identify the continuum fields with macroscopic observables obtained in a two-step process:

1. A pointwise field is obtained as a statistical mechanics phase average.
2. A macroscopic field is obtained as a spatial average over the pointwise field.

We have seen that the pointwise fields obtained in the first step are defined as phase averages with respect to a probability density function. Typically a molecular dynamics (MD) simulation is purely deterministic in nature, meaning that at a given instant in time, we have a complete microscopic description of the system. Due to this knowledge, the probability density function introduced in the Irving–Kirkwood procedure reduces to a Dirac delta distribution supported on the point in the phase space corresponding to the state of the system. If $(\boldsymbol{x}^{\mathrm{MD}}(t), \boldsymbol{v}^{\mathrm{MD}}(t))$ denotes the evolution of an MD simulation, then the probability density function W^{MD} corresponding to an MD simulation is given by

$$W^{\mathrm{MD}}(\boldsymbol{x}, \boldsymbol{v}; t) = \prod_{\alpha} \delta(\boldsymbol{x}_\alpha - \boldsymbol{x}_\alpha^{\mathrm{MD}}(t)) \delta(\boldsymbol{v}_\alpha - \boldsymbol{v}_\alpha^{\mathrm{MD}}(t)). \tag{4.3.1}$$

Therefore, in an MD setting, the pointwise fields obtained in step 1 are localized to the particle positions. Next, we spatially average these fields with respect to a normalized weighting function that has compact support, thus obtaining expressions for the continuum fields that can be numerically evaluated using the data generated in a MD simulation.

Spatial averaging

A macroscopic quantity is by necessity an average over some spatial region surrounding the continuum point where it is nominally defined. Thus, if $f(\boldsymbol{x}, t; W)$ is an Irving–Kirkwood-pointwise field, such as density, stress or internal energy, the corresponding macroscopic field $f_w(\boldsymbol{x}, t)$ is given by

$$f_w(\boldsymbol{x}, t) = \int_{\mathbb{R}^3} w(\boldsymbol{y} - \boldsymbol{x}) f(\boldsymbol{y}, t; W)\, d\boldsymbol{y}, \tag{4.3.2}$$

where $w(\boldsymbol{r})$ is a suitable weighting function.

It is important to note that due to the linearity of the phase averaging in the Irving–Kirkwood procedure, the averaged macroscopic function $f_w(\boldsymbol{x}, t)$ satisfies the same balance equations as does the pointwise measure $f(\boldsymbol{x}, t)$.

Weighting function

The weighting function $w(\boldsymbol{r})$ is a real-valued function[11] with units of volume^{-1} which satisfies the normalization condition

$$\int_{\mathbb{R}^3} w(\boldsymbol{r}) d\boldsymbol{r} = 1. \tag{4.3.3}$$

This condition ensures that the correct macroscopic field is obtained when the pointwise field is uniform. For a spherically-symmetric function, $w(\boldsymbol{r}) = \hat{w}(r)$, where $r = \|\boldsymbol{r}\|$. The normalization condition in this case is

$$\int_0^\infty \hat{w}(r) 4\pi r^2 dr = 1.$$

The simplest choice for $\hat{w}(r)$ is a spherically-symmetric uniform function over a specified radius r_w, given by

$$\hat{w}(r) = \begin{cases} 1/V_w & \text{if } r \leq r_w, \\ 0 & \text{otherwise}, \end{cases} \tag{4.3.4}$$

where $V_w = \frac{4}{3}\pi r_w^3$ is the volume of the sphere. This function is discontinuous at $r = r_w$. If this is a concern, a "mollifying function" [Mur07] that smoothly takes $w(r)$ to zero at r_w over some desired range can be added (see (4.4.6)). Other possible choices include for example Gaussian functions [Har82], or spline function used in meshless methods [BKO$^+$96] (see [AT10] for details). Many physical interpretations can be given to the weighting function. See [MB94] for further details.

One possible interpretation for a positive-valued w with compact support (as described above) can be related to the physical nature of the experimental probe measuring the continuum fields. In this case, the size of the compact support represents the length scale over which continuum fields are being measured. An alternative approach described by Murdoch and Bedeaux [MB94] is based on the requirement that "repeated spatial averaging should produce nothing new". In other words, spatially averaging a quantity that was al-

[11] It was mentioned in [AT10] that the weighting function is a positive-valued function based on our interpretation of it being related to the nature of the experimental probe. We thank I. Murdoch for directing us to an alternate interpretation which allows the weighting function to take on negative values. See [MB94] for details.

ready spatially averaged should give the same average. This leads to a definite form for the weighting function that also takes on negative values.

It is straightforward to see that substituting the expression given in (4.3.1) for the probability density function into (4.3.2) and performing the spatial averaging defined there using any weighting function discussed above, we obtain expressions for continuum fields that can be numerically evaluated using the data generated from an MD simulation. For example, let us look at the mass density field given in (4.2.7) and repeated here with $W = W^{\mathrm{MD}}$:

$$\rho(\boldsymbol{x}, t) = \sum_{\alpha} m_\alpha \langle W^{\mathrm{MD}} \mid \boldsymbol{x}_\alpha = \boldsymbol{x} \rangle. \tag{4.3.5}$$

Spatially averaging this distribution with respect to the weighting function results in

$$\rho_w(\boldsymbol{x}, t) = \sum_{\alpha} m_\alpha w(\boldsymbol{x}_\alpha^{\mathrm{MD}} - \boldsymbol{x}), \tag{4.3.6}$$

where ρ_w denotes the continuum mass density field obtained by the spatial averaging of the pointwise field ρ with respect to the weighting function w. Similarly, all other continuum definitions for an MD simulation are obtained from their probabilistic versions. Following

is a catalog of definitions for continuum fields that can be evaluated in any MD simulation:

$$\boldsymbol{p}_w(\boldsymbol{x},t) = \sum_\alpha m_\alpha \boldsymbol{v}_\alpha w(\boldsymbol{x}_\alpha^{\mathrm{MD}} - \boldsymbol{x}), \tag{4.3.7}$$

$$\boldsymbol{v}_w(\boldsymbol{x},t) = \frac{\boldsymbol{p}_w(\boldsymbol{x},t)}{\rho_w(\boldsymbol{x},t)}, \tag{4.3.8}$$

$$\boldsymbol{\sigma}_w(\boldsymbol{x},t) = \boldsymbol{\sigma}_{w,\mathrm{k}}(\boldsymbol{x},t) + \boldsymbol{\sigma}_{w,\mathrm{v}}(\boldsymbol{x},t), \tag{4.3.9}$$

$$\epsilon_w(\boldsymbol{x},t) = \epsilon_{w,\mathrm{k}}(\boldsymbol{x},t) + \epsilon_{w,\mathrm{v}}(\boldsymbol{x},t), \tag{4.3.10}$$

$$\boldsymbol{q}_w(\boldsymbol{x},t) = \boldsymbol{q}_{w,\mathrm{k}}(\boldsymbol{x},t) + \boldsymbol{q}_{w,\mathrm{v}}(\boldsymbol{x},t), \tag{4.3.11}$$

$$\boldsymbol{\sigma}_{w,\mathrm{k}}(\boldsymbol{x},t) = -\sum_\alpha m_\alpha (\boldsymbol{v}_\alpha^{\mathrm{rel}} \otimes \boldsymbol{v}_\alpha^{\mathrm{rel}}) w(\boldsymbol{x}_\alpha^{\mathrm{MD}} - \boldsymbol{x}), \qquad \boldsymbol{v}_\alpha^{\mathrm{rel}} = \boldsymbol{v}_\alpha^{\mathrm{MD}} - \boldsymbol{v}, \tag{4.3.12}$$

$$\rho_w \epsilon_{w,\mathrm{k}}(\boldsymbol{x},t) = \frac{1}{2}\sum_\alpha m_\alpha \|\boldsymbol{v}_\alpha^{\mathrm{MD}}\|^2 w(\boldsymbol{x}_\alpha^{\mathrm{MD}} - \boldsymbol{x}), \tag{4.3.13}$$

$$\boldsymbol{q}_{w,\mathrm{k}}(\boldsymbol{x},t) = \frac{1}{2}\sum_\alpha m_\alpha \|\boldsymbol{v}_\alpha^{\mathrm{rel}}\|^2 \boldsymbol{v}_\alpha^{\mathrm{rel}} w(\boldsymbol{x}_\alpha^{\mathrm{MD}} - \boldsymbol{x}), \tag{4.3.14}$$

$$\begin{aligned}\boldsymbol{\sigma}_{w,\mathrm{v}}(\boldsymbol{x},t) = \frac{1}{2}\sum_{\substack{\alpha,\beta \\ \alpha\neq\beta}} \int_{\mathbb{R}^3} w(\boldsymbol{y}-\boldsymbol{x}) \times \\ \int_{s=0}^1 \left\langle -\boldsymbol{f}_{\alpha\beta} W^{\mathrm{MD}} \mid \boldsymbol{x}_\alpha = \boldsymbol{y} + s\boldsymbol{z}, \boldsymbol{x}_\beta = \boldsymbol{y} - (1-s)\boldsymbol{z} \right\rangle ds \otimes \boldsymbol{z}\, d\boldsymbol{z}\, d\boldsymbol{y},\end{aligned} \tag{4.3.15}$$

$$\begin{aligned}\epsilon_{w,\mathrm{v}}(\boldsymbol{x},t) &= \int_0^t \frac{1}{\rho}\left(\boldsymbol{\sigma}_w : \nabla_{\boldsymbol{x}} \boldsymbol{v}_w - \bar{g}_{w,\mathrm{S}}(\boldsymbol{x},t)\right) dt, \\ \bar{g}_{w,\mathrm{S}}(\boldsymbol{x},t) &= \frac{1}{2}\sum_{\substack{\alpha,\beta \\ \alpha\neq\beta}} \boldsymbol{f}_{\alpha\beta}^{\mathrm{MD}} \cdot (\boldsymbol{v}_\alpha^{\mathrm{MD}} - \boldsymbol{v}_\beta^{\mathrm{MD}}) w(\boldsymbol{x}_\alpha^{\mathrm{MD}} - \boldsymbol{x}),\end{aligned} \tag{4.3.16}$$

$$\begin{aligned}\boldsymbol{q}_{w,\mathrm{v}}(\boldsymbol{x},t) = \frac{1}{2}\sum_{\substack{\alpha\beta \\ \alpha\neq\beta}} \int_{\mathbb{R}^3} w(\boldsymbol{y}-\boldsymbol{x}) \int_{\mathbb{R}^3} \boldsymbol{z} \quad \times \\ \int_{s=0}^1 \left\langle \boldsymbol{f}_{\alpha\beta} \cdot \left(\frac{\boldsymbol{v}_\alpha + \boldsymbol{v}_\beta}{2} - \boldsymbol{v}\right) W^{\mathrm{MD}} \mid \boldsymbol{x}_\alpha = \boldsymbol{y} + s\boldsymbol{z}, \boldsymbol{x}_\beta = \boldsymbol{y} - (1-s)\boldsymbol{z} \right\rangle ds\, d\boldsymbol{z}\, d\boldsymbol{y}.\end{aligned} \tag{4.3.17}$$

The expressions for $\boldsymbol{\sigma}_{w,\mathrm{v}}$ and $\boldsymbol{q}_{w,\mathrm{v}}$ given in (4.3.15) and (4.3.17) respectively, can be further simplified by the following simple change of variables:

$$\boldsymbol{y} + s\boldsymbol{z} = \boldsymbol{u}, \qquad \boldsymbol{y} - (1-s)\boldsymbol{z} = \boldsymbol{v}, \tag{4.3.18}$$

which implies that

$$\boldsymbol{z} = \boldsymbol{u} - \boldsymbol{v}, \qquad \boldsymbol{y} = (1-s)\boldsymbol{u} + s\boldsymbol{v}. \tag{4.3.19}$$

The Jacobian of the transformation is

$$J = \det \begin{bmatrix} \nabla_{\boldsymbol{u}} \boldsymbol{z} & \nabla_{\boldsymbol{v}} \boldsymbol{z} \\ \nabla_{\boldsymbol{u}} \boldsymbol{y}_{\perp} & \nabla_{\boldsymbol{v}} \boldsymbol{y}_{\perp} \end{bmatrix} = \det \begin{bmatrix} \boldsymbol{I} & -\boldsymbol{I} \\ (1-s)\boldsymbol{I} & s\boldsymbol{I} \end{bmatrix} = 1. \tag{4.3.20}$$

Using (4.3.18), (4.3.19) and (4.3.20), $\boldsymbol{q}_{w,\mathrm{v}}$ simplifies to

$$\begin{aligned} &\boldsymbol{q}_{w,\mathrm{v}}(\boldsymbol{x}, t) = \\ &\frac{1}{2} \sum_{\substack{\alpha\beta \\ \alpha \neq \beta}} \int_{\mathbb{R}^3 \times \mathbb{R}^3} \left\langle \boldsymbol{f}_{\alpha\beta} \cdot \left(\frac{\boldsymbol{v}_\alpha + \boldsymbol{v}_\beta}{2} - \boldsymbol{v} \right) W^{\mathrm{MD}} \mid \boldsymbol{x}_\alpha = \boldsymbol{u}, \boldsymbol{x}_\beta = \boldsymbol{v} \right\rangle (\boldsymbol{u} - \boldsymbol{v}) b(\boldsymbol{x}; \boldsymbol{u}, \boldsymbol{v}) \, d\boldsymbol{u} \, d\boldsymbol{v}, \\ &\qquad = \frac{1}{2} \sum_{\substack{\alpha\beta \\ \alpha \neq \beta}} \boldsymbol{f}_{\alpha\beta}^{\mathrm{MD}} \cdot \left(\frac{\boldsymbol{v}_\alpha^{\mathrm{MD}} + \boldsymbol{v}_\beta^{\mathrm{MD}}}{2} - \boldsymbol{v}_w \right) (\boldsymbol{x}_\alpha^{\mathrm{MD}} - \boldsymbol{x}_\beta^{\mathrm{MD}}) b(\boldsymbol{x}; \boldsymbol{x}_\alpha^{\mathrm{MD}}, \boldsymbol{x}_\beta^{\mathrm{MD}}), \end{aligned} \tag{4.3.21}$$

where

$$b(\boldsymbol{x}; \boldsymbol{u}, \boldsymbol{v}) = \int_{s=0}^{1} w((1-s)\boldsymbol{u} + s\boldsymbol{v} - \boldsymbol{x}) \, ds,$$

is called the *bond function*. Similarly, $\boldsymbol{\sigma}_{w,\mathrm{v}}$ simplifies to

$$\boldsymbol{\sigma}_{w,\mathrm{v}}(\boldsymbol{x}, t) = \frac{1}{2} \sum_{\substack{\alpha,\beta \\ \alpha \neq \beta}} -\boldsymbol{f}_{\alpha\beta}^{\mathrm{MD}} \otimes (\boldsymbol{x}_\alpha^{\mathrm{MD}} - \boldsymbol{x}_\beta^{\mathrm{MD}}) b(\boldsymbol{x}; \boldsymbol{x}_\alpha^{\mathrm{MD}}, \boldsymbol{x}_\beta^{\mathrm{MD}}). \tag{4.3.22}$$

Hence, equations (4.3.6)-(4.3.14), (4.3.16), (4.3.21) and (4.3.22), are the most simplified form of continuum fields that can be evaluated in an MD simulation. These expressions constitute a generalization to many-body potentials of expressions originally given by Hardy [Har82] for the special case of pair potentials (noting that our expressions for the internal energy density and heat flux vector which have modified forms). Other commonly-used definitions like the virial stress [Cla70] and the Tsai traction [Tsa79] can be obtained as limiting cases of the above relations (see [AT10] for details). We therefore see that our formulation is unified in the sense that it shows how all of these relations are related and provides a single framework that encompasses them all.

4.4 Numerical experiments

It was mentioned at the end of Section 4.2.4 that the definitions obtained in the new derivation are quite different and some qualitative differences were identified. We now try to see how the definitions vary quantitatively. Various stress tensors obtained through this unified framework were studied in [AT10] by the authors. In this section, we describe molecular dynamics simulations that are carried out to compare the following two quantities:

$$\epsilon^{\mathrm{ik}}_{w,\mathrm{v}}(\boldsymbol{x},t) = \frac{1}{\rho}\sum_{\alpha}\mathcal{V}_\alpha w(\boldsymbol{x}^{\mathrm{MD}}_\alpha - \boldsymbol{x}) - \epsilon^{\mathrm{ik}}_{w,\mathrm{v}}(\boldsymbol{x},0), \tag{4.4.1}$$

$$\epsilon_{w,\mathrm{v}}(\boldsymbol{x},t) = \int_0^t \frac{1}{\rho}\left(\boldsymbol{\sigma}_w : \nabla_{\boldsymbol{x}}\boldsymbol{v}_w - \bar{g}_{w,\mathrm{S}}(\boldsymbol{x},t)\right)\,dt. \tag{4.4.2}$$

Here $\epsilon^{\mathrm{ik}}_{w,\mathrm{v}}$ is the local spatial average of the potential part of the specific internal energy in the original Irving–Kirkwood formulation. $\epsilon_{w,\mathrm{v}}$ is the corresponding expression in the new formulation taken from (4.3.16). The constant in (4.4.1) is chosen in order to compare the above two equations from a fixed datum. To explore the role of the two parts of the integrand in (4.4.2), we define

$$\epsilon^1_{w,\mathrm{v}}(\boldsymbol{x},t) := \int_0^t \frac{1}{\rho}\left(\boldsymbol{\sigma}_w : \nabla_{\boldsymbol{x}}\boldsymbol{v}_w\right)\,dt, \tag{4.4.3}$$

$$\epsilon^2_{w,\mathrm{v}}(\boldsymbol{x},t) := -\int_0^t \frac{1}{\rho}\bar{g}_{w,\mathrm{S}}(\boldsymbol{x},t)\,dt, \tag{4.4.4}$$

so that $\epsilon_{w,\mathrm{v}} = \epsilon^1_{w,\mathrm{v}} + \epsilon^2_{w,\mathrm{v}}$.

Interatomic potential

Since the unified framework applies to arbitrary multi-body potentials, it would have been ideal to choose a multi-body potential for our numerical experiments. Unfortunately, since as mentioned in the introduction, there is no rigorous way to distribute the total energy among particles, the expression for $\epsilon^{\mathrm{ik}}_{w,\mathrm{v}}$ in (4.4.1) is ill-defined. Thus the only possibility for comparison is in the special case of pair potential interactions in a system of identical particles. In this case due to symmetry, it is reasonable to divide the energy equally among the particles (see footnote [4]), thus arriving at a plausible definition for $\epsilon^{\mathrm{ik}}_{w,\mathrm{v}}$. We will see that even in this case the expressions in (4.4.1) and (4.4.2) are not equivalent. In more general cases, we argue that only the new expression in (4.4.2) is well-defined.

Our system consists of particles arranged in a face-centered cubic crystal, stacked together in the form of $15 \times 15 \times 15$ unit cells, interacting through a modified Lennard-Jones type

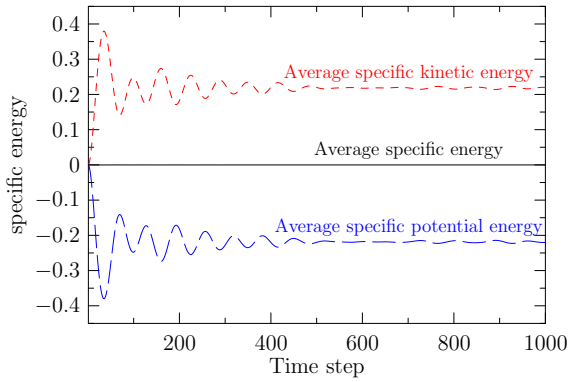

Figure 4.2: Plot showing the average specific potential energy and the average specific kinetic energy. Since this is a constant energy simulation, their sum (*black solid line*) is always constant.

potential. The Lennard-Jones parameter, ϵ and σ are arbitrarily set to 1. The potential has the following form:

$$\phi(r) = 4\left[\frac{1}{r^{12}} - \frac{1}{r^6}\right] - 0.0078r^2 + 0.0651. \tag{4.4.5}$$

The above equation has been rendered dimensionless by expressing lengths in units of σ and energy in units of ϵ. As seen in the above equation, the standard Lennard-Jones potential is modified by the addition of a quadratic term. This is done to ensure that $\phi(r_{\text{cut}}) = \phi'(r_{\text{cut}}) = 0$, where $r_{\text{cut}} = 2.5$, denotes the cutoff radius for the potential. We refer to this as the "Modified Lennard-Jones potential". The ground state of this potential is an fcc crystal with a lattice constant of $a = 1.556$. Thus, the dimension of the sample at ground state is given by its length $l = 15 \times 1.556 = 23.34$. We use the *velocity Verlet* time integration algorithm to evolve the system.

The weighting function, $w(r)$, is chosen to be a constant with a suitable mollifying function [Mur07],

$$w(r) = \begin{cases} c & \text{if } r < R - \delta \\ \frac{1}{2}c\left[1 - \cos\left(\frac{R-r}{\delta}\pi\right)\right] & \text{if } R - \delta < r < R \\ 0 & \text{otherwise} \end{cases}, \tag{4.4.6}$$

where $\delta = 0.12$, R is the radius of the sphere which forms the compact support and $c = 1 - (\delta/R)^3 + 3(\delta/R)^2 - 1.5(\delta/R)$. The constant c is chosen to normalize the weighting function.

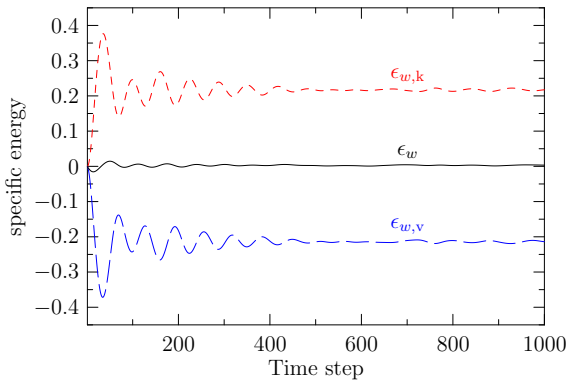

(a)

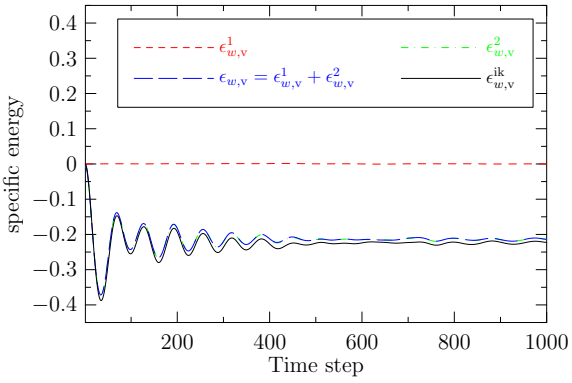

(b)

Figure 4.3: Evolution of specific internal energy for a constant energy simulation with periodic boundary conditions. (a) Plot showing the evolution of the potential part, $\epsilon_{w,\mathrm{v}}$, and the kinetic part, $\epsilon_{w,\mathrm{k}}$, of the specific internal energy. The total specific internal energy (shown in black solid line) is not strictly constant. (b) Plot comparing the evolution of the potential part of the specific internal energy with its analogue, $\epsilon^{\mathrm{ik}}_{w,\mathrm{v}}$, in the original Irving–Kirkwood procedure.

Experiment 1

We begin with a *constant energy* molecular dynamics simulation with *periodic boundary conditions*. The atoms in the system are randomly perturbed to induce a temperature of $T = 0.145$ in Lennard-Jones units after equilibration. Fig. 4.2 shows the evolution of the average specific potential energy, i.e., the total potential energy divided by the mass ($= N$ in our case), and average specific kinetic energy, which add up to a constant specific internal energy. (The average specific internal energy is constant since this is a constant energy simulation.)

Now, suppose we are interested in evaluating the continuum quantities given in (4.4.1) and (4.4.2) at the center of our system. To do this, we choose $R = 0.4l$, which corresponds to a length of 6 unit cells, for the radius of the compact support of the weighting function.

Fig. 4.3(a) shows a plot of the potential and kinetic part of the specific energy at the center of the sample calculated using the weighting function given in (4.4.6). It is clear from the plot that the total specific energy at the center of the sample has some oscillations up to about 200 time steps before these oscillations become negligible. This reminds us that although we are performing a constant energy simulation, the *specific* internal energy at a point need not be constant. Fig. 4.3(b) compares the different expressions for the potential part of the specific internal energy given in (4.4.1) and (4.4.2). The plots for $\epsilon_{w,\mathrm{v}}$ and $\epsilon^{\mathrm{ik}}_{w,\mathrm{v}}$ are in good agreement. It is also clear from the plot that the contribution of $\epsilon^{1}_{w,\mathrm{v}}$ to $\epsilon_{w,\mathrm{v}}$ is negligible.

Experiment 2

In this experiment, we continue with the same system with periodic boundary conditions. We begin with the particles at their equilibrium positions, with temperature $T = 0$. We allow the system to evolve for the first 1000 time steps during which we observe small fluctuations due to numerical noise. We then instantaneously increase the temperature to $T = 0.2$ using a simple velocity rescaling thermostat and maintain this temperature for the rest of the simulation. Again, we are interested in studying the continuum fields at the center of the sample. We choose the radius of the compact support $R = 0.4l$ for the weighting function, as in the previous experiment. Fig. 4.4(a) shows the plot of $\epsilon_{w,\mathrm{v}}$, $\epsilon_{w,\mathrm{k}}$, and the total specific internal energy at the center of the sample for this case. Fig. 4.4(b) compares $\epsilon_{w,\mathrm{v}}$ with $\epsilon^{\mathrm{ik}}_{w,\mathrm{v}}$. It is clear from this plot that both $\epsilon_{w,\mathrm{v}}$ and $\epsilon^{\mathrm{ik}}_{w,\mathrm{v}}$ are in good agreement with each other. It is interesting to see that the contribution to $\epsilon_{w,\mathrm{v}}$ due to $\epsilon^{1}_{w,\mathrm{v}}$ remains negligible

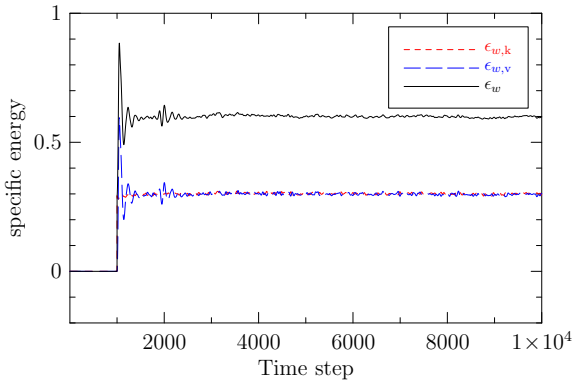

(a)

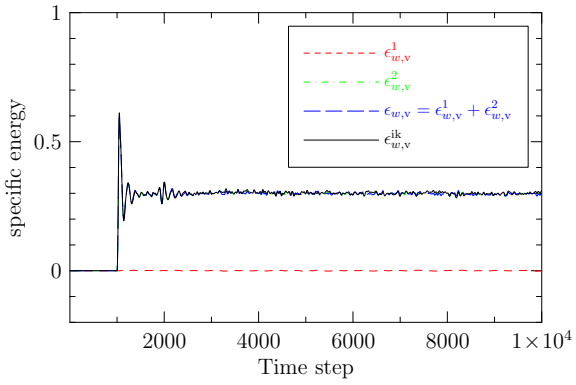

(b)

Figure 4.4: Evolution of specific internal energy for a constant temperature (applied after first 1000 time steps) simulation with periodic boundary conditions. (a) Plot showing the evolution of the potential part, $\epsilon_{w,\mathrm{v}}$, and the kinetic part, $\epsilon_{w,\mathrm{k}}$, of the specific internal energy (b) Plot comparing the evolution of the potential part of the specific internal energy with its analogue, $\epsilon^{\mathrm{ik}}_{w,\mathrm{v}}$, in the original Irving–Kirkwood procedure.

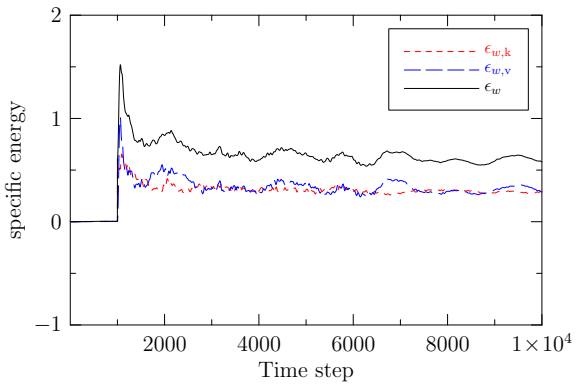

(a)

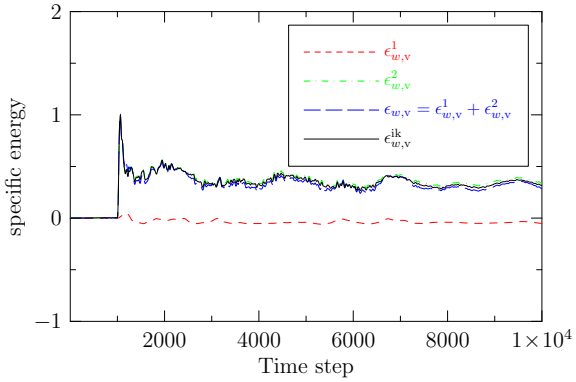

(b)

Figure 4.5: Evolution of specific internal energy for a constant temperature (applied after first 1000 time steps) simulation *without* periodic boundary conditions, using an averaging domain of radius $R = 0.4l$. (a) Plot showing the evolution of the potential part, $\epsilon_{w,\mathrm{v}}$, and the kinetic part, $\epsilon_{w,\mathrm{k}}$, of the specific internal energy. (b) Plot comparing the evolution of the potential part of the specific internal energy with its analogue, $\epsilon^{\mathrm{ik}}_{w,\mathrm{v}}$, in the original Irving–Kirkwood procedure.

even after increasing the temperature of the system.

Experiment 3

The setup is similar to the previous experiment except that now we do not apply periodic boundary conditions. This means that the sample is free to expand once the temperature of the sample is increased. The plots shown in Fig. 4.5 correspond to $R = 0.4l$. Fig. 4.5(a) shows the plot of $\epsilon_{w,\mathrm{v}}$, $\epsilon_{w,\mathrm{k}}$ and the total specific energy at the center of the sample, and Fig. 4.5(b) compares $\epsilon_{w,\mathrm{v}}$ with $\epsilon^{\mathrm{ik}}_{w,\mathrm{v}}$. In this case we see from Fig. 4.5(b) that unlike the previous two experiments there is a small negative contribution to $\epsilon_{w,\mathrm{v}}$ due to $\epsilon^1_{w,\mathrm{v}}$ — although the magnitude is still very small. Note that the longer wavelength oscillations in energy

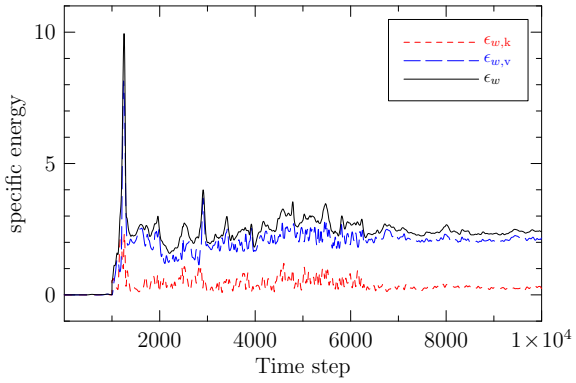

(a)

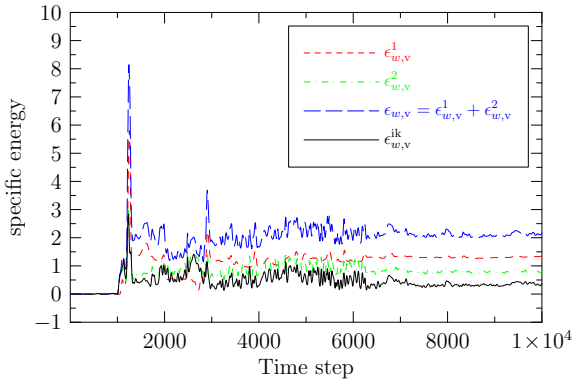

(b)

Figure 4.6: Evolution of specific internal energy for a constant temperature (applied after first 1000 time steps) simulation *without* periodic boundary conditions, using an averaging domain of radius $R = 0.1l$. (a) Plot showing the evolution of the potential part, $\epsilon_{w,\mathrm{v}}$, and the kinetic part, $\epsilon_{w,\mathrm{k}}$, of the specific internal energy. (b) Plot comparing the evolution of the potential part of the specific internal energy with its analogue, $\epsilon^{\mathrm{ik}}_{w,\mathrm{v}}$, in the original Irving–Kirkwood procedure.

in these plots correspond to the pulsing of the sample as it expands and contracts about its mean thermally-expanded size.

It is also interesting to see how these continuum fields change as the averaging domain size is decreased. As mentioned previously, as the weighting function tends to the Dirac delta distribution, we expect the continuum fields to also become localized with increasing magnitude. To see if this is indeed the case, we decrease the size of the averaging domain by choosing $R = 0.1l$, which corresponds to a length of 1.5 unit cells. Fig. 4.6 shows the plots for this case. Comparing Fig. 4.6(a) with Fig. 4.5(a), we see that $\epsilon_{w,\mathrm{k}}$ remains the same, while $\epsilon_{w,\mathrm{v}}$ for the smaller averaging domain is about four times larger than its value for the larger domain. Similarly comparing Fig. 4.6(b) with Fig. 4.5(b), we see that for the smaller domain, $\epsilon_{w,\mathrm{v}}$ is greater than four times $\epsilon^{\mathrm{ik}}_{w,\mathrm{v}}$, whereas they were equal for the larger domain. Moreover, the contribution due to $\epsilon^{1}_{w,\mathrm{v}}$ to the specific internal energy is larger than that due to $\epsilon^{2}_{w,\mathrm{v}}$. This clearly shows that for small averaging domains, the two definitions given by (4.4.1) and (4.4.2) are quite different in nature. Based on our observations, we can conclude that $\epsilon_{w,\mathrm{v}}$ tends to localize more strongly with the averaging domain size than does $\epsilon^{\mathrm{ik}}_{w,\mathrm{v}}$.

To rationalize these results, let us consider what happens to these definitions as the weighting function tends to a delta distribution. In this case, $\epsilon^{\mathrm{ik}}_{w,\mathrm{v}}$ (see (4.4.1)) localizes to the particle positions. The same also happens to all terms in the definition of $\epsilon_{w,\mathrm{v}}$ (see (4.4.2)) *except* for σ_w. This term localizes to the lines joining the particles rather than onto the particles themselves. This observation provides a qualitative explanation, although not complete, for the different behavior of the two definitions shown above.

4.5 Summary

In this paper, we present a two-step *unified framework* for the evaluation of continuum field expressions from molecular simulations: (1) pointwise continuum fields are obtained using a generalization of the Irving–Kirkwood procedure to arbitrary multi-body potentials, and (2) spatial averaging is applied to obtain the corresponding macroscopic quantities. The latter lead to expressions suitable for computation in molecular dynamics simulations. It is shown that the important commonly-used microscopic definitions for continuum fields are recovered in this process as special cases.

In generalizing the Irving–Kirkwood to arbitrary many-body potentials we have had to address two ambiguities inherent in the original procedure which lead to non-uniqueness in the resulting expressions. The first ambiguity arises due to the non-uniqueness of the

partitioning of the force on an atom as a sum of central forces, which is directly related to the non-uniqueness of the potential energy representation in terms of distances between particles. This is in turn related to the shape space of the system. The conclusion is that the pointwise stress tensor is *not* unique, however we show in [AT10] that the macroscopic stress obtained via spatial averaging becomes unique as the spatial averaging domain is taken to infinity.

The second ambiguity in the original Irving–Kirkwood procedure arises due to the arbitrary decomposition of energy between particles. We show that this decomposition can be completely avoided through an alternative derivation for the energy balance equation. This leads to new definitions for the specific internal energy and the heat flux vector. In particular, the resulting potential part of the specific internal energy does not depend on the arbitrary partitioning of the potential energy to individual particles, and the resulting heat flux vector does not contain the "transport part" which is not invariant with respect to the addition of a constant to the potential energy function.

The new definition for the specific internal energy is compared with the original Irving–Kirkwood definition through a series of numerical experiments. Although our expression applies to arbitrary many-body potentials, we have chosen to perform the comparisons for the special case of a system of identical particles interacting through a pair potential since this is the only case where the original Irving–Kirkwood internal energy density is well-defined. This is due to the ambiguity in the decomposition of energy between the particles in the original Irving–Kirkwood derivation (and existing extensions to the approach). In our numerical experiments, we observe that both definitions agree for weighting functions with support given by a ball of radius 0.6 unit cells and larger. However, as the weighting function tends to a delta distribution, the two definitions scale differently. A qualitative theoretical explanation for this difference is given based on the limiting behavior of the two definitions as the averaging domain tends to a point.

It would also be of interest to compare the new expression for the heat flux vector to the original Irving–Kirkwood expression. In order to do this, one has to study the transport part of the heat flux. To our knowledge, this has not been done in the past because the transport part is normally lumped into either the kinetic or potential parts of the heat flux and not observed separately. Our new derivation shows that its existence is directly related to the arbitrariness in the energy decomposition. Preliminary numerical studies of some systems (not reported here) suggest that the transport part of the heat flux vector, which is absent in the new derivation, tends to be negligible. Further work is necessary to determine whether

this is a general result.

Chapter 5

Thesis summary

In this work, various continuum notions for atomistic systems have been systematically obtained under a unified framework.[1]

In Chapter 2, we obtained material fields for atomistic systems by carrying out the Murdoch–Hardy procedure on a reference configuration of discrete particles. One of the key feature of this procedure is that these fields are obtained without defining a deformation map. Additionally, we have shown that the relationship between the spatial and material fields are identically satisfied in a distributional sense. An interesting observation from our derivation is that the atomistic first Piola–Kirchhoff stress tensor does not have a kinetic contribution, which in the atomistic Cauchy stress tensor accounts for thermal fluctuations. We showed that this effect is also included in the atomistic first Piola–Kirchhoff stress tensor through the motion of particles with the example of an ideal gas. Finally, we demonstrated the validity of our definition for the first Piola–Kirchhoff stress through a numerical example involving finite deformation of a slab containing a notch under tension.

In Chapter 3, we studied the non-uniqueness of the atomistic stress tensor arising from the non-uniqueness of the force decomposition, which in turn is due to the choice of the potential energy representation. A geometric interpretation of force decomposition was given using rigidity theory and its non-uniqueness is characterized. This analysis resulted in a decomposition of the atomistic stress into an irrotational part that depends on the choice of potential energy representation, and a solenoidal part that is independent of it. A similar decomposition is constructed in continuum mechanics using the generalized Beltrami

[1] Some portions of this chapter are adopted verbatim from the summary sections of Chapter 2, Chapter 3 and Chapter 4, which have been written as three separate papers for publication in peer-reviewed journals.

representation, which is a version of Helmholtz decomposition for symmetric tensor fields. We identified various analogies between the two decompositions and obtained an atomistic equivalent to the continuum strain tensor. We numerically compared the two decompositions and demonstrated their equivalence for a linear elasticity boundary-value problem of an anisotropic infinite plate with a hole under uniaxial stress at infinity.

In Chapter 4, we addressed an ambiguity in the original Irving–Kirkwood procedure that arises due to the arbitrary decomposition of energy between particles. We showed that this decomposition can be completely avoided through an alternative derivation for the energy balance equation. This lead to new definitions for the specific internal energy and the heat flux vector. In particular, the resulting potential part of the specific internal energy does not depend on the arbitrary partitioning of the potential energy to individual particles, and the resulting heat flux vector does not contain the "transport part" which is not invariant with respect to the addition of a constant to the potential energy function. The new definition for the specific internal energy was compared with the original Irving–Kirkwood definition through a series of numerical experiments.

Bibliography

[Adm] N. C. Admal. Modified Lennard–Jones potential for Argon.

[Adm10] Nikhil Chandra Admal. A unified interpretation of stress in molecular systems. Master's thesis, University of Minnesota, Department of Aerospace Engineering and Mechanics, Minneapolis, MN 55455, 2010.

[AT10] N. C. Admal and E. B. Tadmor. A unified interpretation of stress in molecular systems. *Journal of Elasticity*, 100:63–143, 2010.

[AT11] N. C. Admal and E. B. Tadmor. Stress and heat flux for arbitrary multibody potentials: A unified framework. *The Journal of Chemical Physics*, 134:184106, 2011.

[AT14] N. C. Admal and E. B. Tadmor. The non-uniqueness of the atomistic stress tensor and its relationship to the generalized Beltrami representation. 2014. In preparation.

[Bel92] E Beltrami. Osservazioni sulla nota precedente. *Atti Accad. Lincei Rend*, 1(5):141–142, 1892.

[Ber58] N. Bernardes. Theory of solid Ne, Ar, Kr, and Xe at 0K. *Phys. Rev.*, 112(5):1534–1539, 1958.

[BKO+96] T. Belytchko, Y. Krongauz, D. Organ, M. Fleming, and P. Krysl. Meshless methods: An overview and recent developments. *Computer Methods in Applied Mechanics and Engineering*, 139:3–47, 1996.

[Cau28a] Augustin Cauchy. *Exercises de mathématique*, volume 3, chapter Sur l'éequilibre et le mouvement d'un système du points matériels sollicités par des forces d'attraction ou de répulsion mutuelle, pages 227–252. Chez de Bure Frères, Paris, 1828.

[Cau28b] Augustin Cauchy. *Exercises de mathématique*, volume 3, chapter De la pression ou tension dans un système de points matériels, pages 253–277. Chez de Bure Frères, Paris, 1828.

[Che06] Y. P. Chen. Local stress and heat flux in atomistic systems involving three body forces. *The Journal of Chemical Physics*, 124:054113, 2006.

[Cla70] R. Clausius. On a mechanical theorem applicable to heat. *Philosophical Magazine*, 40:122–127, 1870.

[CRD01] J. Cormier, J. M. Rickman, and T. J. Delph. Stress calculation in atomistic simulations of perfect and imperfect solids. *Journal of Applied Physics*, 89(1):99–104, 2001.

[CW96] Robert Connelly and Walter Whiteley. Second-order rigidity and prestress stability for tensegrity frameworks. *SIAM Journal on Discrete Mathematics*, 9(3):453–491, 1996.

[DB84] M.S. Daw and M.I. Baskes. Embedded-atom method: Derivation and application to impurities, surfaces, and other defects in metals. *Phys. Rev. B*, 29:6443–6453, 1984.

[Del05] T. J. Delph. Conservation laws for multibody interatomic potentials. *Modeling and Simulation in Materials Science and Engineering*, 13:585–594, 2005.

[EA94] F. Ercolessi and J. B. Adams. Interatomic potentials from first-principles calculations - the force-matching method. *Europhysics Letters*, 26(8):583–588, 1994.

[EEL+07] W. E, B. Engquist, X. T. Li, W. Q. Ren, and E. Vanden-Eijnden. Heterogeneous multiscale methods: A review. *Comm. Comp. Phys.*, 2(3):367–450, 2007.

[Ella] R. E. Elliott. A EAM Dynamo potential for Al due to Ercolessi and Adams.

[Ellb] R. E. Elliott. EAM Model Driver which reads Dynamo setfl and setfl table files for Embedded-Atom Method (EAM) and Finnis Sinclair potentials.

[FRC05] Roger Fosdick and Gianni Royer-Carfagni. A stokes theorem for second-order tensor fields and its implications in continuum mechanics. *International Journal of Non-Linear Mechanics*, 40(2):381–386, 2005.

[FS03] Roger Fosdick and Karl Schuler. Generalized Airy stress functions. *Meccanica*, 38(5):571–578, 2003.

[Ghi10] Riccardo Ghiloni. The Hodge decomposition theorem for general three-dimensional vector fields, without cuts. 2010.

[GR79] Vivette Girault and P-A Raviart. Finite element approximation of the Navier-Stokes equations. *Lecture Notes in Mathematics, Berlin Springer Verlag*, 749, 1979.

[Gur62] Morton E Gurtin. On helmholtz's theorem and the completeness of the Papkovich-Neuber stress functions for infinite domains. *Archive for Rational Mechanics and Analysis*, 9(1):225–233, 1962.

[Gur63] M.E. Gurtin. A generalization of the beltrami stress functions in continuum mechanics. *Archive for Rational Mechanics and Analysis*, 13(1):321–329, 1963.

[Har82] Robert. J. Hardy. Formulas for determining local properties in molecular dynamics simulation: Shock waves. *The Journal of Chemical Physics*, 76(01):622–628, 1982.

[Hör90] L. Hörmander. *The analysis of linear partial differential operators: Distribution theory and Fourier analysis*. Springer Study Edition. Springer-Verlag, 1990.

[HPB05] Hendrik Heinz, Wolfgang Paul, and Kurt Binder. Calculation of local pressure tensors in systems with many-body interactions. *Physical Review E*, 72:066704, 2005.

[HRS02] Robert J. Hardy, Seth Root, and David. R. Swanson. Continuum properties from molecular simulations. *AIP Conference Proceedings*, 620:363–366, 2002.

[IK50] J. H. Irving and G. Kirkwood. The statistical mechanics theory of transport processes. iv. the equations of hydrodynamics. *The Journal of Chemical Physics*, 18(06):817–829, 1950.

[KO01] J. Knap and M. Ortiz. An analysis of the quasicontinuum method. *J. Mech. Phys. Sol.*, 49(9):1899–1923, 2001.

[Lee12] John Lee. *Introduction to smooth manifolds*, volume 218. Springer, 2012.

[Lek63] S. G. Lekhnitskii. *Theory of elasticity of an anisotropic elastic body*. Holden-Day Series in Mathematical Physics, 1963.

[LVLT10] Richard Lehoucq and Anatole Von Lilienfeld-Toal. Translation of walter nolls derivation of the fundamental equations of continuum thermodynamics from statistical mechanics. *Journal of Elasticity*, 100:5–24, 2010.

[Mal69] L. E. Malvern. *Introduction to the mechanics of a continuous medium*. Prentice-Hall, Upper Saddle River, 1969.

[Max70] J. C. Maxwell. On reciprocal figures, frames and diagrams of forces. *Translations of the Royal Society of Edinburgh*, XXVI:1–43, 1870.

[Max74] J. C. Maxwell. Van der waals on the continuity of the gaseous and liquid states. *Nature*, 10:477–80, 1874.

[MB93] A. I. Murdoch and D. Bedeaux. On the physical interpretation of fields in continuum mechanics. *International Journal of Engineering Science*, 31(10):1345–1373, 1993.

[MB94] A. I. Murdoch and D. Bedeaux. Continuum equations of balance via weighted averages of microscopic quantities. *Proceedings of the Royal Society of London A*, 445:157–179, 1994.

[MJP09a] Kranthi K. Mandadapu, Reese E. Jones, and Panayiotis Papadopoulos. Generalization of the homogeneous nonequilibrium molecular dynamics method for calculating thermal conductivity to multibody potentials. *Physical Revew E*, 80(4):047702, 2009.

[MJP09b] Kranthi K. Mandadapu, Reese E. Jones, and Panayiotis Papadopoulos. A homogeneous nonequilibrium molecular dynamics method for calculating thermal conductivity with a three-body potential. *The Journal of Chemical Physics*, 130(20):204106, 2009.

[MR83] Gisele Marechal and Jean-Paul Ryckaert. Atomic versus molecular description of transport properties in polyatomic fluids: n-butane as an illustration. *Chemical Physics Letters*, 101(6):548–554, 1983.

[MRT06] S. Morante, G. C. Rossi, and M. Testa. The stress tensor of a molecular system: An exercise in statistical mechanics. *The Journal of Chemical Physics*, 125:034101–1–034101–11, 2006.

[Mur82] A. I. Murdoch. The motivation of continuum concepts and relations from discrete considerations. *Journal of Applied Mathematics and Mechanics*, 36:163–187, 1982.

[Mur03] A. I. Murdoch. On the microscopic interpretation of stress and couple stress. *Journal of Elasticity*, 71:105–131, 2003.

[Mur06] A. I. Murdoch. Some primitive concepts in continuum mechanics regarded in terms of objective space-time molecular averaging: The key role played by inertial observers. *Journal of Elasticity*, 84:69–97, 2006.

[Mur07] A. I. Murdoch. A critique of atomistic definitions of the stress tensor. *Journal of Elasticity*, 88:113–140, 2007.

[Mur12] A. I. Murdoch. *Physical Foundations of Continuum Mechanics*. Cambridge University Press, New York, 2012.

[Nol55] Walter Noll. Die herleitung der grundgleichungen der thermomechanik der kontinua aus der statistichen mechanik. *Journal of Rational Mechanics and Analysis*, 4:627–646, 1955.

[PS82] Christopher C Paige and Michael A Saunders. Lsqr: An algorithm for sparse linear equations and sparse least squares. *ACM Transactions on Mathematical Software (TOMS)*, 8(1):43–71, 1982.

[RB00] Robert E. Rudd and J. Q. Broughton. Concurrent coupling of length scales in solid state systems. *Physical Status Solidi B*, 217:251–291, 2000.

[RR04] Michael Renardy and Robert C Rogers. *An introduction to partial differential equations*, volume 4. Springer, 2004.

[RT10] G. C. Rossi and M. Testa. The stress tensor in thermodynamics and statistical mechanics. *The Journal of Chemical Physics*, 132:074902, 2010.

[SMC04] L. E. Shilkrot, R. E. Miller, and W.A. Curtin. Multiscale plasticity modeling: Coupled atomistic and discrete dislocation mechanics. *J. Mech. Phys. Sol.*, 52(4):755–787, 2004.

[SMT+99] V. B. Shenoy, R. Miller, E.B. Tadmor, D. Rodney, R. Phillips, and M. Ortiz. An adaptive methodology for atomic scale mechanics: The quasicontinuum method. *J. Mech. Phys. Sol.*, 47:611–642, 1999.

[SW85] H. Stillinger and A. Weber. Computer simulation of local order in condensed phases of silicon. *Physical Review B*, 31:5262–5271, 1985.

[TEPS13] Ellad B Tadmor, Ryan S Elliott, Simon R Phillpot, and Susan B Sinnott. NSF cyberinfrastructures: A new paradigm for advancing materials simulation. *Current Opinion in Solid State and Materials Science*, 17(6):298–304, 2013.

[Ter88] J. Tersoff. Empirical interatomic potential for silicon with improved elastic properties. *Phys. Rev. B*, 38(14):9902–9905, 1988.

[TES+11] EB Tadmor, RS Elliott, JP Sethna, RE Miller, and CA Becker. The potential of atomistic simulations and the Knowledgebase of Interatomic Models. *JOM Journal of the Minerals, Metals and Materials Society*, 63(7):17–17, 2011.

[TM09] E. B. Tadmor and Ronald E. Miller. A unified framework and performance benchmark of fourteen multiscale atomistic/continuum coupling methods. *Modelling and Simulation in Materials Science and Engineering*, 17:053001, 2009.

[TM11] Ellad B Tadmor and Ronald E Miller. *Modeling materials: continuum, atomistic and multiscale techniques*. Cambridge University Press, 2011.

[TME12] Ellad B Tadmor, Ronald E Miller, and Ryan S Elliott. *Continuum mechanics and thermodynamics: from fundamental concepts to governing equations*. Cambridge University Press, 2012.

[TNO08] Daichi Torii, Takeo Nakano, and Taku Ohara. Contribution of inter- and intramolecular energy transfers to heat conduction in solids. *The Journal of Chemical Physics*, 128:044504, 2008.

[TOP96] E. B. Tadmor, M. Ortiz, and R. Phillips. Quasicontinuum analysis of defects in solids. *Philosophical Magazine A*, 73(6):1529–1563, 1996.

[TPM09] A. P. Thompson, S. J. Plimpton, and W. Mattson. General formulation of pressure and stress tensor for arbitrary many-body interaction potentials under periodic boundary conditions. *The Journal of Chemical Physics*, 131:154107, 2009.

[Tsa79] D. H. Tsai. The virial theorem and stress calculation in molecular dynamics. *The Journal of Chemical Physics*, 70(03):1375–1382, 1979.

[UMP13] Manfred H Ulz, Kranthi K Mandadapu, and Panayiotis Papadopoulos. On the estimation of spatial averaging volume for determining stress using atomistic methods. *Modelling and Simulation in Materials Science and Engineering*, 21(1):15010–15024, 2013.

[VTSA14] Juan M Vanegas, Alejandro Torres-Sánchez, and Marino Arroyo. Importance of force decomposition for local stress calculations in biomembrane molecular simulations. *Journal of Chemical Theory and Computation*, 10(2):691–702, 2014.

[WAD95] Eligiusz Wajnryb, Andrzej R. Altenberger, and John S. Dahler. Uniqueness of the microscopic stress tensor. *The Journal of Chemical Physics*, 103(22):9782–9787, 1995.

[XB04] S.P. Xiao and T. Belytschko. A bridging domain method for coupling continua with molecular dynamics. *Computer Methods in Applied Mechanics and Engineering*, 193:1645–69, 2004.

[ZIH+04] J. A. Zimmerman, E. B. Webb III, J. J. Hoyt, R. E. Jones, P. A. Klein, and D. J. Bammann. Calculation of stress in atomistic simulation. *Modeling and Simulation in Material Science and Engineering*, 12:S319–S332, 2004.

[ZT04] Junfang Zhang and B. D. Todd. Pressure tensor and heat flux for inhomogeneous nonequilibrium fluids under the influence of three body forces. *Physical Review E*, 69:031111, 2004.

[ZWS08] Jonathan A. Zimmerman, Edmund B. Webb, and Steven C. Seel. Reconsideration of continuum thermomechanical quantities in atomic scale simulations. *Mathematics and Mechanics of Solids*, 13:221–266, 2008.

Appendix A

Thermal contribution to the atomistic first Piola–Kirchhoff stress tensor in an ideal gas

Recall that the atomistic Cauchy stress $\boldsymbol{\sigma}_w$ defined in (2.3.9) has a kinetic contribution whereas the definition of the first Piola–Kirchhoff $\boldsymbol{P}_w$ in (2.3.27) does not. This leads to an apparent contradiction when considering the relation between these two measures. In particular, when a system is not deformed, we expect $\boldsymbol{\sigma}_w = \boldsymbol{P}_w$.

To investigate this issue, we consider the example of an ideal gas enclosed in a container at non-zero temperature. Since an ideal gas is modeled as a collection of non-interacting particles, the potential part of the Cauchy stress tensor away from the container boundaries is identically zero. This enables us to focus on the kinetic contribution alone. We show below that although $\boldsymbol{P}_w$ does not have an explicit kinetic-like term, the time-average of $\boldsymbol{P}_w$ recovers the kinetic contribution.

Consider an ideal gas confined within a cubic container. The ideal gas particles do not interact with each other, but do interact with the particles of the container through a strong short-range potential which keeps the gas particles strictly inside the container without diffusing into the container walls. The particles are initially given random velocities corresponding to the set temperature, and the system is allowed to establish thermal equilibrium. Suppose we are now interested in calculating the stress at the center of the cube. In order to do this, we choose a weighting function w whose support is centered at the center of the cube. Assume that the size of the support is small, so that it is away from the boundaries and

therefore does not include any of the current bonds[1] which lie close to the inner-boundary of the container walls.

Clearly, the potential part of the atomistic Cauchy stress, calculated using (2.3.12), is always zero because the support of w is away from the boundaries. Thus, the only contribution to the atomistic Cauchy stress comes from the kinetic part, which receives contributions from particles crossing the support of the weighting function. At the same time, it is clear from (2.3.27) that the atomistic first Piola–Kirchhoff stress is non-zero whenever a particle α that lies within the support of w in the reference configuration, interacts with a particle β of the container. The contribution to $\boldsymbol{P}_w$ due to this interaction is given by

$$-\boldsymbol{f}_{\alpha\beta} \otimes (\boldsymbol{X}_\alpha - \boldsymbol{X}_\beta) \int_{s=0}^{1} w((1-s)\boldsymbol{X}_\alpha + s\boldsymbol{X}_\beta - \boldsymbol{X})\, ds. \tag{A.0.1}$$

Although the magnitude of the vector $\boldsymbol{X}_\alpha - \boldsymbol{X}_\beta$ is large, the multiplying factor in (A.0.1) scales it down.[2] In other words, while the contribution to the atomistic Cauchy stress is due to the velocity of particles, the contribution to the atomistic first Piola–Kirchhoff stress is due to the interaction of particles lying inside the support of the weighting function in the reference configuration with container particles. For an ideal gas in a container, we expect the time average of the first Piola–Kirchhoff stress to be equal to the time average of the Cauchy stress. Although it is difficult to prove this assertion in full generality, we show that the it holds exactly when computing the traction across a plane (in the manner of Tsai) as described below.

Tsai [Tsa79] proposed a method for calculating the atomistic Cauchy stress tensor using the traction vector on a plane with normal $\boldsymbol{n}$. For instance, the $1k$ $(k = 1, 2, 3)$ component of the Cauchy stress tensor at a point $\boldsymbol{x}$, is given by $t_k(\boldsymbol{x}, \boldsymbol{n})/A$, where the traction vector $\boldsymbol{t}(\boldsymbol{x}, \boldsymbol{n})$ is calculated by passing a plane of area A, with normal $\boldsymbol{n} = (1, 0, 0)$, through the

[1] See (2.3.19) for the definition of a current bond. In this example, a current bond refers to the line joining a gas particle α, and a container particle β, whenever $\boldsymbol{f}_{\alpha\beta} \neq \boldsymbol{0}$.

[2] By assumption, $\boldsymbol{X}_\alpha$ is close to the center of the cube, and $\boldsymbol{X}_\beta$ is close to the boundary. Therefore, $\boldsymbol{X}_\alpha - \boldsymbol{X}_\beta$ is of the order of the size of the cube. For a constant weighting function, the factor resulting due to the integral in (A.0.1) is equal to the fraction of $\boldsymbol{X}_\alpha - \boldsymbol{X}_\beta$ that lies within the support of w, divided by the volume of the support of w.

point $\boldsymbol{x}$. The Tsai traction $\boldsymbol{t}(\boldsymbol{x}, \boldsymbol{n})$ is given by the expression [AT10]

$$\boldsymbol{t}(\boldsymbol{x}, \boldsymbol{n}) = \lim_{T\to\infty} \frac{1}{AT} \left[\int_0^T \sum_{\alpha\beta\cap\mathfrak{l}} \boldsymbol{f}_{\alpha\beta} \frac{(\boldsymbol{x}_\alpha - \boldsymbol{x}_\beta)\cdot\boldsymbol{n}}{|(\boldsymbol{x}_\alpha - \boldsymbol{x}_\beta)\cdot\boldsymbol{n}|}\, dt - \sum_{\alpha\leftrightarrow\mathfrak{l}}^{T} \frac{m_\alpha \boldsymbol{v}_\alpha(t_\leftrightarrow)(\boldsymbol{v}_\alpha(t_\leftrightarrow)\cdot\boldsymbol{n})}{|\boldsymbol{v}_\alpha(t_\leftrightarrow)\cdot\boldsymbol{n}|} \right], \tag{A.0.2}$$

where $\sum_{\alpha\beta\cap\mathfrak{l}}$ indicates the summation over all current bonds α–β that cross the plane $\mathfrak{l}$, $\sum_{\alpha\leftrightarrow\mathfrak{l}}^{T}$ indicates summation over all particles that cross[3] $\mathfrak{l}$ in the interval $[0, T]$, and $t_\leftrightarrow$ indicates the time at which the particle crosses the plane. It is shown in [AT10] that the Cauchy stress tensor obtained from the Tsai traction is a special case of $\boldsymbol{\sigma}_w$ defined in (2.3.9). Specifically, the traction vector $\boldsymbol{t}(\boldsymbol{x}, \boldsymbol{n})$ defined in (A.0.2) is obtained as the limit:

$$\boldsymbol{t}(\boldsymbol{x}, \boldsymbol{n}) = \lim_{i\to\infty} \bar{\boldsymbol{\sigma}}_{w_i} \boldsymbol{n}, \tag{A.0.3}$$

where the w_i's are a sequence of weighting functions whose support is tending to a plane normal to $\boldsymbol{n}$, and $\bar{\boldsymbol{\sigma}}_w$ is the time-averaged atomistic Cauchy stress tensor. A similar derivation can be carried out to obtain a definition for the atomistic first Piola–Kirchhoff stress tensor from the nominal (referential) Tsai traction vector $\boldsymbol{T}(\boldsymbol{X}, \boldsymbol{N})$, defined using a plane passing through $\boldsymbol{X}$, with normal $\boldsymbol{N}$. The resulting definition for $\boldsymbol{T}$ is given by

$$\boldsymbol{T}(\boldsymbol{X}, \boldsymbol{N}) = \lim_{T\to\infty} \frac{1}{AT} \int_0^T \sum_{\alpha\beta\cap\mathfrak{L}} \boldsymbol{f}_{\alpha\beta} \frac{(\boldsymbol{X}_\alpha - \boldsymbol{X}_\beta)\cdot\boldsymbol{N}}{|(\boldsymbol{X}_\alpha - \boldsymbol{X}_\beta)\cdot\boldsymbol{N}|}\, dt, \tag{A.0.4}$$

where $\sum_{\alpha\beta\cap\mathfrak{L}}$ indicates a summation over all reference bonds that cross the plane $\mathfrak{L}$.

We now show that for the ideal gas example, the Cauchy and first Piola–Kirchhoff stress tensors obtained from the corresponding Tsai tractions agree at the center of the cube and any other point away from the boundaries. This requires that $\boldsymbol{t} = \boldsymbol{T}$ away from the boundaries. In order to calculate $\boldsymbol{t}$ and $\boldsymbol{T}$, we consider a plane $\mathfrak{L}$ that passes through the center of the cube and cuts through it. (Since the system remains undeformed, the planes $\mathfrak{l}$ and $\mathfrak{L}$ coincide.) Since the system consists of non- interacting particles, without loss of generality, we may focus our attention on a single particle α. Moreover, we assume that the particle α, in its reference configuration[4], is located on the negative side[5] of the plane $\mathfrak{L}$.

[3] Multiple crossings by a single particle are included in the summation.

[4] A reference configuration is arbitrarily chosen to be the configuration at $t = 0$.

[5] The half of the cube towards which the normal of the plane points is referred to as the positive side of the plane. The other side is the negative.

Clearly, since no current bonds cross $\mathfrak{L}$, the integral of the first term on the right-hand side of (A.0.2) is identically zero for all $T > 0$. Let t_1 and t_2 be the first two consecutive crosses of particle α through the plane $\mathfrak{L}$. In the time interval $[0, t_1]$, the particle α may interact with the particles of one half of the container. Although there is an interaction, the term on the right-hand side of (A.0.4) does not contribute to $\boldsymbol{T}$ in the interval $[0, t_1]$. This is because, in the interval $[0, t_1]$, every reference bond α–β, where β is a particle in the container walls lies entirely on the negative side of the plane, and hence does not cross $\mathfrak{L}$. On the other hand, it is obvious that there is no contribution to $\boldsymbol{t}$ in the interval $[0, t_1]$, as none of the particles cross $\mathfrak{L}$. In the interval $[t_1, t_2]$, the kinetic contribution to $\boldsymbol{t}$ is given by

$$m_\alpha(\boldsymbol{v}_\alpha(t_1) - \boldsymbol{v}_\alpha(t_2)), \tag{A.0.5}$$

where we have used the equality $\boldsymbol{v}_\alpha(t_1) \cdot \boldsymbol{n} = \boldsymbol{v}_\alpha(t_2) \cdot \boldsymbol{n}$. The contribution to $\boldsymbol{T}$ in the interval $[t_1, t_2]$ is non-zero, because every reference bond α–β, where β is a particle of the container, now crosses the plane. Therefore, the contribution to $\boldsymbol{T}$ in the interval $[t_1, t_2]$ is given by

$$\begin{aligned}&\left[\int_{t_1}^{t_2} \left(\sum_{\alpha\beta\cap\mathfrak{L}} \boldsymbol{f}_{\alpha\beta}\right) dt\right] \frac{(\boldsymbol{X}_\alpha - \boldsymbol{X}_\beta) \cdot \boldsymbol{N}}{|(\boldsymbol{X}_\alpha - \boldsymbol{X}_\beta) \cdot \boldsymbol{N}|}, \\ &= m_\alpha(\boldsymbol{v}_\alpha(t_1) - \boldsymbol{v}_\alpha(t_2)).\end{aligned} \tag{A.0.6}$$

The second equality is the result of Newtons second law applied to particle α. Due to the equality of (A.0.5) and (A.0.6), it follows that $\boldsymbol{t} = \boldsymbol{T}$. Therefore, we have shown that in the case of an ideal gas, the atomistic first Piola–Kirchhoff and the Cauchy stress tensors are equal.